ELUCIDATING THE ROLE OF SMALL MOLECULE SIGNALS IN BACTERIAL DEVELOPMENT

A Dissertation

by

QUTAIBA OMAR ABABNEH

Submitted to the Office of Graduate and Professional Studies of
Texas A&M University
in partial fulfillment of the requirements for the degree of

DOCTOR OF PHILOSOPHY

Chair of Committee,	Jennifer Herman
Committee Members,	Frank Raushel
	Paul Straight
	Deborah A. Siegele
Head of Department,	Gregory D. Reinhart

August 2015

Major Subject: Biochemistry

ABSTRACT

The nucleotide second messengers pppGpp and ppGpp ((p)ppGpp) are responsible for the global down-regulation of transcription, translation, DNA replication, and growth rate during stringent response. More recent studies suggest that (p)ppGpp is also an important effector in many non-stringent processes, including virulence, persister cell formation, and biofilm production. In *Bacillus subtilis*, (p)ppGpp production is controlled by bifunctional synthetase/hydrolase, RelA, and two monofunctional synthetases, YwaC and YjbM. We observed that a *relA* mutant grows exclusively as unchained, motile cells in contrast to the wildtype (PY79), which grows as both motile, unchained and nonmotile, chained cells. The phenotypic switch from non-motile, chained cells to unchained, motile cells is promoted by the alternative sigma factor, SigD. We found that the *relA* mutant is trapped in a SigD ON state during exponential growth, implicating RelA and (p)ppGpp levels in the regulation of cell chaining and motility in *B. subtilis*. Furthermore, we showed that this cell chaining and motility is directly regulated by the GTP-sensing protein, CodY. (p)ppGpp accumulation inhibits GTP synthesis and CodY has three putative binding sites in the *sigD*-containing *fla*/*che* operon. Our current model is that (p)ppGpp synthesis leads to decreased levels of GTP and a concomitant decrease in CodY-GTP mediated repression of *fla/che* operon transcription. This work highlighted the critical role of basal (p)ppGpp levels in significantly skewing developmental decision-making outcomes.

Entry into sporulation is governed by Spo0A, which accumulates as cells enter stationary phase and is activated by a phosphorylation cascade initiated by sensor kinases

in response to environmental cues. Environmental cues are critical to successful sporulation, as prior studies have shown that expression of constitutively active Spo0A is not sufficient to induce sporulation during exponential growth. However, previous reports indicate that a gradual increase in Spo0A-P, mediated through artificial expression of the kinase KinA, is sufficient to trigger sporulation during exponential growth. We report here that sporulation via KinA induction requires an extracellular factor or factors (FacX) that only accumulates to sufficient levels during post-exponential growth. FacX is retained by dialysis with a cutoff smaller than 500 Dalton, can be concentrated, and is susceptible to proteinase K digestion, similar to quorum-sensing peptides shown to be involved in promoting sporulation. However, unlike previously characterized peptides, FacX activity is not dependent on SigH or Spo0A, and does not require the oligopeptide transporters Opp and App. We also find that *B. subtilis* can be induced to sporulate following the acute induction of active Spo0A in media containing FacX. These results indicate that there is no formal requirement for gradual Spo0A-P accumulation in successful sporulation and instead support the idea that sporulation requires both sufficient levels of active Spo0A and at least one other signal or condition.

DEDICATION

To my parents, wife and son.

ACKNOWLEDGEMENTS

Thanks to my supervisor Jennifer Herman for giving me the honor of being your first graduate student. Thank you for being both patient and supportive throughout my graduate program.

Thanks to my examining committee members, Drs. Frank Raushel, Deborah Siegele and Paul Straight for your helpful insights and constructive comments throughout the course of this research.

Thanks to my friends in Herman Lab, Emily Brown, Yi Duan, Sarah Hartman, Allyssa Miller and Anthony Sperber for every second I spent with you.

Thanks to Straight Lab and Young Lab members for your help and assistance.

Thanks to Dr. Larry Dangot and Dr. Chris Hoelfer for all your help in FacX puriication.

Thanks to Dr. William Park, Daisy Wilbert and Rafael Almanzar for all your administrative assistance and advice.

TABLE OF CONTENTS

Page

LIST OF FIGURES

LIST OF TABLES

CHAPTER I

INTRODUCTION

Unicellular organisms, such as bacteria, were once thought to live as communities of clonal uniform cells. However, it is now apparent that under certain conditions, cultures of genetically identical bacteria consist of subpopulations of specialized, differentiated cells. These subpopulations of cells can serve distinct functions within their community. Bacteria must coordinate the activation and regulation of the developmental programs that result in these distinct subpopulations. However, a central question in developmental biology remains outstanding: how is entry into the different developmental programs regulated? The Gram positive bacterium *Bacillus subtilis* is an excellent system to address this question, as it carries out several well-characterized developmental pathways to form subpopulations of cells, each capable of accomplishing distinct functions either alone, or in the context of, multicellular communities (1). Functions that are expressed at the subpopulation level include motility, uptake of exogenous DNA, biofilm formation, extracellular protease synthesis, and sporulation (1). The differentiation of *B. subtilis* cells to perform these functions is regulated in part by both intracellular and extracellular signaling molecules (2). These molecules play critical roles bacterial surviving during environmental & nutritional stresses.

Bacillus subtilis

B. subtilis is a non-pathogenic, rod-shaped, ubiquitous soil-dwelling bacterium and that is an endospore-forming member of the phylum Firmicutes (low GC% content Gram-positive bacteria). Second only to *Escherichia coli*, *B. subtilis* is genetically and physiologically one of the best characterized bacteria, and is used in research laboratories as a model organism to understand diverse cellular processes in other bacteria. Most *B. subtilis* strains used in the laboratory are derivatives of the tryptophan auxotroph, strain 168. The *B. subtilis* 168 strain was isolated after Paul Burkholder and Norman Giles used X-rays to mutagenize the Marburg strain (3). One of the original Marburg isolates called NCIB 3610, is much "wilder" than strain 168 and is widely used in studies involving bacterial multicellular behavior functions, such as biofilm formation, fruiting body formation, and swarming motility. In contrast, strain 168 lacks any of these functions (4). In this study, we used a laboratory domesticated strain PY79, which is a derivative of the 168 strain. In the last decade, PY79 became one of the most widely used strains in large-scale -omics studies (5-8). PY79 is different from 168 due to the absence of the SPβ prophage (9) and the conjugative transposon ICEBs1 (10); and due to replacement of 168-like DNA sequences with DNA sequences from another *B. subtilis* strain called W23 (11). Compared to the undomesticated NCIB 3610 strain, both 168 and PY79 strain are naturally more competent, which make them an attractive model as they are genetically manipulated more easily.

Sporulation

Sporulation is a developmental program initiated in response to nutrient deprivation (12), whereby a vegetative cell becomes a resilient, metabolically dormant, highly protected and morphologically distinct cell type capable of reinitiating growth (germination) upon reintroduction of nutrients (13). Cells sporulate to deal with adverse environmental conditions, whereby the bacteria can preserve the genome until favorable growth conditions return. *B. subtilis* is being equipped with other survival strategies, including biofilm formation and stationary phase, and *B. subtilis* spore characteristics and morphology indicate that sporulation is the last resort designed for survival under extremely harsh environmental conditions [13].

During vegetative growth in nutrient-rich environment, cells replicate their chromosomes, double their length, and divide at the middle of the cell to generate two identical daughter cells. Sporulating cells undergo a number of morphological changes that are distinct from those exhibited by vegetative cells (Fig. 1.1) (14, 15). First, after chromosomes are replicated, the origins of replication are segregated to opposite poles and the chromosomes are remodeled to form the axial filament, an extended conformation of the cell's two chromosomes (16). Next, cells initiate an asymmetric division near one of the cell poles, producing two cellular compartments: the larger compartment is called the mother cell, while the smaller one is designated as the forespore. Initially, the mother cell and the forespore lie side-by side, but eventually the mother cell engulfs the forespore and facilitates the synthesis of protective spore coat

(16). After engulfment, the forespore is wrapped with an outer membrane derived from the mother cell. Next, the spore cortex, which is made of a specialized peptidoglycan and proteinaceous spore coat, is formed between the spore inner and outer membranes. Following spore cortex formation, the forespore cytoplasm is dehydrated and the chromosome is condensed. Lastly, the mother cell lyses, releasing the mature endospore. The spore, which is metabolically dormant and resistant to environmental damage, can be converted into a vegetative cell through a process called germination. This germination process is triggered when the spore senses specific small molecules such as amino acids and sugars (reviewed in (14, 16)).

The process of spore formation is time-consuming, energy-expensive and becomes irreversible after the completion of the early steps even if nutrients become available (17). In this case, cells committed to sporulation will be at a competitive disadvantage compared to those which didn't initiate sporulation. On the other hand, failure to initiate sporulation upon nutrient deprivation decreases the chance of survival if the nutrients continue to be exhausted. Thus, the decision of whether or not to initiate the sporulation pathway is highly regulated and tightly linked to physiological status and environmental conditions (18).

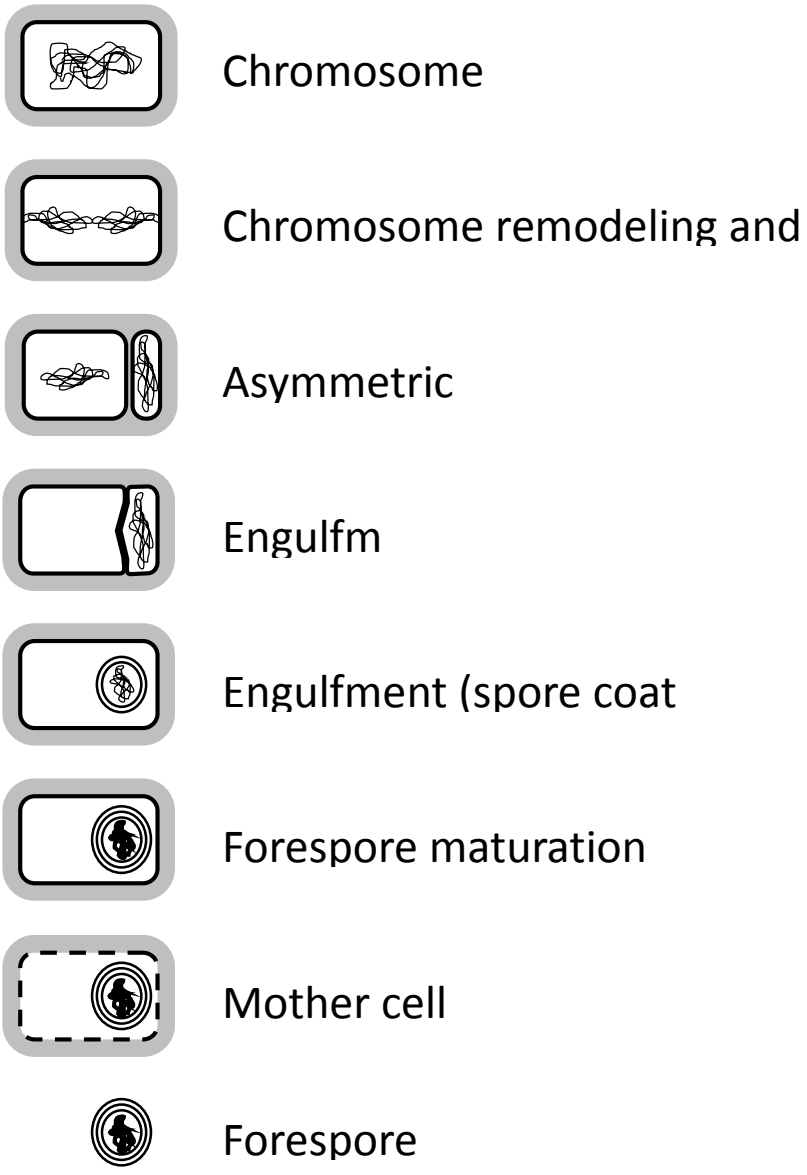

FIGURE 1.1 Morphological changes during sporulation (start from top to bottom). First, replicated chromosomes are replicated. Then, chromosomes are remodeled and segregated into each pole. Next, the cell divides near one of the poles, giving the large mother cell and the small forespore cell. The two cells initially lie side- by-side, then the mother cell engulf forespore. After the completion of engulfment, the forespore is released into the mother cell cytoplasm wrapped in an outer membrane derived from the mother cell. Next, the coat proteins are deposited in the forepsore surface and a peptidoglycan layer is synthesized in the space between the outer and inner membranes. After that, forespore cytoplasm is dehydrated and the chromosome is condensed. Finally, the mother cell lyses and the mature spore is released into the environment.

Entry into sporulation

Kinases

B. subtilis uses a complex genetic and protein network, called the phosphorelay, to decide whether to initiate sporulation or not (14). The phosphorelay is responsible for the phosphorylation and activation of the master regulator of sporulation, Spo0A (Fig. 1.2). In order to initiate sporulation, cells detect the signals generated during nutrient deprivation and increased cell density (15, 19). This sensing function is accomplished by one of five histidine kinases: KinA-D (20). These kinases respond to environmental cues by autophosphorylating a conserved histidine residue in an ATP-dependent manner (20). KinA and KinB are the main kinases responsible for initiation of sporulation (20, 21). However, the exact physiological signal(s) that is sensed by KinA and KinB is still unclear. KinA and KinB have been shown to sense and respond to changes in ATP levels (22, 23). KinC on the other hand is activated in response to unknown signals and it has been implicated in regulating cannibalism and biofilm formation in a phosphorelay dependent manner (24). Despite being reported to directly phosphorylate Spo0A (20), KinC activity is not sufficient for triggering sporulation at native levels, as cells lacking both KinA and KinB are unable to sporulate. Nevertheless, increasing the KinC protein levels was reported to be sufficient for sporulation (25). Based on these results, Devi and coworkers suggested that KinC activation leads to low levels of Spo0A phosphorylation (Spo0A-P) (24).

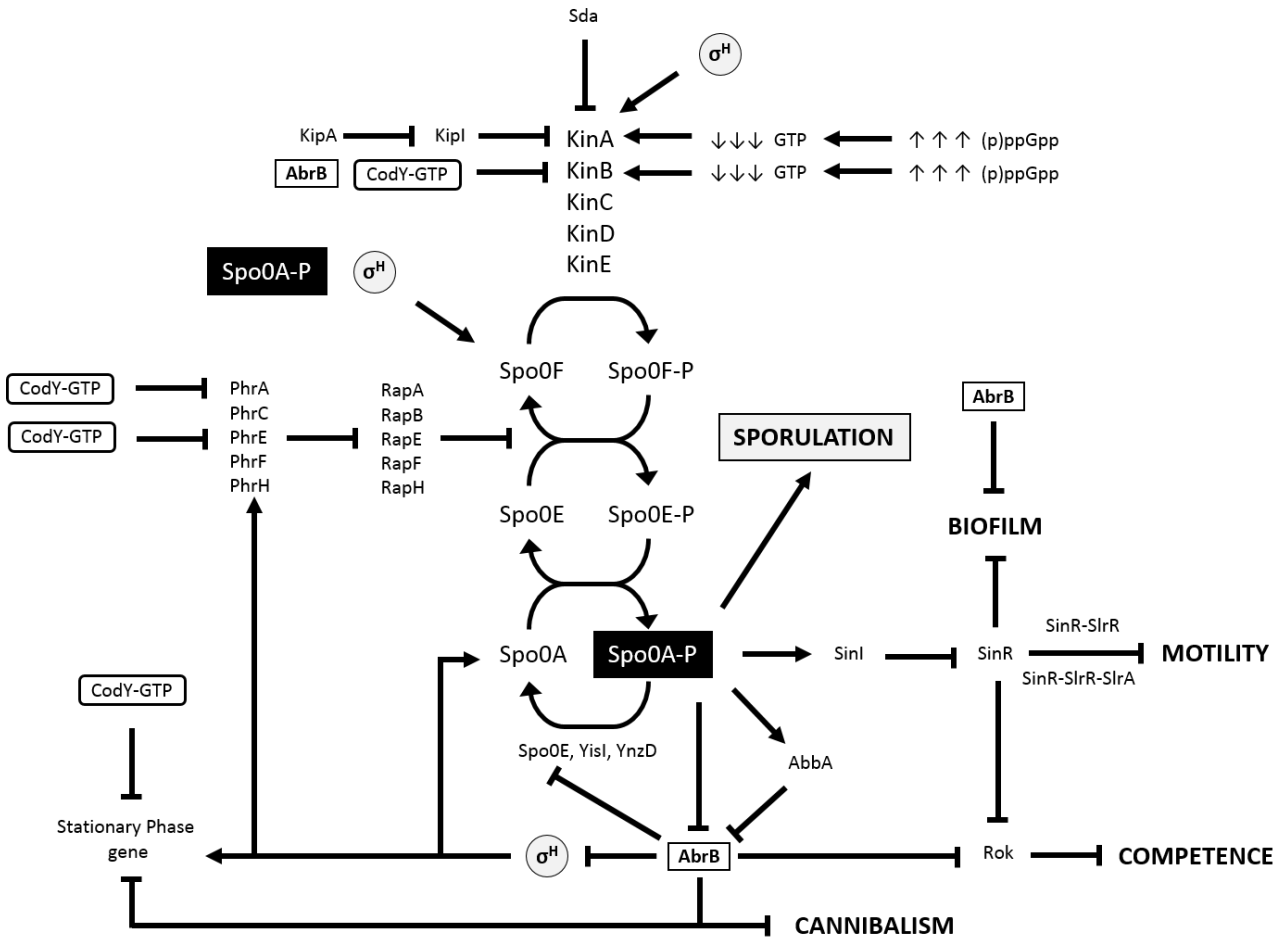

FIGURE 1.2 Regulatory network controlling the decision to initiate sporulation and other developmental processes. Lines with arrowheads indicate positive regulation and lines with blunt ends indicate negative regulation.

These low levels of Spo0A-P promote cells to form biofilms and produce the cannibalism toxin (24). Also, since KinC activity only results in low Spo0A levels, it may help cells avoid the sporulation initiation decision, as KinC-induced Spo0A-P levels are below the threshold required for triggering sporulation (24). In fact, cells can only accumulate high enough levels of Spo0A-P to initiate sporulation when KinA becomes activated (26). Lastly, KinD has been proposed to act as a phosphatase under certain condition and thereby delay the onset of sporulation (4), while no role for KinE in sporulation initiation has been reported so far (27).

Upon KinA and KinB autophosphorylation, the phosphoryl groups are transferred to aspartate residues on Spo0F (28). Spo0F-P then transfers the phosphoryl group to a histidine of phosphotransferase Spo0B, which finally phosphorylates a conserved aspartic acid in the regulatory domain of Spo0A to generate activated Spo0A-P (Fig. 1.2) (28). Spo0A-P regulates the initiation of sporulation by binding to conserved DNA sequence TGNCGAA, called the '0A box', present in the promoter regions in gene members of the Spo0A regulon. Spo0A-P directly regulates the expression of approximately 121 genes (29), including those involved in axial filament formation and asymmetric cell division (17).

Kinase activity is negatively regulated by interactions with the anti-kinases KipI and Sda (Fig. 1.2). Anti-kinase KipI was shown to block KinA autophosphorylation *in vitro* without affecting phosphoryl group transfer to the phosphorelay (30). KipI activity in turn is antagonized by a protein called KipA (31). Sda on the other hand, blocks both

KinA autophosphorylation and its ability to transfer phosphoryl group to its target, Spo0F (32).

Phosphatases

In addition to kinase inhibition by KipI and Sda, the phosphorelay is modulated by a number of phosphatases (Spo0F phosphatase, Rap A, B, E and H) that remove the phosphoryl groups from Spo0F or Spo0A (33-38). In addition, Spo0A-P can be dephosphorylated by Spo0E, YnzD, and YisI (39). The Rap proteins contain six 34-residue tetratricopeptide repeats involved in protein-protein interactions (34), and their activity is negatively regulated by small peptides encoded by *phr* genes. Thus far, the pheromone peptides PhrC, PhrA, PhrE, PhrF and PhrH have been recognized as inducers of sporulation (Fig. 1.2) (40-44). Each peptide is encoded in an operon with a Rap phosphatase and inhibits the activity of its cognate Rap protein (45). Each *phr* gene is co-transcribed with its cognate *rap* gene from a housekeeping, σ^A-dependent promoter upstream of the operon. However, a second promoter internal to the *rap* genes and immediately upstream of *phrC*, *phrE* and *phrF* genes have been identified. Transcription from this second promoter is controlled by the stationary phase alternative sigma factor σ^H (46). The regulation of *phr* expression by σ^H contributes to the cell-density control of sporulation. As cells transition from exponential growth to stationary phase, σ^H activity increases (47). The second internal promoter increases the amount of Phr peptide produced relative to its cognate Rap protein, such that the Rap phosphatase activities become more

inhibited as cell density increases (48). Once the Phr proteins are made, they are cleaved and secreted from the cell, accumulating in the culture supernatant, where they are processed by proteases into mature peptides and subsequently reimported by the oligopeptide uptake system Opp and App (48, 49). Once imported into the cytoplasm, Phr peptides bind to and inhibit the phosphatases directly (44, 50, 51). Regulation of the kinases, anti-kinases, phosphatases and Phr peptides activities is critical for determining Spo0A-P levels and allows cells to sense many environmental and cellular signals, and ultimately, integrate them into a cellular decision; for example, whether or not to sporulate

Spo0A

The gene encoding Spo0A is transcribed from two promoters: a σ^A-dependent promoter and a σ^H-dependent promoter (52, 53). σ^A is the housekeeping sigma factor, while σ^H is the stationary phase alternative sigma factor. Spo0A regulates its own transcription and three 0A boxes or operators, O1, O2 and O3, are located in the *spo0A* gene promoter region (54, 55). Spo0A-P binds to O2 during exponential growth, where it inhibits transcription from the σ^H-dependent promoter. As cells transition from exponential to stationary phase, Spo0A-P binds O1 to repress transcription from the σ^A-dependent promoter, but also binds O3 to activate transcription from the σ^H -dependent promoter (55).

Spo0A-P, directly and indirectly regulates more than 200 genes (29, 56). Genes regulated directly by Spo0A-P binding to their promoter are divided into two classes:

Genes activated by high levels of Spo0A-P due to their low affinity binding sites, and genes activated by low Spo0A-P levels which have high affinity binding sites (27, 29). Low Spo0A-P levels have been shown to activate the expression of *kinA*, *spo0F* and *sigH*, as well as the *spo0A* gene, which serves as a positive feedback mechanism to increase the capacity of the phosphorelay to activate Spo0A (Fig. 1.2) (27). Additionally, a subset of genes are indirectly activated by low Spo0A-P levels through inactivation of the repressor regulator AbrB, which represses transcription from genes required for sporulation initiation such as *sigH* (*spo0H*) (27). Spo0A-P directly inhibits the transcriptional repression of AbrB and activates the expression of an AbrB inhibitor called AbbA (Fig 1.2) (57). On the other hand, high Spo0A-P levels play a critical role in regulating entry into sporulation, as well as controlling the expression of genes involved in the early stages of sporulation (27).

The different Spo0A-P levels accumulating during growth are an important determinant in the decision-making process in which cells choose a developmental path to follow. Low Spo0A-P has been implicated in biofilm formation and immunity to toxins, whereas higher levels of Spo0A-P induce sporulation. These two developmental choices are dependent on SinR and its inhibitor SinI (58, 59). SinR is a transcriptional repressor that controls genes involved in motility, biofilm formation, and genetic competence in *B. subtilis* (60, 61). The promoter region of *sinI* contains 0A boxes with varying affinities for Spo0A-P. When Spo0A-P levels are low, Spo0A-P binds to the high affinity 0A boxes and activates SinI expression, leading to SinR inhibition and biofilm formation (Fig. 1.2) (27). In addition, SinR inhibition by SinI alleviates repression of *rok* expression by SinR

(61). Once synthesized, Rok blocks DNA competence through inhibiting ComK, the master regulator of competence (62). Rok is also known to inhibit antimicrobial peptide synthesis (63). Thus, blocking competence and antimicrobial peptide synthesis might promote cells to choose the sporulation initiation option. When Spo0A-P is abundant in the cells, the low affinity *sinI* 0A boxes are bound by Spo0A-P, which represses *sinI* expression. This leads to inhibition of biofilm formation by SinR (59, 61), and once again poises cells for sporulation. The intersection of SinR and Spo0A is a critical point in the decision-making process, as cells have to choose between mutually exclusive developmental paths.

Several studies have concluded that sporulation only requires that cells exceed a threshold level of Spo0A-P (22, 64, 65). This idea was challenged by the observation that sporulating and non-sporulating sometimes produce similar levels of Spo0A-P (66). This result indicated that, in addition to Spo0A-P levels, other signals or downstream events are required to initiate sporulation. In support of this hypothesis, it was observed that sporulation can be reversed even after many *spo* genes have been activated by Spo0-P, and only becomes irreversible when the sporulation-specific mother sigma factor, σ^E, is activated following asymmetric division (67).

GTP and sporulation

Sporulation initiation has long been associated with a reduction in GTP pools (68, 69). The intracellular GTP levels decrease as cells transition from exponential to

stationary phase, and is accompanied by de-repression of genes controlled by the GTP-sensing transcriptional regulator CodY (70-73). Transcription of *kinB, phrA* and *phrB* has been shown to be repressed by active GTP-CodY (Fig. 1.2) (74), and as discussed earlier, these proteins are important for Spo0F phosphorylation during entry into sporulation (Fig. 1.2). In addition, the drop in GTP levels has an indirect positive effect on *kinA* and *kinB* transcription, independent of CodY (23).

Cell chaining and motility

Autolysins

Cell division in bacteria involves requires coordination of three major events: chromosome replication, chromosome segregation, and cell division between two chromosome-containing daughter cells. In *B. subtilis*, daughter cells may remain joined by a shared layer of peptidoglycan following division, leading to cell chains. Specific cell wall hydrolytic enzymes, called autolysins, break down the peptidoglycan layer along the septum, thereby releasing the daughter cells from each other (75). However, under certain growth conditions, dividing cells are not separated and remain joined through multiple rounds of divisions, thereby forming long chains (76).

Exponentially growing cultures of *B. subtilis* are heterogeneous and comprised of two cell types, individual motile cells and long chains of sessile cells (76). Although 35 putative autolysin genes has been found in the *B. subtilis* genome, only three autolysin

(LytC, LytD and LytF) have been implicated in the cell chaining heterogeneity (77). LytC is an N-acetylmuramoyl-l-alanine amidase that functions during vegetative growth and sporulation (78, 79), while LytD is the major glucosaminidase in *B. subtilis* and have been implicated in cell separation and certain antibiotic mediated cell lysis (80). LytF (a γ-d-glutamate meso-diaminopimelate muropeptidase) is involved in cell separation and motility (81). Interestingly, only the expression of autolysin LytF was found to be necessary and sufficient for cell separation (75).

The gene encoding *lytC* is located in a three gene operon *lytABC*. LytA is a membrane lipoprotein that is believed to be involved in LytC and LytB secretion, while LytB binds to LytC to enhance its activity (79). Transcription of *lytABC* operon requires σ^A and the alternative sigma factor, σ^D, which also regulates genes required for flagella-mediated motility. On the other hand, *lytD* and *lytF* are exclusively expressed from σ^D-dependent promoters (78, 80-82). Moreover, transcription of *lytC*, *lytD* and *lytF* peak in late exponential phase (the beginning of so-called "transition" phase) and decrease during stationary phase (79). The temporal expression of *lytC*, *lytD* and *lytF* coincide with the increased σ^D accumulation (83). σ^D "ON" cells grow as unchained, motile cells and due to the active expression of autolysin and motility genes. On the other hand, σ^D "OFF" cells do not express the autolysin or motility genes and grow as non-motile chains (75).

Autolysins, LytC, LytD and LytF have a secondary function to septal peptidoglycan breakdown which is activating motility in *B. subtilis* (77). Although the role of autolysins in motility is still unclear, three models have been suggested to explain

how autolysins are involved in motility. The first model suggest that autolysins play a role in remodeling the peptidoglycan layer to facilitate flagella penetration and/or to allow flagellum biosynthesis (84). The second model suggests that the autolysins activate motility simply by separating cells in the long chains, as chained cells might generate conflicting forces due to uncoordinated flagellar rotation (85). Lastly, Kearns and coworkers suggested that autolysins might be required for proper flagellum function (75).

Motility

Motility allows bacteria to move toward favorable environmental conditions and away from adverse conditions. The most simple kind of motility requires flagella, large, membrane-anchored, multi-protein machines that rotate to generate force like propellers (86). *B. subtilis* possesses two different kinds of motility: swimming and swarming motility. Swimming motility takes place as individual cells use flagella to move their bodies in three dimensions through an aqueous environment (87). In addition to swimming motility, *B. subtilis* moves in two dimensions on top of solid surfaces using flagella from a group of rafted cells (88). This type of behavior is called swarming motility.

Swarming motility is different from swimming motility in the following respects: swarming cells secrete a wetting agent called a surfactant, which reduces surface tension and aids cell movement (86). In addition, swarming is a social behavior, whereby cells

move as dynamic assemblages of cells called rafts (88). Finally, swarming cells possess an increased number of flagella per cell compared to swimming cells (86, 88, 89).

Flagella structure and regulation

Each flagellum is composed of more than 20 proteins that assemble into three architectural domains, the basal body, the hook, and the filament, in a highly sequential fashion (86). The basal body is embedded in the inner membrane, and functions to anchor the flagellar structure to the plasma membrane, to provide the proton motive force required for flagellar rotation, and to act as a secretion apparatus that exports the distal components during flagella assembly. The basal body is the first architectural domain assembled and consists of a stack of protein rings which are embedded in the lipid bilayer. Following assembly of the basal body rings, the secretion apparatus exports several proteins that polymerize to form the outward growing structure known as the rod. The rod extends from the basal body rings and crosses the peptidoglycan layer. Motor proteins that harvest the energy required for rotation of flagella are also found around the basal body. The hook is assembled onto the rod and extends toward the cell exterior. By acting as a flexible joint, the hook is responsible for changing the rotation angle of the helical filament that functions as a propeller. Once the hook is complete, the filament monomer protein called flagellin, is secreted and polymerizes to form the helical structure of the flagellum. Upon completion, the flagellum is capable of rotating

clockwise or counterclockwise and can extend many times the length of the cell body (90-92).

Genes that encode the flagellar proteins are located in several operons and transcribed in nearly the same order in which the functional flagellum is assembled. The gene encoding the filament protein flagellin, *hag*, is the last gene to be transcribed (90, 91). Depending on the similarity of their promoters, flagellar genes are generally grouped into three regulatory hierarchies called class I-III (Fig. 1.3) (93). Class I genes encode the master transcriptional regulators that activate the expression of Class II genes. Class II genes encodes most of the structural components that form the basal body, the secretion apparatus, and the hook. Lastly, class III genes encode the filament and the motor proteins.

In *B subtilis*, SwrA is designated as the master regulator of flagellar gene expression (Fig. 1.3) (94). However, SwrA is not required for flagellum biosynthesis, as *swrA* mutants swim but do not swarm (76). SwrA activates transcription from the large flagellar and chemotaxis operon, *fla/che*, which contains class II genes (76). Inactivation of SwrA was shown to reduce expression from the *fla/che* operon and basal body number approximately twofold. Conversely, overexpression of SwrA elevates expression from the *fla/che* operon by twofold and increases the number of flagella per cell (76, 95). Unlike the wildtype *B. subtilis* strain NCBI 3610, the domesticated laboratory strains 168 and its derivatives PY79, do not swarm due to a frame-shift mutation in *swrA* open reading frame (95). In fact, the *swrA* gene was originally identified as a spontaneous gain-of-function mutation in a laboratory strain with an

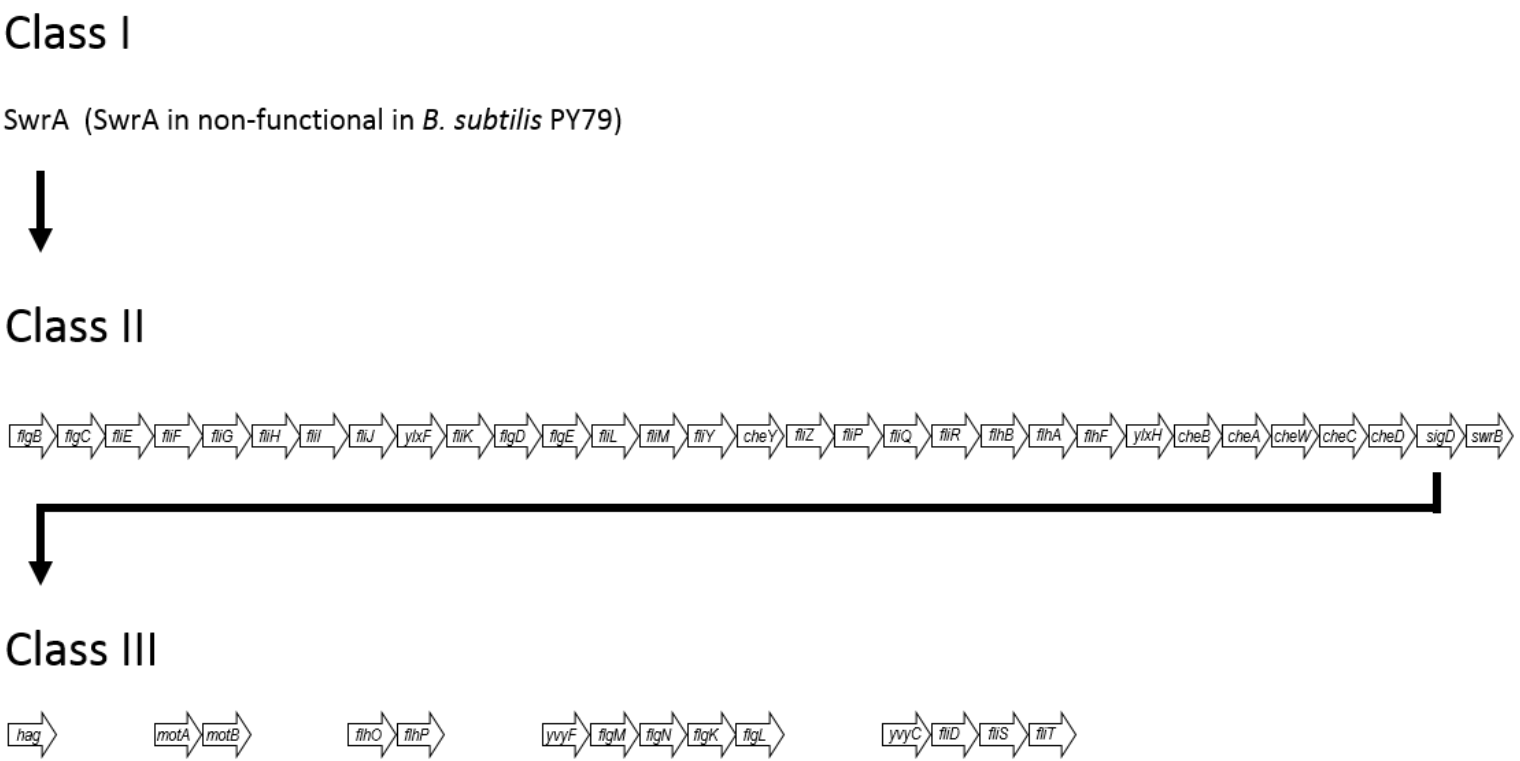

FIGURE 1.3 Hierarchical organization of flagellum assembly genes. Flagella synthesis cascade for model and Gram-positive bacterium *B. subtilis* (C) divided into class I, class II, and class III flagellar genes.

improved motility allele called *ifm* (94). The *ifm* allele restored the *swrA* open reading frame and SwrA function, resulting in an increase in the number of flagella per cell and the proportion of motile cells in the population (76, 94). Finally, SwrA is transcribed from both σ^A and σ^D -dependent promoters, and SwrA can indirectly autoactivate its own transcription via its σ^D-dependent promoter, as the *sigD* gene encoding σ^D, is found in the *fla/che* operon and is activated by SwrA (96).

Activation of the $P_{fla/che}$ promoter by SwrA is proposed to require the response regulator DegU since SwrA doesn't contain any identifiable DNA-binding motifs. Additionally SwrA mediated activation of $P_{fla/che}$ promoter is lost in cells lacking a functional DegU (96, 97). DegU is associated with the transcriptional regulation of motility, competence, biofilm formation and sporulation (98). DegU has been shown to both activate and repress flagellar gene expression depending on its phosphorylation state and concentration. Low levels of phosphorylated DegU (DegU-P) bind to an inverted repeat-like sequence upstream of the *fla/che* promoter and activate transcription (97, 99, 100). In contrast, at high levels DegU-P binds to a different inverted repeat-like sequence downstream of the *fla/che* promoter where it blocks activation of $P_{fla/che}$ (97). Interestingly, similar to *swrA* mutants, *degU* mutants do not swarm but can still swim. Furthermore, SwrA overexpression in the *degU* mutant background doesn't restore swarming motility, suggesting that either both proteins function in the same regulatory pathway or that DegU has a function that is downstream of the $P_{fla/che}$ promoter (96).

The 31-gene-long *fla/che* operon contains the gene, *sigD*, encoding the alternative sigma factor, σ^D (101). The *sigD* gene is located at the 3′ end of the operon,

25 kb away from the *fla/che* operon promoter, and its product controls the expression of several autolysins and the class III flagellar genes (75). The *fla/che* transcript level gradually decreases along the operon and the *sigD* gene position is important for determining the proportion of cells in the population with σ^D ON or OFF states. Moving the *sigD* gene closer to the start of the operon increases the number of σ^D ON cells (102). As discussed earlier, cells that have high levels of active σ^D express both the autolysin and flagellar genes and grow as separate, motile cells. In contrast, cells that have low levels of active σ^D do not express the autolysin or flagellar genes and grow as non-motile chains (75). The expression from the *fla/che* operon in the σ^D ON cells was reported to be fourfold higher than the expression detected in the σ^D OFF cells, suggesting that cells become motile if the σ^D levels exceeds a certain threshold (102). Thus, it is proposed that the position of the *sigD* gene along with noise in *fla/che* promoter activation contribute to the observed chaining and motility population heterogeneity of exponentially growing *B. subtilis* culture (92).

A small peptide called, SlrA, is responsible for the observed gradual decrease in the *fla/che* transcript level along the operon (103, 104). Overexpression of *srlA* results in *B. subtilis* cultures exclusively growing as nonmotile chains (103). SlrA has been shown to reduce *fla/che* operon transcript abundance through paralogous DNA binding proteins: SinR and SlrR (103, 105-107). SinR and SlrR control biofilm formation and SlrR is repressed by SinR. The SlrA/SinR/SlrR effect on *fla/che* operon transcript levels is suggested to occur after transcription initiation and it might involve a transcription elongation factor, a transcriptional terminator, or RNA turnover (92). Thus, SlrA-SinR-

SlrR directly inhibits the accumulation of σ^D class II flagellar proteins, and indirectly deactivates the σ^D regulon, including the class III flagellar proteins and σ^D-dependent autolysins. In addition, SinR and SlrR forms a heterodimer that binds and represses the *hag*, *lytF* and *lytC* promoters (107).

Two promoters drive transcription of the *fla/che* operon: P_{D3} and P_A (108). The σ^A-dependent P_A promoter is both necessary and sufficient for *fla/che* operon expression and motility, while the σ^D-dependent P_{D3}, which is located upstream of P_A, is not sufficient to promote motility (108, 109). Two additional σ^D-dependent promoters, P_{ylxF3} and P_{sigD}, are found within *fla/che* operon upstream of genes encoding flagellar hook components and *sigD*, respectively (104, 108, 109). The three σ^D-dependent promoters may contribute to a positive-feedback mechanism to enhance σ^D expression above the threshold required for cells to attain a σ^D ON state and become motile.

The σ^D protein is prevented from association with the RNAP polymerase until the hook–basal body assembly is completed by direct interaction with the anti-sigma protein FlgM. FlgM is exported outside the cell by components of the flagellar secretion apparatus (110-112) where it is degraded by the proteases Epr and WprA (112). Once liberated from FlgM sequestration, σ^D directs RNAP to express the gene encoding flagellin. Transcriptional regulation by FlgM serves to ensure that the biosynthesis of the energy-expensive and energy-consuming flagellum is tightly regulated and that the last components of the flagellar apparatus are not expressed until the secretion apparatus and basal body are fully assembled (112).

In addition to being regulated by secretion, FlgM autoinhibits its own expression because it has a σ^D-dependent promoter, P_{flgM}, upstream of *flgM* (113). However, this autoinhibitory regulatory mechanism is opposed through the activation of FlgM expression by DegU-P (114). Phosphorylated DegU binds to two different DNA sequences upstream of the P_{flgM} promoter (97, 115), where it functions to lower the σ^D threshold required to activate expression from the P_{flgM} promoter (114). The precise mechanism by with the σ^D threshold is lowered by DegU-P is unclear.

Intracellular signaling molecules and differentiation

Prokaryotes use nucleotide-based second messengers to regulate diverse cellular processes, including developmental decision-making. Mono-cyclic (cAMP and cGMP), di-cyclic (c-di-GMP and c-di-AMP) or linear nucleotides (ppGpp and pppGpp) play important roles in integrating many signals received from outside the cell with target molecules present inside the cell (Fig. 1.4).

Cyclic AMP and cyclic GMP

cAMP was discovered by the Nobel prize laureate Earl Sutherland in 1957 while studying the mechanism of hyperglycaemic action of epinephrine and glucagon (116). A few years later, cGMP was found in rat urine (117), but it wasn't until 1974 that cGMP was discovered in prokaryotes (118).

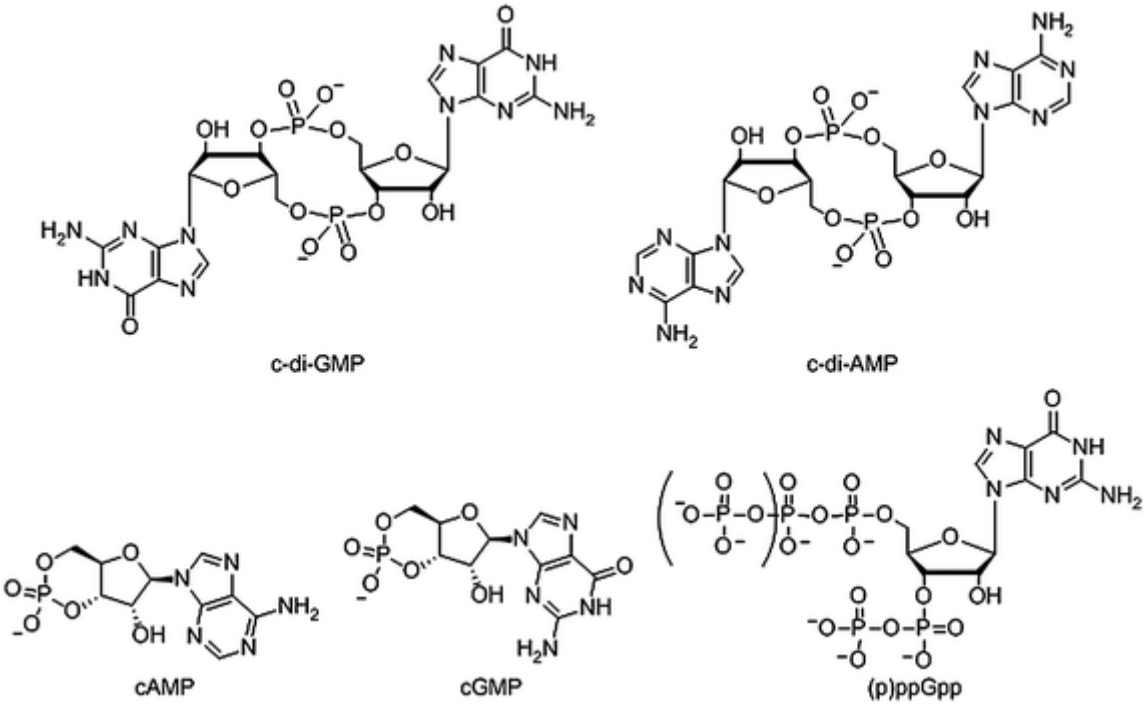

FIGURE 1.4 Structure of mono- and di-cyclic nucleotides signalling molecules in bacteria (119).

cAMP and cGMP are synthesized from ATP and GTP by adenylate and guanylyl cyclases, respectively, and are degraded back to AMP and GMP by the cAMP and cGMP specific phosphodiesterase, respectively (119). During carbon starvation in prokaryotes, cAMP activates a transcription factor, cAMP receptor protein (CRP), to alleviate catabolite repression during the utilization of alternative carbon sources (120). In addition, cyclic AMP is a central player in both direct and indirect regulation of various cellular processes including biofilm formation (121), virulence (122), flagellum biosynthesis (123) and motility (124). On the other hand, the physiological significance of cGMP signaling in prokaryotes remains largely unexplored. However, several reports indicate that cGMP might be important for survival under starvation during stationary phase (125, 126). Also, cGMP has been shown to control cyst development in the α–proteobacterium *Rhodospirillum centenum* (127).

Cyclic di-GMP and cyclic di-AMP

The ubiquitous signaling molecule c-di-GMP was discovered by Benziman and coworkers in *Gluconacetobacter xylinus* as a modulator of cellulose synthase (128). The synthesis of c-di-GMP is catalyzed by Diguanylate cyclases (DGCs) from two molecules of GTP, whereas phosphodiesterases (PDEs) breakdown c-di-GMP into pGpG or GMP (129, 130). The intracellular concentration of c-di-GMP within a cell is maintained by the balancing activities of DGCs and PDEs. The DGCs catalyze the synthesis of cyclic

di-GMP using either the GGDEF (130) or GGEEF (131) domains, whereas PDEs use either EAL (132) or HD-GYP (133) domains to hydrolyze c-di-GMP.

In bacteria, cyclic di-GMP signaling has been implicated in regulating adhesion to surfaces, biofilm formation, cell cycle, motility, virulence and others (134-136); it exerts its regulatory action by binding to a wide variety of effector proteins and receptors. The list of c-di-GMP targets includes the following: 1) PilZ domain-containing proteins, which lack any enzymatic activities, but bind to c-di-GMP to regulate enzymes and proteins through protein-protein interaction (137, 138); 2) Enzymes such as polynucleotide phosphorylase (PNPase) (139); 3) Transcription factors or repressors, such as FleQ from *Pseudomonas aeruginosa* (140), VpsT from *Vibrio cholerae* (141), Clp from *Xanthomonas axopodis* (142) and Bcam1349 from *Burkholderia cenocepacia* (143); 4) Riboswitches that regulate translation (144) or transcription (145); 5) GGDEF and/or EAL domain-containing proteins that are no longer catalytically proficient (146-149).

The most recent signaling nucleotide to be discovered was cyclic di-AMP. Hopfner and coworkers identified c-di-AMP during a structural study on DNA integrity scanning protein (DisA) from *B. subtilis* (150). Cyclic di-AMP is synthesized from two molecules of ATP by diadenylyl cyclase (DAC) domain-containing proteins and is degraded to pApA by phosphodiesterases (PDE). The most well-studied c-di-AMP synthase protein is DisA, an octameric protein from *B. subtilis* that has two functions; first, it binds DNA via its C-terminal helix–hairpin–helix DNA-binding domain (HhH) and scans DNA integrity. Second, it synthesizes c-di-AMP using the N-terminal DAC

domain (151). The DAC domain in DisA protein is connected to the HhH domain through a specific linker domain (150). Therefore, c-di-AMP synthesis by DAC domain is allosterically inhibited when the HhH domain binds damaged DNA (152). Failure to synthesize c-di-AMP in *B. subtilis* has been shown to cause a delay in sporulation (152). Moreover, c-di-AMP is suggested to play an important role in maintaining DNA integrity during various types of stresses (153). Finally, c-di-AMP has been implicated in regulating fatty acid synthesis (154), growth in conditions of low-potassium (155), and cell wall homeostasis (156, 157).

(p)ppGpp and the stringent response

In order to be able to sense and respond to changes in quality of the environment, including nutritional stress, bacteria are equipped with a multitude of response regulatory mechanisms. The global response to nutrient scarcity and environmental stress leads to a complex metabolic adjustment known as the stringent response (SR). The SR enables bacteria to divert resources from division and growth to amino acid biosynthesis; at the same time induction of stringent response leads to the expression of stationary phase genes required for survival (158, 159). The global responses associated with the stringent response are signaled by the intracellular accumulation of two small molecules, ppGpp and pppGpp, collectively referred to as (p)ppGpp (158). (p)ppGpp discovered by Cashel and Gallant while analyzing a thin layer chromatography (TLC) to analyze the nucleotide pools present in the extracts of amino acid-starved *Escherichia*

coli (160). (p)ppGpp appeared as two spots on the TLC plate and were termed "magic spots" (MSI and MSII, pppGpp and ppGpp, respectively).

For years, SR was thought to only be activated during amino acid starvation. However, later work demonstrated that SR is also activated during under conditions of limited phosphate (161) fatty acids (162) carbon (163), nitrogen (164) and iron (165), suggesting that SR is a general response to nutrient status.

(p)ppGpp metabolism

The cellular concentration of (p)ppGpp is governed by the activities of a diverse family of RelA/SpoT Homologues enzymes (RSH enzymes) (Fig. 1.5). RelA and SpoT are the enzymes responsible for (p)ppGpp accumulation in *E. coli* (166). In bacteria, the RSH enzymes are typically found in two forms: larger bifunctional enzymes with both (p)ppGpp synthase and hydrolase activities termed long RSH, and smaller monofunctional enzymes with only synthase activity referred to as small alarmone synthases (SASs) (167). Although it has not yet been identified in bacteria, a third kind RSH was found in eukaryotes that possesses hydrolase activity only and is referred to as a small alarmone hydrolases (SAHs) (168).

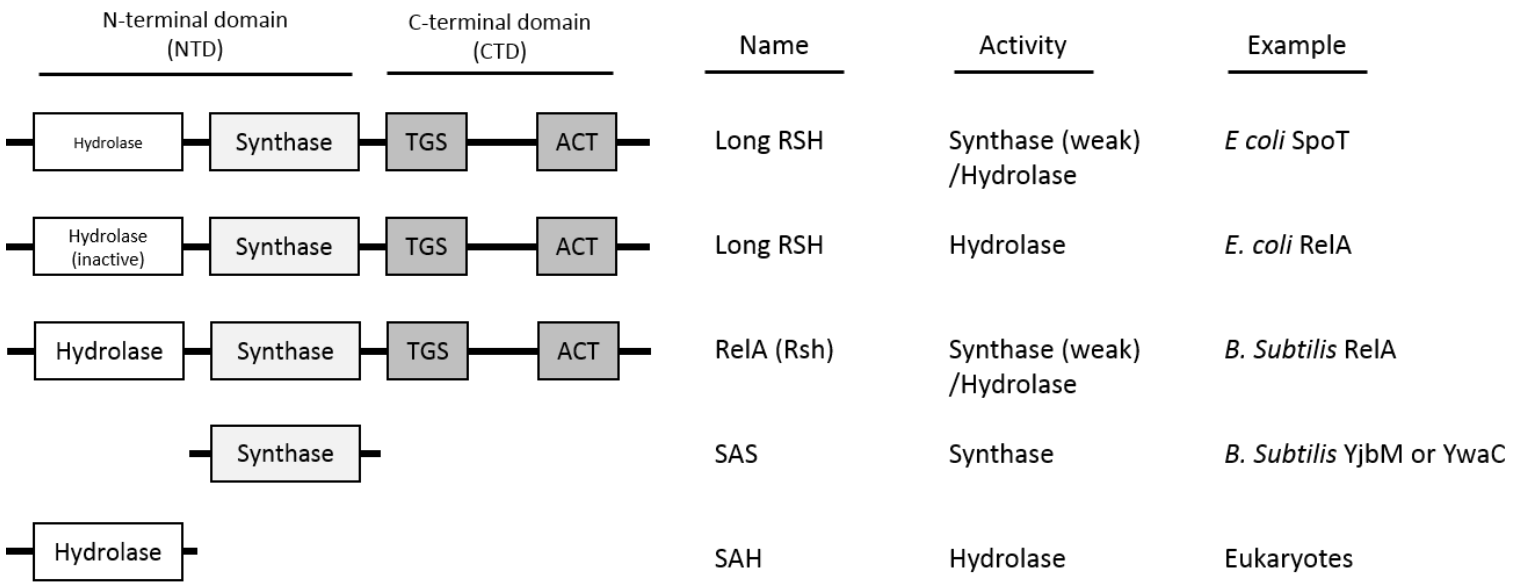

FIGURE 1.5 (p)ppGpp metabolic enzymes domain organization**.** RSH: RelA/SpoT Homologue; SAS: Small alarmone synthases; SAH: Small alarmone hydrolases; ACT: Aspartokinase, chorismate mutase, and TyrA; TGS: Threonyl-tRNA Synthetase, GTPase, and SpoT.

The bulk of the SR studies have been carried out in the Gram-negative model organism *E. coli*. In *E. coli*, the cellular concentration of (p)ppGpp is governed by the activities of by two enzymes, RelA, a monofunctional synthase, and SpoT, a bifunctional hydrolase-synthase enzyme (166). RelA is ribosome-associated and is activated when the ribosome stalls on a messenger RNA at the acceptor site due to the lack of a charged amino-acyl-tRNA (169). Active RelA is released from the ribosome and utilizes GTP and ATP to generate numerous molecules of pppGpp, which are rapidly converted to ppGpp (170, 171). After pppGpp synthesis, RelA rebinds the ribosome where it restarts the binding, release and pppGpp synthesis cycle (171). RelA doesn't fit into either the long RSH or SAS enzymes profiles. Despite having a similar size and structure as the bifinctional RSH enzymes, it has only a (p)ppGpp synthase enzyme activity, as the (p)ppGpp hydrolase domain is inactivated by point mutations (170). RelA has two distinct domains, the N-terminal domain (NTD), which harbors the catalytic domain and the regulatory C-terminal domain (CTD), which controls oligomerization and/or functional conformation independent of ribosome binding (172).

SpoT possesses both synthase and hydrolyase activities, however, the synthetase activity is weaker than the RelA synthase activity (158). SpoT synthesizes both ppGpp and pppGpp under various stress conditions, including fatty acid, carbon, iron, and phosphorus starvation (159). Moreover, through a manganese-dependent phosphohydrolase domain, SpoT is responsible for the hydrolysis of ppGpp to GDP and pyrophosphate (PPi), or the hydrolysis of pppGpp to GTP and PPi (162, 165, 173, 174). SpoT hydrolase activity is enhanced by interaction with the GTP-sensing protein CgtA

(175, 176). This interaction with CgtA ensures that low (p)ppGpp levels are produced during growth in nutrient-rich conditions, where GTP levels are high (177).

Over the past two decades, our understanding of the enzymes that regulate (p)ppGpp synthesis and degradation have, especially in Gram positive bacteria, has increased dramatically, beginning with a study on the RSH enzymes from the Gram positive bacterium *Streptococcus dysgalactiae.* This study revealed a new type of RSH enzyme called Rel_{seq} which possessed both strong synthase and hydrolyase activities in single polypeptide, similar to those found in the distinct *E.coli* proteins RelA and SpoT, respectively (178). This new type of RSH enzyme, which is referred to as Rsh to distinguish it, has been shown to be widely distributed among Gram positive bacteria (167). Like the *E.coli* RelA, the bifunctional Rsh of Gram-positives is responsible for (p)ppGpp accumulation during amino acid starvation and therefore is proposed to interact with a complex of ribosomes, uncharged tRNA, and mRNA (179). Since Rsh possesses both strong (p)ppGpp synthase and hydrolyase activities, it has been proposed to be responsible for modulating both the duration and the magnitude of the stringent response (159).

Genetic, biochemical and structural analysis of Rel_{seq} demonstrate that the synthase and hydrolase activities are reciprocally controlled by two distinct, mutually exclusive, conformational mechanisms (180, 181). The synthase and hydrolase functions of *E.coli* SpoT and Rsh enzymes are found to exist in two opposing states: the hydrolase-ON/synthase-OFF and the hydrolase-OFF/synthase-ON states (180, 181). The Rsh from Gram positive bacteria has a two domain structures linked by a flexible hinge.

The catalytic sites for both (p)ppGpp synthesis and degradation reside in the NTD and share an overlapping three-helix bundle which facilitates intramolecular allosteric signaling between the two sites (181). Therefore, the binding of nucleotides at either the synthase of hydrolase active site initiates structural changes that render the substrate coordination and metal cofactor unfavorable for the opposing catalytic activity (181). The Rsh CTD contains two regulatory elements: The ACT (aspartokinase, chorismate mutase, and TyrA) domain which binds small effector molecules that allosterically regulate the enzyme activities, and another domain called the TGS (Threonyl-tRNA Synthetase, GTPase, and SpoT) (159). Removal of $RelA_{Seq}$ CTD causes the (p)ppGpp synthase to be constitutively activated, suggesting that CTD might interacts with NTD to inhibit (p)ppGpp synthase activity and activate hydrolase activity (178).

The genomes of Gram positive bacteria also encode proteins with a single nucleotidyl-transferase domain necessary for (p)ppGpp synthesis (SAS domains) that lack both the regulatory CTD domain and the Mn2+-dependent hydrolase domain required for (p)ppGpp degradation (162, 182-186). RelP and RelQ from Firmicutes are the most extensively characterized SAS domain-containing enzymes (167, 182). To date, RelV from Vibro species, has been the only SAS homologue identified in the Gram-negative bacteria (184).

The physiological contribution of the newly discovered SAS enzymes is unclear. However, several studies suggest that SAS activity may be important in maintaining low basal levels of (p)ppGpp under non-stressful, balanced growth conditions, as their inactivation suppressed the slow growth phenotype caused by high basal levels of

(p)ppGpp when the Rsh hydrolase is inactivated (167, 182, 185). For example, the *S. aureus* genes, *relP* and *relQ*, were demonstrated to contribute to the essentiality of the Rsh hydrolase activity and *relP (yjbM)* and *relQ (ywaC)* genes from *B. subtilis* accumulated spontaneous mutations when the RelA is inactivated (187, 188). Finally, its suggested that SAS might be involved in (p)ppGpp synthesis under specific stress conditions such as oxidative and alkaline stress (185, 189).

Pleiotropic effects of the stringent response on cellular physiology

(p)ppGpp regulates a broad range of physiological adaptations that rely heavily on changes in transcription. Other critical cellular processes regulated by (p)ppGpp include, DNA replication, translation and metabolism. Table 1.1 provides a summary for the primary targets of (p)ppGpp in Gram-negative and Gram-positive bacteria.

(p)ppGpp effects on transcription

The most profound regulatory feature of (p)ppGpp is exerted on transcription. In *E. coli* and other Gram-negative bacteria, (p)ppGpp regulates transcription initiation by controlling RNA polymerase (RNAP) transcriptional specificity, leading to down-regulation of genes required for rapid growth, such as rRNA and tRNA genes. At the same time, it activates genes required for amino acid biosynthesis and transport, nutrient acquisition, virulence, and various stress response pathways (159). Transcriptional

regulation by (p)ppGpp is mainly accomplished through direct interactions with RNAP, or indirectly through interaction with alternative sigma factor and transcription factors (159). The direct interaction of (p)ppGpp with RNAP is dependent on the RNAP-binding transcriptional regulator DksA (190, 191). (p)ppGpp binds to an interface between the RNAP β′ and ω subunits where it acts as an allosteric modulator (192-194). DskA uses its N-terminal α- helical coil-coil tip to interact with the RNAP secondary channel, sensitizing RNAP to the effects of (p)ppGpp and reducing the stability of the promoter open complex at target promoters such as those driving transcription of rRNA and tRNA (190, 195). This promoter selectivity is due to the unique kinetic properties of the RNAP-promoter complex. As a rule, if the promoter sequence between the -10 element and transcriptional start site is GC-rich, then the RNAP-promoter complex formed at this *cis* element is inherently unstable and can be further destabilized by interaction of RNAP with both (p)ppGpp and DksA (196). Genes with promoters of this class are repressed by (p)ppGpp and DskA. On the other hand, genes with AT-rich promoter sequence between the -10 element and transcriptional start site form more stable RNAP-promoter complexes and are activated by (p)ppGpp and DskA (197). Indirect transcription regulation by (p)ppGpp also occurs through sigma factor competition. The amount of the *E. coli* housekeeping sigma factor σ^{70} bound to RNAP decreases during SR, whereas some alternative sigma factors, like σ^{S}, $\sigma^{32,}$ σ^{54}, are dependent on ppGpp for their production (198). Therefore, these alternative sigma factor compete with σ^{70} for the RNAP during SR (199). Sigma factor competition would

affects mainly rRNA and tRNA genes, which require high concentrations of σ^{70} holoenzyme due to nature of their unstable promoter-RNAP complex (196, 197).

Another indirect transcriptional control by (p)ppGpp occurs through the regulation of initiating nucleotide (iNTP) concentration (200). In Gram-negative bacteria, rRNA promoters are sensitive to small changes in the concentration of the iNTP (ATP or GTP) (201). In addition, (p)ppGpp has been shown to act as a competitive inhibitor of adenlylosuccinate synthase and IMP dehydrogenase, enzymes in the ATP and GTP biosynthesis pathways, respectively (202, 203). Finally, some studies have suggested that (p)ppGpp might compete with the iNTP for binding to the RNAP active site (204, 205).

In Gram positive bacteria, (p)ppGpp does not regulate transcription directly; instead (p)ppGpp exerts its effect indirectly by lowering the intracellular GTP levels in the cell (206). No homologue of DksA has been found in Gram-positive bacteria. Additionally, in *B. subtilis*, (p)ppGpp does not interact directly with RNAP and the (p)ppGpp binding site on RNAP from *E. coli* was found to be absent (74, 193). Thus, evidence for direct (p)ppGpp-mediated RNAP control in Gram-positive bacteria is absent.

Upon SR induction in *B. subtilis*, (p)ppGpp accumulation causes a dramatic drop in GTP and a subsequent increase in ATP pools by two mechanisms. First, GTP is

TABLE 1.1 Summary for (p)ppGpp target in Gram positive and Gram negative bacteria.

GRAM NEGATIVE	GRAM POSITIVE
TRANSCRIPTION	
RNAP DskA σ factor	GTP and CodY Transcription start site (rrn)
TRANSLATION	
GTPases IF-2 EF-G	GTPases IF-2
REPLICATION	
DNA primase (initiation step)	DNA primase (Elongation)
[GTP]	
GuaB (IMP dehydrogenase) HprT (Hypoxanthine phosphoribosyltransferase)	GmK (Guanylate kinase) HprT (hypoxanthine phosphoribosyltransferase)

consumed during (p)ppGpp synthesis, leading to a depletion of the cellular pools. Second, two key enzymes in GTP biosynthesis pathway are inhibited by (p)ppGpp (207-209). The enzymes hypoxanthine phosphoribosyltransferase (HprT) and guanylate kinase (Gmk), which catalyze transition from hypoxanthine to inosine monophosphate and GMP to GDP, respectively, are inhibited by even micromolar concentrations of (p)ppGpp (210), much lower levels than that the 1-2 mM concentrations of (p)ppGpp detected during SR (158). Thus (p)ppGpp is likely to act as a potent inhibitor of hypoxanthine phosphoribosyltransferase and guanylate kinase in vivo. (p)ppGpp mediated changes in GTP and ATP levels have two major effects on transcription. First, the lowered levels directly affect promoters which require guanine or adenine as the initiating nucleotides of transcription (23, 74, 208, 211). The *B. subtilis* ribosomal RNA (*rrn*) operons use GTP as their initiating nucleotide, therefore upon SR induction, transcription of *rrn* operons is down-regulated because less GTP is available for transcription initiation (74, 207-209). Second, many promoters are indirectly affected by the decrease in GTP levels through several mechanisms. First, promoters whose initiating nucleotide of transcription is ATP are activated because of the concomitant increase of ATP accompanying the decrease of GTP levels by (p)ppGpp (208,211). An example of such promoter are those found upstream the amino acid biosynthesis genes (208, 210, 211). Second, GTP (along with branched chain amino acids (BCAA)), acts as a co-factor of the transcriptional repressor CodY (212). In the absence of GTP, CodY undergoes a conformational change that lead to de-repression of CodY target genes (70, 213).

(p)ppGpp inhibits translation

(p)ppGpp directly inhibits the activity of the translation elongation factors EF-Tu and EF-G (214-216). (p)ppGpp also interacts with the translation initiation factor IF2 by binding to the same site as GTP, where it may interfere with the initiation complex formation (217). (p)ppGpp inhibits initiation factors when ppGpp levels become equimolar to GTP levels during SR, thus the ratio of ppGpp to GTP in the cell is important (217). In addition, ppGpp induces the expression of ribosome modulating factor, which in turn induces the formation of inactive ribosomes (218). Finally, (p)ppGpp accumulation induces degradation of both stable RNAs and ribosomal proteins (219-221).

(p)ppGpp effects on DNA replication

Inhibition of DNA synthesis during SR was originally described for *B. subtilis* and *E. coli* chromosomes (222). Subsequent studies showed that the same phenomenon occurs for other replicons such as plasmids (222). In general, (p)ppGpp mediates DNA replication inhibition at the initiation stage in *E. coli* (223), while in *B. subtilis*, (p)ppGpp was reported to inhibit replication fork elongation by interacting directly with primase (222, 224). In *E coli*, Ferullo and colleagues reported that (p)ppGpp inhibits replication initiation in a manner dependent on SeqA and Dam methylase (225). Finally,

(p)ppGpp accumulation in *S. aureus* has been shown to inhibit the activity of replication enzyme primase by binding to the active site (196).

CodY

The *B. subtilis codY* gene was first identified during a transposon screen for regulators controlling the expression of the dipeptide permease operon (*dpp*) involved in dipeptide scavenging during nutrient limitation (226). Mutations that allowed the expression of *dpp* during growth in nutrient rich conditions mapped to an operon named *cod* (control of *dpp*). The *cod* operon consists of four genes: *codVWXY*. Out of the four genes, only deletion of *codY* gene was found to be required for repression of *dpp* in nutrient-rich medium (71). Soon after, CodY was also found to be involved in regulating the histidine utilization operon (*hut* operon) and two early competence genes (227).

CodY is a global, DNA-binding transcriptional regulator that directly and indirectly controls the expression of hundreds of genes during exponential growth, primarily through repression (70, 228). CodY derepression during late exponential and early stationary phase allows expression of genes important transition phase (227). The CodY regulon include genes involved in stationary phase adaptive responses such as amino acid biosynthesis (7, 70, 73), peptide, sugar and amino acid transport (227, 229-231), protein degradation (7), carbon overflow pathways (232), genetic competence (233), antibiotic production (234), motility (235), chemotaxis (7) and sporulation (7). In addition, several stress tolerance and virulence pathways are under CodY control,

including toxin production (236, 237), DNA repair (238), antioxidant systems (237, 239), and capsule or S-layer biosynthesis (240).

CodY is highly conserved among the low G+C Gram-positive bacteria. CodY contains GTP-binding motif and a Helix-Turn-Helix (HTH) DNA-binding motif (70). The conformational change of CodY responsible for binding or release of DNA is modulated by interaction with two types of effectors, GTP and the branched chain amino acids (BCAA), isoleucine, leucine and valine (73, 212). The binding of either GTP or BCAAs alone can enhance CodY's affinity for DNA, however, the binding of GTP and BCAAs together have been shown to synergistically enhance the stability of the CodY-DNA interaction in *B. subtilis* (212). Using electrophoretic gel mobility shift assays, it was shown that isoleucine binds CodY with the highest affinity, followed by valine and then leucine (73). GTP binds to conserved residues at three putative regions in the N-terminus called G1, G3 and G4. The CodY N-terminus harbors the G1 region, while both G3 and G4 are located at C- terminus (241, 242). Unlike CodY, the GTP-binding motifs are typically found in GTPase proteins at a single domain (70). The affinity of CodY for GTP could be dramatically decreased by substituting glycine to asparagine in G1 motif, which ultimately result in reduction in the binding affinity of CodY to DNA (70). CodY monitors the nutritional status of the cell by sensing the intracellular concentration of GTP and BCAA, which are high during rapid growth in nutrient rich conditions. CodY-mediated repression of late exponential and early stationary phase genes is alleviated as BCAAs and GTP levels decrease when nutrients are limiting (243). Interestingly, CodY homologues of *Streptococcus mutans* and *Lactococcus lactis* are not

affected by the drop in GTP levels when nutrients are limited (244, 245). These homologues were found to contain a substitution of glycine to serine in the G1 motif (244, 245).

The CodY protein binds as a dimer to an AT-rich, DNA palindromic consensus sequence of AATTTTCNGAAAATT (70, 72, 228). However, DNA fingerprinting assays have shown that several CodY regulated genes have CodY-protected sequences with low homology to the consensus sequence (233, 243). Moreover, tandem overlapping CodY-binding motifs with three to five nucleotide mismatches from the consensus sequence were found in CodY regulated genes having low consensus sequence homology (246). Based on this observation, it was proposed that a 24 bp tandem consensus sequence should be included in the CodY DNA-binding consensus motif, in addition to the canonical 15-bp palindromic consensus motif (246). Other studies have also proposed to expand the CodY DNA-binding motif size to 17 or 21 bp (228, 246, 247). Finally, a mode of hierarchical expression of CodY regulated genes have been supported by a recent study (248). As cells transition from exponential to the stationary phase, GTP levels gradually drops and CodY regulated genes are de-repressed. Genes or promoters which contain CodY-bindings sites and have a weak affinity for CodY are expected to be relieved from CodY repression before genes that have sites with stronger CodY binding affinity (248).

Transcriptional regulation by CodY has been shown to occur through two distinct mechanisms. First, CodY has been shown to bind to upstream regulatory elements around the promoter region of genes, where it typically inhibits transcription initiation

(234). Second, CodY can act as a "road-block" to RNAP moving along DNA during transcription by binding to sites located downstream of the transcriptional start site (228). Binding of CodY to these downstream sites results in truncated transcripts and stimulates RNAP disassociation from the DNA (249). In summary, CodY mediated regulation of gene expression is fine-tuned by complex mechanisms that depend on the effector concentrations (GTP and BCAA) as well as the strength, number and location of the CodY binding sites.

Intersection of (p)ppGpp, GTP and CodY

CodY-dependent genes become derepressed as GTP levels fall. When (p)ppGpp rise, such as during SR, GTP levels fall due (see (p)ppGpp effects on transcription section). Therefore, intracellular GTP and is at the metabolic intersection between CodY activity and (p)ppGpp synthesis (Fig. 1.6). The relationship between CodY, GTP and (p)ppGpp has been shown to control a number of processes in Gram-positive bacteria. For example, in *B. subtilis* the ability to uptake exogenous DNA (competence) is induced through drop in GTP levels (69). In one study, it was found that a *relA* mutant, compromised in (p)ppGpp production, was exhibited higher GTP levels compared to wildtype as cells transitioned from the exponential to the stationary phase (207). The development of genetic competence, which peaks in early transition phase, was significantly lower in the *relA* mutant compared to the wildtype (207). GTP levels are reported to fall ~60-80% between exponential growth and transition phase (68), leading

the authors to hypothesize that the reduction in competence could be the result of higher GTP levels. The competence of the *relA* mutant strain was restored when CodY was inactivated or when GTP levels were dropped by the addition of decoyinine, an inhibitor of a key enzyme (GMP synthetase) in GTP synthesis pathway (250). The authors proposed that as cells exit exponential phase, the RelA-induced (p)ppGpp accumulation causes a drop in intracellular GTP levels, which in turn alleviates CodY repression of competence genes. In another example, *S. aureus* defective in the ability to induce SR was shown to be less virulent than the wildtype (251). The SR-defective *S. aureus* strain was unable to effectively reduce GTP during infection, such that the CodY-dependent repression of virulence genes was not alleviated. Virulence was fully restored when CodY was inactivated in this SR-defective *S. aureus* strain (251). Similarly, the loss of virulence in *Listeria monocytogenes relA* mutant could be restored by mutations in the *codY* gene (252).

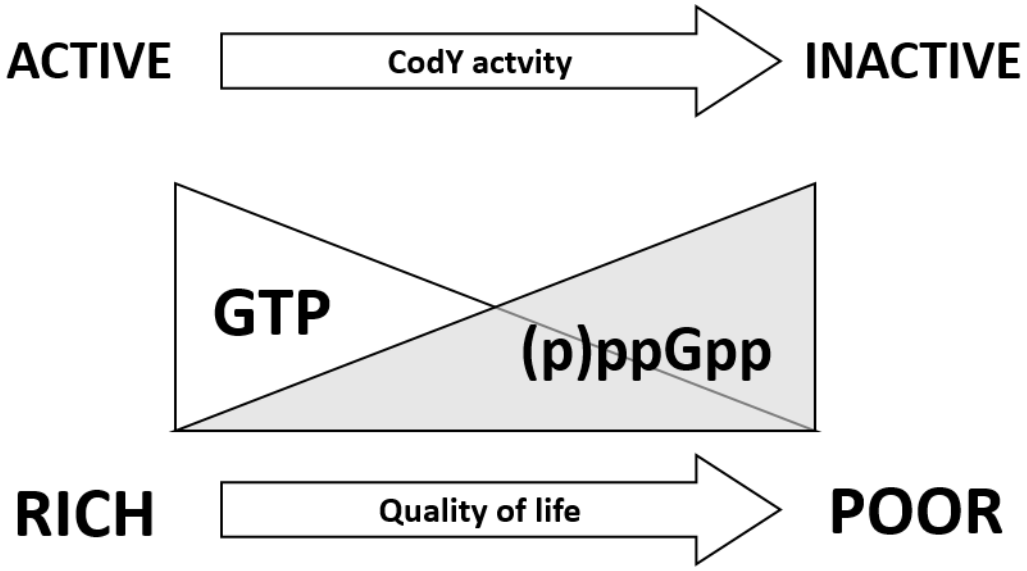

FIGURE 1.6 Simplified cartoon of the concentration dependent effects of (p)ppGpp on GTP levels and CodY activity. In *B. subtilis*, an inverse relationship exist between (p)ppGpp and GTP levels. Under nutrient rich conditions CodY is active, repressing more than 100 genes. Nutrient limitation triggers (p)ppGpp accumulation, which causes a drop in GTP levels. Subsequently, CodY regulated genes are de-repressed due to BBCA and GTP depletion, many genes involved in amino acid biosynthesis, nutrient acquisition and transport, and other stress responses are activated.

CHAPTER II

RelA INHIBITS *BACILLUS SUBTILIS* MOTILITY AND CHAINING*

Introduction

Genetic regulation makes it possible for cells possessing identical genomes to differentiate into subpopulations of phenotypically and physiologically distinct cell types. The Gram-positive bacterium *Bacillus subtilis* is an excellent model system in which to study the molecular mechanisms underlying differentiation because it produces several well-characterized cell types including spores, competent cells, biofilm formers, non-motile chained cells and motile unchained cells. These different cell types are produced through both stochastic and responsive phenotypic switching mechanisms (253-255). For example, the proportion of chained, non-motile cells versus unchained, motile cells in a culture of exponentially growing wild-type *B. subtilis* is driven by stochastic switching between the ON and OFF states of SigD (76, 104), an alternative sigma factor which drives expression of the genes responsible for daughter cell separation and motility. However, stochastic determinants are only one part of SigD regulation, as the proportion of cells in the SigD ON state also increases as cells transit* ion out of exponential growth (70, 99, 235, 256). In this study, we focus on the

* This chapter is reprinted with permission from "RelA inhibits *Bacillus subtilis* motility and chaining" by Ababneh Q. and Herman J. ,2015. *J. Bacteriol.* 197:128–137, 2015 by American Society for Microbiology.

role of a conserved, intracellular signaling molecule in triggering the switch to a SigD ON state.

The bacterial "alarmone" (also called "magic spot"), consisting of pppGpp and ppGpp (hereafter referred to as (p)ppGpp), acts as an important second messenger molecule, linking both intra and extracellular environmental cues with global changes in transcription, translation, and DNA replication (159, 199, 257). In *E. coli* and *B. subtilis*, (p)ppGpp levels are estimated to be present at levels of less than 20 pmols per optical density unit during exponential growth (158, 258-260), but rapidly rise to mM levels in response to adverse growth conditions such as amino acid starvation (158). High levels of (p)ppGpp lead to an arrest of DNA replication and cell division, reduced lipid synthesis, a global reduction in transcription and translation (159, 199, 257, 261), and increased tolerance to cell stress (257, 262, 263). Levels of (p)ppGpp are strongly correlated with growth rate (258) and ribosomal pool size (264), and one study found that various sub-stringent concentrations of (p)ppGpp regulate differential sets of genes, suggesting that (p)ppGpp concentration may be associated with graded responses in gene expression (265).

In *B. subtilis* (p)ppGpp levels are predominately determined by the net activity of RelA, a dual function (p)ppGpp synthetase and hydrolase, as well as two additional (p)ppGpp synthetase enzymes, YwaC and YjbM (185). (p)ppGpp is synthesized at low, but detectable levels during exponential growth, primarily through the activity of RelA (185). RelA is also responsible for the high levels of (p)ppGpp that accumulate in *B. subtilis* during stringent response (185, 266). Less is known about the contribution of

YwaC and YjbM activity to (p)ppGpp accumulation. *ywaC* is under the control of at least three stress response sigma factors, SigW, SigV, and SigM and encodes the protein responsible for the increase in (p)ppGpp observed during alkaline shock (185, 267-269). Based on microarray data, *yjbM* is the second gene in an operon of otherwise experimentally uncharacterized genes in *B. subtilis* (270). Expression profiles suggest that the level of *yjbM* transcription peaks during rapid growth and transition state in rich media (185, 270). In addition, YjbM contributes, albeit less substantially than RelA, to the basal levels of (p)ppGpp present during exponential growth (185).

When *relA* is deleted or depleted of a RelA variant that possesses hydrolase but not synthetase activity ($RelA_{D264G}$), *B. subtilis* grows slowly (185) and is prone to growth rate suppressors (185, 187, 209). RelA mutants have also been shown to exhibit pleotropic phenotypes including reduced competence (207) and delayed sporulation (207). Absolute levels of (p)ppGpp are likely elevated in the *relA* deletion and hydrolase mutant since these mutants lack the major activity responsible for breaking down (p)ppGpp synthesized by the remaining synthetases, YwaC and YjbM (185, 209). Consistent with the idea that (p)ppGpp levels are elevated, the slow-growth phenotype of the *relA* mutant can be complemented by introduction of an allele of *relA* that encodes only the (p)ppGpp hydrolase and through loss-of-function mutations in *ywaC* and/or *yjbM* (185). It is likely that small differences in (p)ppGpp levels during exponential growth account for the observed phenotypes; however, any variances in (p)ppGpp levels present in the *relA* mutant and wild-type during exponential growth (when stringent response is not induced) are not quantifiable using current methodologies.

In this study we show that the *relA* mutant grows exclusively as swimming, unchained cells during exponential growth phase; this unchained phenotype contrasts sharply with the wild-type, domesticated strain PY79, which exhibits a primarily chained phenotype during exponential growth in rich laboratory media (75). We also find that the *relA* mutant exhibits an accelerated swim front in a swim plate assay, consistent with the increased population of swimming cells we observe microscopically. Analysis of SigD synthesis and activity indicate that the *relA* mutant is trapped in a SigD ON state during exponential growth. Thus, our results show cell chaining and motility in *B. subtilis* is regulated by RelA through its activity as a (p)ppGpp hydrolase.

Materials and methods

General methods

The strains and plasmids used in this study are listed in Table 2.1 Sequences of primers are listed in Table 2.2 The *B. subtilis* strains used in this study were grown at 37°C in CH medium (271) or Luria-Bertani (LB) broth (10 g/L tryptone, 5 g/L yeast extract, 5 g/L NaCl). All samples were grown in volumes of either 25 ml or 50 ml in 250 ml baffled flasks in shaking waterbath set at 280 rpm. LB plates were supplemented with 1.5% Bacto agar. *Escherichia coli* strains DH5α and TG-1 were used for isolation of plasmids and were grown in LB medium. When needed, antibiotics were included at the following concentrations: 100 μg ml^{-1} spectinomycin, 7.5 μg ml^{-1} chloramphenicol,

TABLE 2.1 Strains and plasmids used in this study

Strain	Genotype	Reference
BJH001	PY79 (wild-type)	(272)
BQA003	Δ*yjbM*::*erm*	This work
BQA006	Δ*ywaC*::*erm*	This work
BQA009	Δ*relA*::*spec*	This work
BQA010	Δ*relA*::*erm*	This work
BQA022	Δ*sigD*::*tet*	(76)
BQA046	*amyE*::P_{hag}-*lacZ (cat)*	This work
BQA047	*amyE*::P_{lytA}-*lacZ (cat)*	This work
BQA050	*amyE*::P_{lytA}-*lacZ (cat)*, Δ*relA*::*spec*	This work
BQA051	*amyE*::P_{lytA}-*lacZ (cat)*, Δ*relA*::*spec*	This work
BQA057	$hag^{HagT209C}$	This work
BQA059	Δ*relA*::*spec* / Δ*sigD*::*tet*	This work
BQA062	$hag^{HagT209C}$, Δ*relA*::*spec*	This work
BQA067	*amyE*::P_{relA}-*relA (spec)*	This work
BQA068	*amyE*::P_{relA}-*relA (spec)*, Δ*relA*::*erm*	This work
BQA071	*amyE*::P_{hag}-*lacZ (cat)*, Δ*sigD*::*tetR*	This work
BQA072	*amyE*::P_{lytA}-*lacZ (cat)*, Δ*sigD*::*tetR*	This work
BQA073	*amyE*::P_{hag}-*lacZ (cat)*, *sacA*::P_{relA}-*relA (spec)*, Δ*relA*::*erm*	This work
BQA074	*amyE*::P_{lytA}-*lacZ (cat)*, *sacA*::P_{relA}-*relA (spec)*, Δ*relA*::*erm*	This work
BQA075	*sacA*::P_{relA}-*relA (spec)*, Δ*relA*::*erm*	This work
BQA076	Δ*hag::erm*	*Bacillus* Genetic Stock Center
BQA080	$hag^{HagT209C}$, *amyE*::P_{relA}-*relA (spec)*, Δ*relA*::*spec*	This work
BQA081	Δ*relA*::*spec*, Δ*yjbM*::*erm*	This work
BQA082	Δ*relA*::*spec*, Δ*ywaC*::*erm*	This work
BQA083	*amyE*::P_{hy}-*sigD (kan)*, Δ*sigD*::*tet*, Δ*relA*::*erm*	This work
BQA084	*amyE*::P_{hag}-*lacZ (cat)*, Δ*sigD*::*tetR*, Δ*relA*::*spec*	This work
BQA085	*amyE*::P_{lytA}-*lacZ (cat)*, Δ*sigD*::*tetR*, Δ*relA*::*spec*	This work
BQA086	*amyE*::P_{hag}-*lacZ (cat)*, Δ*relA*::*spec*, Δ*yjbM*::*erm*	This work
BQA087	*amyE*::P_{lytA}-*lacZ (cat)*, Δ*relA*::*spec*, Δ*yjbM*::*erm*	This work
BQA088	*amyE*::P_{hag}-*lacZ (cat)*, Δ*relA*::*spec*, Δ*ywaC*::*erm*	This work
BQA089	*amyE*::P_{lytA}-*lacZ (cat)*, Δ*relA*::*spec*, Δ*ywaC*::*erm*	This work
DS874	*amyE*::P_{hy}-*sigD (kan)*	Daniel B. Kearns
EUB004	*trpC2* Δ*relA::erm*, *aprE::Pspac-relA*$_{D264G}$ *(spec)*	(185)

TABLE 2.1 continued

Plasmid	Description	Reference
pDR111	*amyE::*P*hyperspank (spec) (amp)*	David Z. Rudner
pMiniMAD2	*ori*^{BsTs} *(amp) (erm)*	(273)
pDG1661	*amyE::lacZ (cat)*	*Bacillus* Genetic Stock Center
pJW053	Δ*yjbM::spec*	This work
pJW054	Δ*relA::spec*	This work
pJW055	Δ*yjbM::erm*	This work
pJW058	Δ*relA::erm*	This work
pJW063	Δ*ywaC::spec*	This work
pJW064	Δ*ywaC::erm*	This work
pKM079	*B. subtilis chromosomal integration vector (spec)*	David Z. Rudner
pKM082	*B. subtilis chromosomal integration vector (erm)*	David Z. Rudner
pQA014	*amyE::*P$_{lytA}$*-lacZ (cat)*	This work
pQA015	*amyE::*P$_{hag}$*-lacZ (cm)*	This work
pQA017	*hag*^{HagT209C}	This work
pQA020	Δ*amyE::P*$_{relA}$*-relA (spec)*	This work

TABLE 2.2 Oligonucleotides used in this study

Primer	Sequence (5' to 3')
oJW052	GGCCGGCCGTGCTCTTCCTTTCCGCCCTGT
oJW053	CATGTCGACTCCCCCAATTCCGAACCAGTT
oJW054	GCAGGATCCGGTAAAGGGGAAGAAGAGCATG
oJW055	GATGAATTCTCCGCCCAGCGCCTTATT
oJW056	GAACGGCCGGGCTTTATTATCGGCTGTCCC
oJW057	CAAGTCGACTTCGTTCGCCATGGAATCACC
oJW058	GTCGGATCCTAAAGGGGTTAGAAAAGAGATTAGTTG
oJW059	CAAGAATTCCCAAGAAAAAGTAACAGATGG
oJW066	GATCGGCCGTCTTGTCGGCGCGATTAA
oJW067	AGAGTCGACCATGTTCGTCATCTCCTTTAA
oJW068	GAAGGATCCTAAAAAAGACGGCACCCA
oJW069	CTCGAATTCCTATGTAGATCATCTATCGGA
oQA063	CAGTCGAATTCTGAAGGGGATCAAGTGAAGC
oQA064	GATAAGGATCCCGCTGCAATATTGTGGTTA
oQA065	CAGTCGAATTCAGTATGCATAGCCGCCAGTT
oQA066	GATAAGGATCCGCAACCCGAAAGAAGCAATA
oQA077	AGGAGGAATTCTCTCCGCATTATCCTCACAAAAAAAG
oQA078	GCATCGAAACCGATATCAGCACAATCTGCTGCATTATCTGC
oQA079	GCAGATAATGCAGCAGATTGTGCTGATATCGGTTTCGATGC
oQA080	CTCCTGGTACCTGAGGAATGATTAGGAGATAGAAATTT
oQA094	CAGTCGAATTCCCTTGACGGCAGAAATAAGC
oQA095	GATAAGGATCCACGACCTCTTCGTCCACTGT

10 µg ml^{-1} tetracycline, and 1 µg ml^{-1} erythromycin (erm) plus 25 µg ml^{-1} lincomycin (MLS), for *B. subtilis* strains; 100 µg ml^{-1} ampicillin, for *E. coli* strains.

Swim plate assay

B. subtilis strains were grown at 37°C in baffled flasks containing CH media to mid-log phase. The cells were pelleted and resuspended at an OD_{600} of 10 in PBS (137 mM NaCl, 2.7 mM KCl, 10 mM Na_2HPO_4, 2 mM KH_2PO_4) containing 0.5% India ink (Higgins). Ten µl of the cell suspension were spotted on the top of 150 x 15 mm LB plates fortified with 0.25% Bacto agar (100 ml/plate), dried for 30 min at room temperature on the benchtop to allow time for absorption, and incubated at 37°C in a loosely covered glass dish containing paper towels soaked with water to generate humid conditions. The swim radius was measured relative to the edge of the origin marked by the India ink.

Microscopy

All fluorescence microscopic analyses were performed with a Nikon Ti-E microscope equipped with a CFI Plan Apo lambda DM 100X objective, and Prior Scientific Lumen 200 Illumination system, C-FL UV-2E/C DAPI, C-FL GFP HC HISN Zero Shift, and C-FL Texas Red HC HISN Zero Shift filter cubes, and a CoolSNAP HQ2 monochrome camera. Membranes were stained with either TMA-DPH (0.02 mM)

or FM4-64 (3 µg ml^{-1}) (Life Technologies) and imaged with exposure times of 200-800 msec. All images were captured, analyzed, and processed using NIS Elements Advanced Research (version 4.10) and Adobe Photoshop (version 12.0).

Flagella were visualized by using the cysteine reactive dye Alexa Fluor 488 C_5 maleimide (Life Technologies) using the method described by (33). Briefly, 1 ml samples of mid-logarithmic cultures were collected at an OD_{600} of 0.5 and cells were pelleted by centrifugation. The pellet was then washed with 1 ml of PBS (137 mM NaCl, 2.7 mM KCl, 10 mM Na2HPO4, and 2 mM KH2PO4), resuspended in 50 µl of PBS containing 5 µg ml^{-1} Alexa Fluor 488 C_5 maleimide, and incubated at room temperature for 5 min. Cells were then washed twice with 0.5 ml PBS. The pellet was resuspended in 50 µl of PBS containing 5 µg ml^{-1} FM4-64 and on a glass slide with a poly-L-lysine (Sigma) treated coverslip.

Western blot analysis

B. subtilis strains were grown to logarithmic growth phases (OD_{600} of 0.4 to 0.7) and 1 or 2 ml samples were collected. Cells were pelleted by centrifugation and resuspended in 50 µl lysis buffer [20 mM Tris pH 7.0, 10 mM EDTA, 1 mg ml^{-1} lysozyme, 10 µg ml^{-1} DNase I, 100 µg ml^{-1} RNase A, with 1 mM PMSF] and incubated 15 min at 37°C. Fifty µl of sample buffer [0.25 M Tris pH 6.8, 4% SDS, 20% glycerol, 10 mM EDTA] containing 10% 2-mercaptoethanol was added to the lysates and the samples were boiled for 5 min prior to loading. Proteins were separated by SDS-PAGE

on precast 4-20% Tris-HCl gels (Bio-Rad), transferred onto nitrocellulose membrane (Pall) at 100 volts for 1 hr in transfer buffer [20 mM Tris, 15 mM glycine and 20% methanol (v/v)] and then blocked in 5% nonfat milk in PBS containing 0.5% Tween-20. Membranes were incubated overnight at 4°C with a 1:5,000 dilution of α-SigD peptide antibody (CIRDDKNVPPEEKIM, Genscript), 1:20,000 dilution of α-SigA (provided by Masaya Fujita, University of Houston), or 1,40,000 α-Hag antibody (provided by Daniel B. Kearns, Indiana University), and washed and incubated with 1:10,000 dilution of horseradish peroxidase-conjugated goat anti-rabbit immunoglobulin G (Bio-Rad). After washing, blots were incubated with SuperSignal West Femto Chemiluminescent substrate (Thermo), according to the manufacturer's instructions.

Flagellin labeling

B. subtilis strains were grown to logarithmic growth phase (OD_{600} of 0.5) and 1 ml samples were collected. Samples were labeled with Alexa Fluor 488 C_5 maleimide labeling as described under microscopy (above) and cell lysates were prepared for SDS-PAGE analysis as described in immunoblot analysis. Proteins were separated by SDS-PAGE on precast 4-20% Tris-HCl gels (Bio-Rad), and visualized by scanning the gels with the Typhoon Trio (GE Healthcare) at 100 μm resolution and an excitation wavelength of 488-nm.

β-galactosidase assays

To assay expression from *lacZ* transcriptional fusions, *B. subtilis* strains were grown at 37°C in baffled flasks containing CH media. One or 2 ml samples were harvested at an OD_{600} of 0.5 by centrifugation in a tabletop, room temperature centrifuge and cell pellets were frozen at -20°C or -80°C. To perform the assays, pellets were thawed on ice and resuspended in 500 µl of Z buffer (40 mM NaH2PO4, 60 mM Na2HPO4, 1 mM MgSO4, 10 mM KCl and 38 mM β-mercaptoethanol, 0.2 mg ml^{-1} lysozyme) and incubated for 15 min at 30°C. The reaction was started by adding 100 µl of 4 mg ml^{-1} O-nitrophenyl β-d-galactopyranoside (in Z buffer) and stopped with 250 µl of 1 M Na2CO3 after a yellow color developed. The optical density of the reaction mixtures was measured at 420 and 550 nm and used to calculate the β-galactosidase specific activity according to the equation: 1000 X [(OD420-(1.75XOD550))/(time × OD600)].

Results

The relA *mutant grows slowly, but exponentially in liquid culture*

Previous studies showed that replacement of *B. subtilis relA* with an antibiotic resistance cassette leads to a slow-growth phenotype. *relA* is in an operon with *dtd* (270), encoding D-amino acid tRNA deacylase (274, 275), an enzyme that removes D-

amino acids from mischarged tRNAs. In order to test if the slow-growth phenotype was attributable to loss of *relA* alone and not due to polar effects on *dtd*, we introduced Δ*relA* into a strain harboring an intact copy of *relA* and its putative promoter region at an ectopic locus (*amyE::*P_{relA}-*relA*) and examined the growth rate of the resultant strain. The Δ*relA* mutant grew more slowly than wild-type on LB plates, consistent with previous reports (185) (Fig. 2.1A). We determined the Δ*relA* mutant also grew more slowly than wild-type in liquid culture (Fig. 2.1B) with a generation time in liquid CH medium at 37°C of 50 min compared to 30 min for wild-type (Fig. 2.1A). Introduction of *amyE::*P_{relA}-*relA* into the Δ*relA* strain complemented the slow-growth phenotype on both plates and in liquid media (Fig. 2.1A and 2.1B), indicating that the slow growth phenotype was solely attributable to the loss of *relA* and not related to polar effects on *dtd*. Despite the slower generation time of the Δ*relA* mutant, the linear phase of exponential growth mirrored that of wild-type, showing a decrease in rate around an OD_{600} of 0.8 to 1.0. This result suggests that the cues triggering the transition out of exponential growth are intact in the Δ*relA* mutant background.

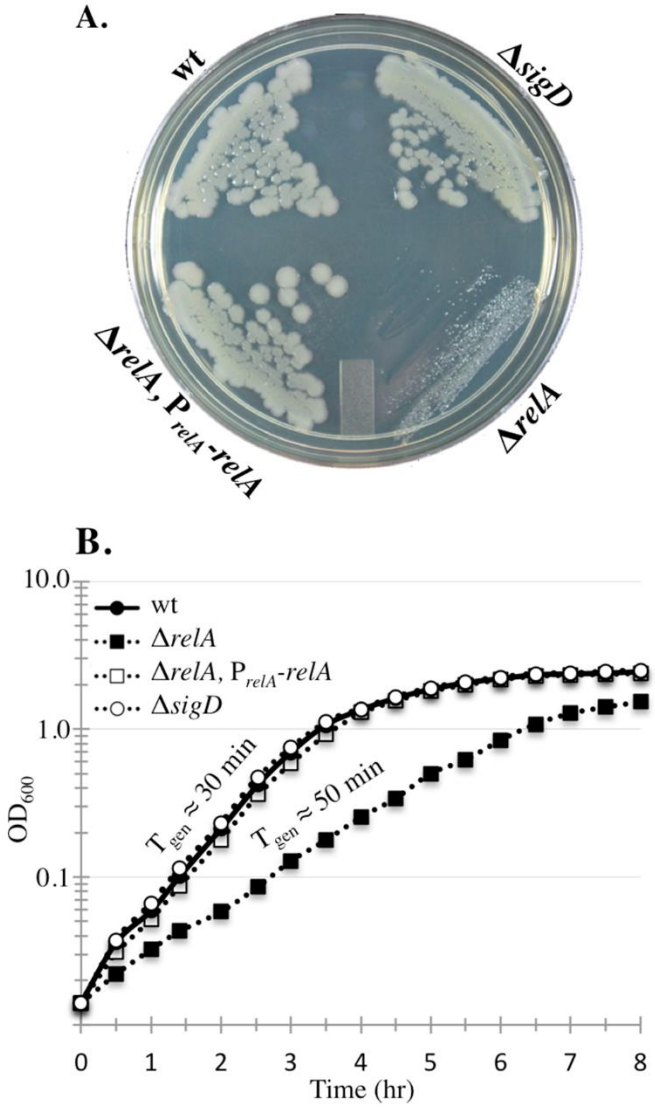

FIGURE 2.1 The *relA* mutant grows slowly and exponentially**.** (A) The indicated strains were streaked on an LB plate incubated for 24 hrs at 37°C. (B) Growth curves of the same strains shown panel 1A grown in liquid CH medium. The average of three independent replicates is plotted for each strain. Wt (BJH001); Δ*relA* (BQA009); Δ*relA*, P_{relA}-*relA* (BQA068); Δ*sigD* (BQA022).

The slow-growing Δ*relA* mutant was previously shown to be prone to the accumulation of growth rate suppressors in *ywaC* and *yjbM*, two other (p)ppGpp synthetase genes (185, 187, 209). When constructing and growing the Δ*relA* strain, we also observed that spontaneous growth rate suppressors arose frequently on plates; sequencing of these suppressors revealed the faster growing strains always possessed mutations in *ywaC* and/or *yjbM* (data not shown), consistent with prior reports (185, 187, 209). Since the Δ*relA* mutant frequently accumulates growth rate suppressors in *ywaC* and *yjbM*, the restoration of wild-type growth we observed in the presence of *amyE::* P_{relA} -*relA* could be attributable to the accumulation of one or more suppressor mutations in these genes as opposed to true complementation. To rule out this possibility, we sequenced the *ywaC* and *yjbM* regions of the complemented Δ*relA* mutant and found the regions encoded the wild-type alleles (data not shown).

A ΔrelA *mutant grows exclusively as unchained cells*

While examining the role of RelA in sporulation, we fortuitously observed that the Δ*relA* mutant grew as a homogeneous population of unchained cells during exponential growth in rich media (Fig. 2.2A and 2.2B). This unchained phenotype is in sharp contrast to PY79, the wild-type, domesticated strain used in this study, which grows as a mixed population of 85% chained and 15% unchained cells under the same growth conditions (Fig. 2.2A and 2.2B). The chaining phenotype was restored in the

relA complementation strain and sequencing of genomic DNA from the same culture pictured in Fig. 2A confirmed that *ywaC* and *yjbM* had not accumulated suppressor mutations. These results indicate that the unchained phenotype is due to the absence of the *relA* gene product and not due to polar effects on *dtd*. Moreover, an inducible allele of *relA* that encodes the (p)ppGpp hydrolase activity, but lacks synthetase activity (D264G substitution in RelA) (185), restored not only wild-type growth rate as previously observed (185), but also the cell chaining in a Δ*relA* background (Fig. 2.2A). In contrast, depletion of $RelA_{D264G}$ in the Δ*relA* background resulted in growth as single cells (Fig. 2.2A). This result is consistent with the unchained phenotype being attributable to the loss of RelA's (p)ppGpp hydrolase function. The presence of chains in all *relA* mutant cultures examined throughout this study correlated with growth rate suppressor mutations in the other (p)ppGpp synthetases (data not shown). Therefore, we found the distinctive, non-chaining phenotype of the *relA* mutant served as a convenient marker to monitor the integrity of *relA* mutant strains used in our experiments. To determine if the unchained phenotype could be attributed to the slow-growth of the Δ*relA* mutant as opposed to a RelA-dependent activity, we examined wild-type cells grown at room temperature in identical media at room temperature. Wild-type cells grown at room temperature had a generation time of ~50 min, comparable to the *ΔrelA* mutant, but grew primarily as chained cells (data not shown), suggesting that slower growth rate alone does not account for the unchained phenotype.

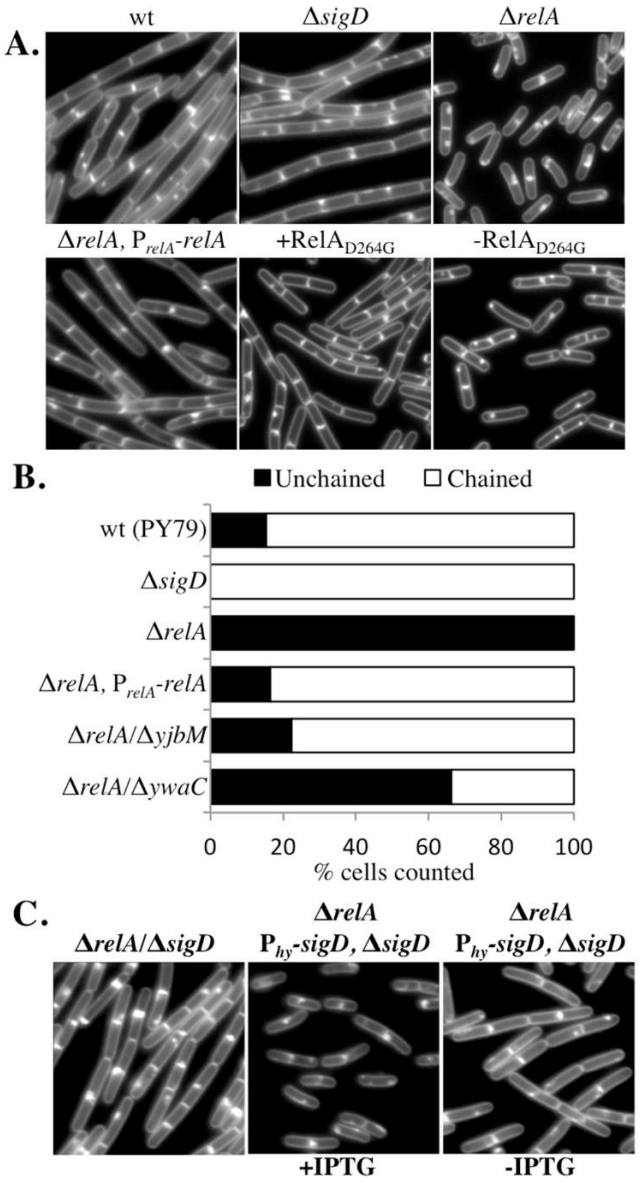

FIGURE 2.2 The Δ*relA* mutant grows exclusively as single cells. (A) Representative images of wt (BJH001), Δ*relA* (BQA009), Δ*relA*, P_{relA}-*relA* (BQA068), Δ*sigD* (BQA022), and P_{spac}-$relA_{D264G}$ (EUB004) cells grown to mid-log in CH medium. For EUB004, cells grown in the presence (+$RelA_{D264G}$) and absence (-$RelA_{D264G}$) of 1 mM IPTG for 120 min are shown. Membranes were stained with TMA. (B) Frequency of chained (three or more cells linked) and unchained (single and doublet) cells across a population. Images from at least three independent cultures were counted and no less than 1,500 cells were quantitated for each strain represented in the graph. (C) Representative images of Δ*relA*/Δ*sigD (*BQA059) and Δ*relA,* P_{hy}-*sigD,* Δ*sigD (*BQA083) cells grown to exponential phase in CH medium. Membranes were stained with TMA.

Deletion of ywaC ***or*** yjbM ***in a*** ΔrelA ***mutant restores cell chaining during exponential growth***

The Δ*relA* mutant lacks the major (p)ppGpp hydrolase activity, so synthesis of (p)ppGpp from YwaC and/or YjbM should lead to a net accumulation of (p)ppGpp in a Δ*relA* mutant background (185). We hypothesized that the unchained phenotype we observed in the Δ*relA* mutant might be due to increased (p)ppGpp levels. Since the basal levels of (p)ppGpp present in the wild-type and Δ*relA* mutant backgrounds fall outside the linear range of detection, we tested this idea genetically using (p)ppGpp synthetase mutants. We hypothesized that if higher levels of (p)ppGpp resulted in loss of chaining, then the Δ*relA*/Δ*yjbM* and Δ*relA*/Δ*ywaC* double mutants should be more chained than the Δ*relA* single mutant. We observed that in comparison to the wild-type (85% chained) and *relA* mutant strain (0% chained), the Δ*relA*/Δ*yjbM* and Δ*relA/*Δ*ywaC* were 78% and 34% chained, respectively (Fig. 2.2B). These results are consistent with the idea that accumulation of (p)ppGpp promotes the switch from chained to unchained cells and also suggest that YjbM is a more significant contributor to (p)ppGpp pools during exponential growth than YwaC.

The proportion of chained versus unchained cells in a population varies with strain and culture conditions, and was previously shown to be regulated by the level of an activated form of the alternative sigma factor, SigD (104). Active SigD stimulates transcription of several genes including the cell wall amidase LytF that promotes post-septational hydrolysis of the peptidoglycan connecting daughter cells (81). As

previously shown, a *sigD* mutant grows exclusively as chains (Fig. 2.2A and 2.2B). In order to determine if the unchained phenotype observed in the *relA* mutant was dependent on SigD activity, we generated a Δ*sigD*/Δ*relA* double mutant by introducing Δ*relA* into the Δ*sigD* background using transformation. We observed, using control DNA, that transformation efficiency of the Δ*sigD* mutant was less than 10% of wild-type. For unknown reasons, the efficiency of introducing the Δ*relA* mutation into the Δ*sigD* mutant was even lower, such that we were only able to obtain one transformant after 15 attempts. In contrast, Δ*relA* could be readily introduced into Δ*sigD* background harboring a copy of P_{relA}-*relA* at an ectopic locus. These results hinted that the combination of Δ*sigD*/Δ*relA* could be synthetically lethal. To further test this idea, we introduced Δ*relA* into a SigD depletion strain in which the only copy of *sigD* is under control of an IPTG regulated promoter. To test for synthetic lethality, the resulting strain was inoculated on media with and without inducer. Surprisingly, the strain grew similar to the Δ*relA* parent on plates whether *sigD* expression was induced with IPTG or not (data not shown). This result suggests that the reduced transformation efficiency we observed is not due to synthetic lethality, rather a reduced ability to obtain transformants. Consistent with this, whole-genome sequencing of the viable Δ*sigD*/Δ*relA* mutant revealed no second-site suppressor mutations. Microscopic analysis of the Δ*sigD*/Δ*relA* mutant revealed an intermediate chaining phenotype different from either the Δ*sigD* or Δ*relA* single mutants (Fig. 2.2C). Moreover, the SigD depletion strain harboring the Δ*relA* mutation appeared similar to Δ*relA* when SigD was expressed (Fig. 2.2C), and

similar to Δ*sigD*/Δ*relA* when SigD was depleted (Fig. 2.2C). These results indicate that SigD is required for the homogenous single-cell phenotype of the Δ*relA* mutant.

The ΔrelA *mutant displays flagella on the cell surface*

We observed that the unchained *relA* mutants observed by microscopy (Fig. 2.2A) appeared highly motile in wet mounts (data not shown), indicating that the unchained cells also possessed active flagella. As mentioned previously, accumulation of active SigD leads to the upregulation of genes responsible for the separation of chained cells into single cells (76, 79, 81, 85). Active SigD also coordinately upregulates synthesis of late flagellar genes (276), including *hag*, the gene encoding flagellin (277). We hypothesized that since the *relA* mutants appeared exclusively unchained and motile by microscopy, the *relA* mutant would also be associated with more flagella than wild-type. In order to directly visualize flagella on intact cells, we engineered strains harboring a HagT209C change in the flagellin subunit, incubated intact cells with a cysteine-reactive dye that stains surface-exposed cysteine residues, and imaged the flagella using epifluorescence microscopy using methodology described previously (276). The *relA* mutant was unchained (as observed in Fig. 2.2A and 2.2B) and presented numerous peritrichous flagella (Fig. 2.3B). In contrast, our wild-type strain grew both as unchained cells that presented flagella and chained cells that generally lacked flagella (Fig. 2.3B). We were unable to quantitate the number of flagella present on the cell surfaces due to difficulty resolving individual filaments

amongst the dense mass on the cell surface. In addition, we observed the presence of significant numbers of shed flagella in the samples that made it difficult to resolve if the flagella were cell-associated. We believe that the shed flagella likely break off due to the sheer forces required to wash and centrifuge the samples during the cysteine labeling (see below). We conclude that the presence of flagella on the surfaces of the unchained *relA* mutant cells suggests that SigD is more active in this strain background compared to wild-type grown under identical conditions.

Although the use of cysteine-reactive dye to observe *B. subtilis* flagella was previously published (276) and we found no fluorescent signal was associated with wild-type cells lacking HagT209C (data not shown), we performed an additional control to visualize the complement of protein species labeled the with cysteine-reactive dye. Intact cells were treated with dye as they would be prior to microscopy, then subjected to SDS-PAGE electrophoresis and laser scanning. A predominant band emitting in the green channel and running at the approximate molecular weight of the flagellin monomer (32 kDa) was present in strains harboring HagT209C for wild-type, the *relA* mutant, and the *relA*-complemented strain, but the band was absent from the flagellin mutant (*Δhag)* and the wild-type PY79 strain which lacks the HagT209C variant (Fig. 2.3B). The amount of flagellin varied greatly even between identical strains in independent trials, despite the fact that samples were normalized by optical density; total protein staining confirmed that approximately equal amounts of protein were loaded for each sample (Fig. 2.3B). We believe the variability seen in flagellin levels is due to shearing of the flagella during the sample handling required for the labeling reaction.

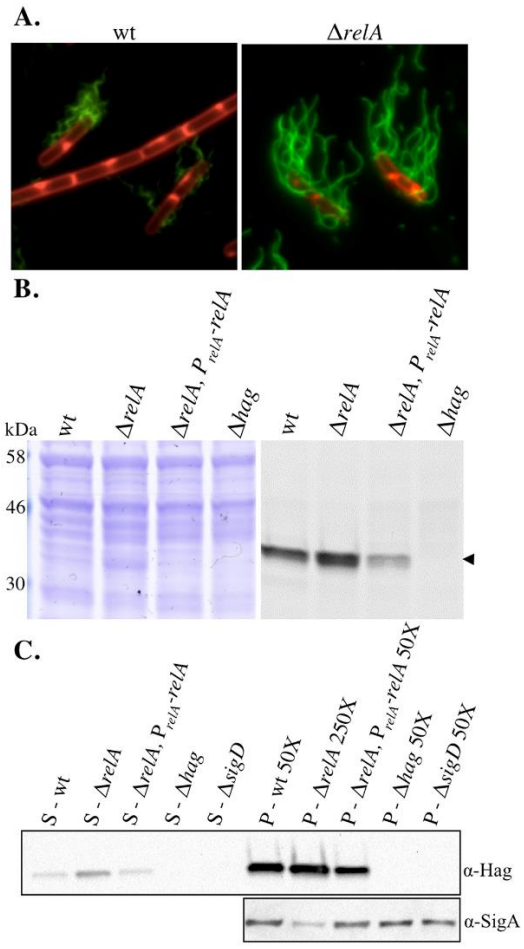

FIGURE 2.3 The *relA* mutant is comprised of mostly flagellated cells. (A) Representative images of mid-log cultures of wt (BQA057) and Δ*relA* (BQA062). Membranes are stained with FM4-64 (red) and flagellin (Hag) is stained with Alexa Fluor C_5 488 maleimide (green). Both strains harbor a point mutation in the chromosomal copy of hag that creates HagT209C. (B) Comparison of flagellin (Hag) protein levels in wt (BQA057), Δ*relA* (BQA062), Δ*relA, P_{relA}-relA* (BQA080) and Δ*hag* (BQA076). Samples were collected from mid-log cultures grown in CH media and stained with Alexa Fluor C_5 488 maleimide. Proteins from cell lysates were separated by SDS-PAGE, stained with coomassie (left panel), and scanned with a laser scanner to visualize fluorescently-labeled protein (right panel). Arrowhead indicates flagellin. (C) Western blot analysis showing flagellin levels (top blot) associated with the culture supernatants (left - S) and cell pellets (right - P) of the indicated strains grown in CH medium to mid-log. wt (BJH001), Δ*relA* (BQA009), Δ*relA*, P_{relA}-*relA* (BQA068), Δ*sigD* (BQA022) and Δ*hag* (BQA076). It was necessary to dilute the cell pellet lysates to the indicated dilutions in order to assess the levels of protein associated with each sample without overexposure. SigA protein serves as a loading control for the cell pellet samples (bottom blot).

We conclude that the fluorescence observed by microscopy is due primarily to labeled flagella, and that while analysis of labeled proteins using SDS-PAGE followed by laser scanning is useful for determining the apparent molecular weight of stained proteins, but is not useful as a quantitative measure of total flagellin levels in *B. subtilis*.

The ΔrelA ***mutant produces more flagellin than wild-type***

In order to quantitate the amount of flagellin associated with the *relA* mutant relative to wild-type, we collected cells and supernatants from exponentially growing cultures and examined flagellin levels using western blot analysis (Fig. 2.3C). The supernatants were collected so we could also assess flagellin that might accumulate in the supernatants due to shedding, shearing, or cell lysis. A predominant band running at the approximate molecular weight of the flagellin monomer (32 kDa) was present in both supernatants and cell lysates of wild-type, the *relA* mutant, and the *relA*-complemented strain, but was absent from the flagellin mutant (Δ*hag)* and the *sigD* mutant (Δ*sigD).* The amount of flagellin associated with the supernatants was negligible compared to the amount associated with the cell bodies, so it was necessary to dilute the cell body lysates 50-fold to visualize all of the samples on the same western blot without overexposure (Fig. 2.3C). Since the amount of flagellin present in the supernatant was minor compared to the cell bodies, we did not analyze this data further. The amount of flagellin present in the wild-type control and the complemented *relA* strain was similar with each of four independent trials and indicated no statistically significant difference

in flagellin levels. The *relA* mutant, in contrast, showed a five-fold increase in flagellin levels compared to wild-type, and it was necessary to dilute the sample five-fold to avoid overexposure (Fig. 2.3C). The SigA antibody serves as a loading control confirming that the diluted sample is loaded in the *relA* mutant lane. These results are consistent with what we observe microscopically (Fig. 2.3A) and suggest that the unchained *relA* mutant population consists primarily of flagellated cells in a SigD ON state.

The ΔrelA *mutant strain exhibits increased mobility on swim plates*

Since the *relA* mutant population is composed exclusively of unchained, flagellated cells we expected that it would also produce a more motile population compared to wild-type. The laboratory strain used in this study (PY79) does not swarm (278), a type of surfaced-based group motility usually facilitated by a bacterially-produced surfactant (278, 279). Therefore, in order to obtain a quantitative assessment of the motility behavior of the population, we performed a swim plate assay, which utilizes a lower concentration of agar and does not require surfactant production (86). All cultures were grown to mid-log (~0.5 OD) spotted in equal volumes and densities on swim plates. The visible edge of the culture, which we refer to as the "swim front" was measured relative to the edge of the original spot over a timecourse (Fig. 2.4A). An example of a swim plate at a 3.5 hr timepoint is shown in Fig. 2.4B. The absolute distance between the edge of the original spot and the swim front (the "swim radius") varied slightly from assay to assay (standard deviations are shown in 2.4A); however,

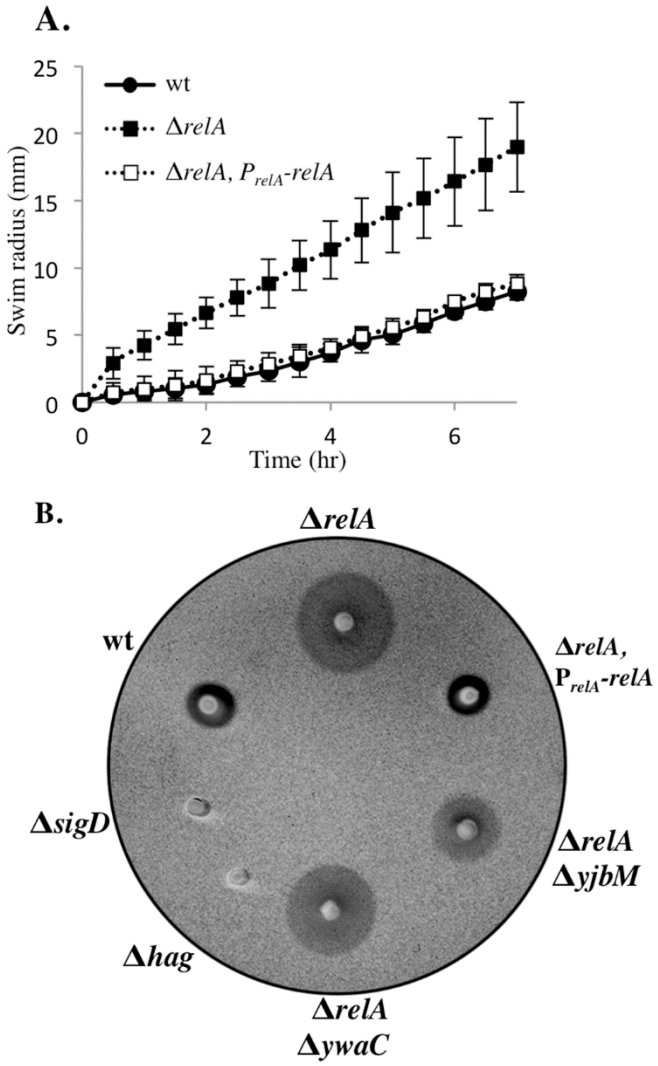

FIGURE 2.4 Loss of *relA* leads to increased mobility on swim plates. (A) Quantitation of swim expansion from plate assays performed with wt (BJH001), Δ*relA* (BQA009) and Δ*relA*, P_{relA}-*relA* (BQA068) on LB fortified with 0.25% of agar. Each symbol indicates the average of measurement from five independent experiments with standard deviations. Measurements were recorded every 30 min for 8 hrs. (B) wt (BJH001), Δ*relA* (BQA009); Δ*relA*, P_{relA}-*relA* (BQA068), Δ*sigD* (BQA022), Δ*hag* (BQA076), Δ*relA*/Δ*yjbM* (BQA081) and Δ*relA*/Δ*ywaC* (BQA082) strains were inoculated on LB fortified with a 0.25% of agar. After 3.5 h incubation at 37°C, the plates were scanned against a black background. The images were inverted to better show contrast.

the maximal rate of migration, calculated from linear regions of the data in Fig. 2.4A, remained essentially constant from experiment to experiment.

The *relA* mutant exhibited two notable phenotypes in the swim plate assay. First, unlike wild-type which exhibited an ~2 hr lag before reaching its maximal swim front migration rate of 2.8 mm/hr, the *relA* mutant had a constant migration rate throughout the course of the experiment (30 min to eight hr) of 4.9 mm/hr. Wild-type cells from exponential cultures, early transition phase (OD_{600} of 1.2), and mid-transition phase (OD_{600} of 1.9) all exhibited similar lags (data not shown). Lag periods for swarming have also been observed previously and may represent a physiological adjustment to growth on a more solid surface (279). The second observable phenotype was that the maximal migration rate of the *relA* mutant was 4.9 mm/hr, significantly faster than that of wild-type at 2.8 mm/hr. The complemented *relA* strain behaved similarly to wild-type (Fig. 2.4A). These results suggest that both the absence of the lag period and the overall increase in maximal swim front migration rate can be attributed to RelA function. As expected, the swim front of strains deficient in either SigD (Δ*sigD*) or flagellin (Δ*hag*) production did not migrate a measurable distance from the culture origin (Fig. 2.4B). The SigD and flagellin non-swimming controls exhibit wild-type growth rates in liquid culture (Fig. 2.1A and data not shown), suggesting that growth rate has little effect on the distance traveled by the swim front in the eight hr timecourse. We conclude that, consistent with the unchained and flagellated phenotype we observed microscopically, the *relA* mutant population is poised to swim during exponential growth phase.

The increased chaining we observed in the Δ*relA*/Δ*yjbM* and Δ*relA*/Δ*ywaC* double mutants (Fig. 2.2C) is consistent with a shift toward a SigD OFF state relative to the *relA* single mutant. If there is reduced SigD activity in the double mutants, then we would also expect a decrease in their ability to swim compared to the *relA* single mutant. To test this hypothesis, we assayed the swim front migration of the Δ*relA*/Δ*yjbM* and Δ*relA/*Δ*ywaC* strains. We observed that both the Δ*relA/*Δ*ywaC* and Δ*relA*/Δ*yjbM* strains possessed smaller swim radii than the Δ*relA* parent alone, but larger radii than wild-type (Fig. 2.4B and 2.5A). The Δ*relA/*Δ*ywaC* strain, which possesses an intact copy of exponentially expressed *yjbM*, consistently exhibited a larger swim radius than the Δ*relA*/Δ*yjbM* strain (Fig. 2.4B and 2.5A), indicating that it more closely resembles the Δ*relA* strain than Δ*relA*/Δ*yjbM*. These results are consistent with the idea that the switch from non-motile (SigD OFF) to motile (SigD ON) states are promoted by increasing (p)ppGpp levels; at the same time, we do not rule out the possibility that the switch is stimulated by another mechanism unrelated to (p)ppGpp accumulation.

Loss of* relA *leads to an increase in SigD levels and activity

The *relA* mutant grows exclusively as unchained, motile cells during exponential growth, consistent with the hypothesis that the *relA* mutant will possess higher levels of active SigD than wild-type during exponential growth. In order to test this hypothesis, we first examined the levels of SigD protein by performing western blot analysis on strains grown to mid-log phase (~0.5 OD). Relative to wild-type, the *relA* mutant

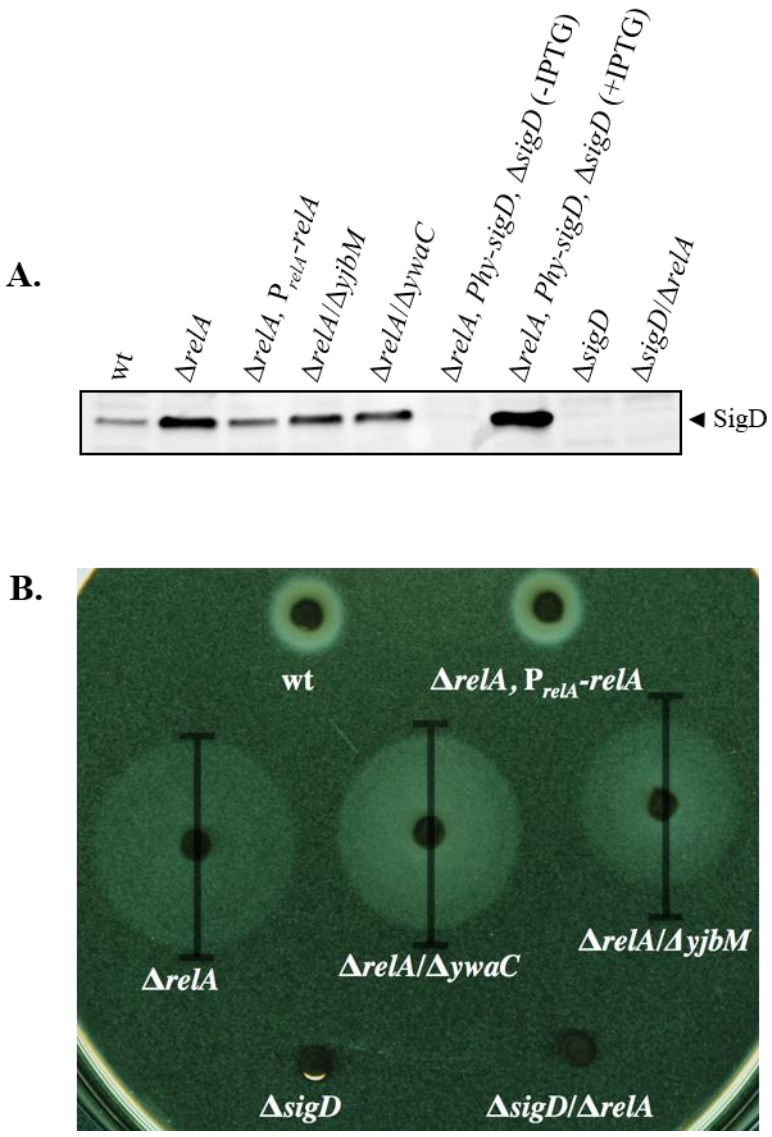

FIGURE 2.5 SigD levels and swimming motility in (p)ppGpp synthetase mutants. (A) Comparison of SigD protein levels in the indicated strains. The SigD depletion strain was grown in the absence (-) or presence (+) of IPTG to regulate *sigD* expression. (B) Swim plate expansion assay. Indicated strains were \inoculated on LB fortified with a 0.25% of agar. After 3.5 h incubation at 37°C, the plates were scanned against a dark background. A scale bar (no units) is drawn through the middle of each swim colony to aid in relative size comparisons.

consistently showed a nearly 10-fold increase in SigD levels (Fig. 2.6A). Approximately wild-type SigD levels were restored in the *relA* complementation strain (Fig. 2.6A), indicating that the increase in SigD levels in the *relA* mutant are due to the absence of a functional RelA protein. We conclude that a RelA-dependent function is required to prevent the accumulation of SigD protein during exponential growth.

Although SigD protein levels are correlated with SigD activity, the relationship is not linear, and several levels of post-translational regulation ultimately determine actual SigD activity (102, 279). In order to determine if the increase in SigD levels we observed also corresponded to an increase in SigD activity, we analyzed expression from two SigD-dependent promoters using transcriptional fusions to a *lacZ* reporter gene. Based on the unchained, flagellated phenotype, the increase in mobility observed on swimming plates, and the increase in SigD abundance, we expected that the *relA* mutant would exhibit significantly higher levels of SigD activity compared to wild-type. The results of β-galatosidase assays performed on samples collected from mid-log growth (~0.5 OD) are shown in Fig. 2.6B. As expected, both P_{hag}, the flagellin promoter and P_{lytA}, which drives expression of proteins important for flagellar activation through peptidoglycan hydrolysis (79), showed significantly higher levels of transcription in the *relA* mutant compared to the wild-type control. The increased expression in the *relA* mutant was dependent on the presence of *sigD* (Fig. 2.6B, Δ*relA*/Δ*sigD*). In contrast, expression was reduced to approximately wild-type levels in the *relA*-complemented strain. The Δ*relA*/Δ*yjbM* and Δ*relA*/Δ*ywaC* mutants exhibit intermediate levels of SigD activity (Fig. 2.6B), consistent with the intermediate chaining (Fig. 2.2B) and swimming

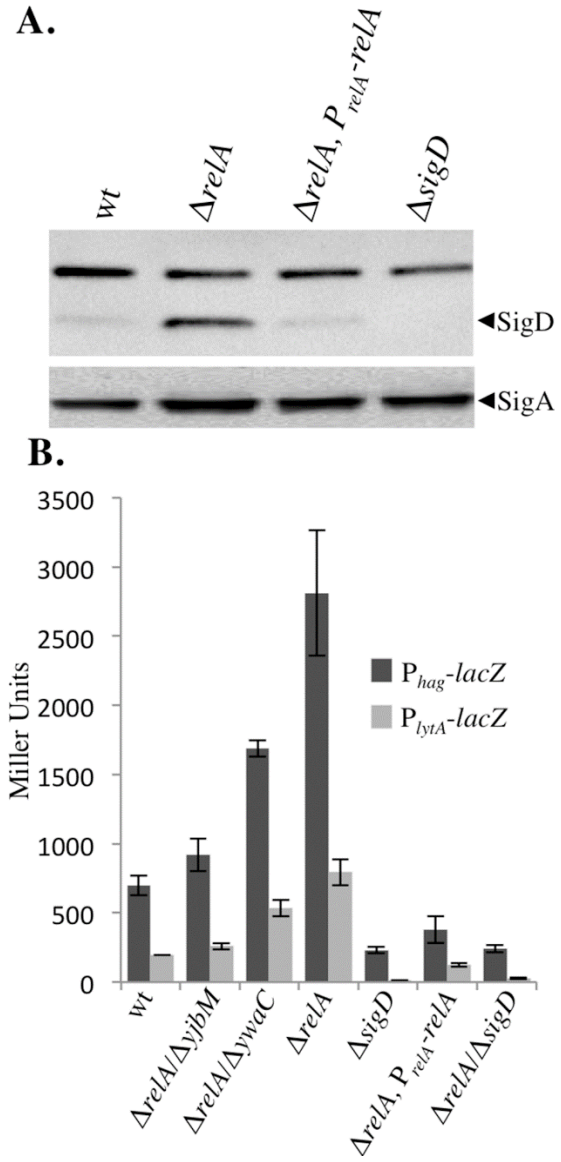

FIGURE 2.6 Loss of *relA* leads to an increase in SigD levels and activity. (A) Comparison of SigD protein levels in wt (BJH001), Δ*relA* (BQA009), Δ*relA,* P_{relA}-*relA* (BQA068) and Δ*sigD* (BQA022). Samples were collected from mid-log cultures grown in CH media. Proteins from cell lysates were separated by SDS-PAGE and analyzed by western blot analysis by probing with either anti-SigD or anti-SigA antibodies as indicated. (B) β-galactosidase assays of P_{hag}-*lacZ* and P_{lytA}-*lacZ* transcriptional activities conducted on wt (BJH046 and BJH047), Δ*relA* (BQA050 and BQA051); Δ*relA/*Δ*yibM* (BQA086 and BQA087), Δ*relA/*Δ*ywaC ((*BQA088 and BQA089)*,* Δ*sigD* (BQA071 and BQA072), Δ*relA,* P_{relA}-*relA* (BQA073 and BQA074) and Δ*relA/*Δ*sigD* (BQA084 and BQA085). Samples were collected from mid-log cultures grown in CH media. Data shown is the mean of three independent replicates with standard deviations.

motility (Fig. 2.3B) phenotypes we observed. We conclude that a RelA-dependent activity regulates the amount of active SigD that accumulates during exponential growth phase and that the Δ*relA* mutant is shifted to a SigD ON state during exponential growth.

Discussion

Nucleotide second messengers like ci-d-GMP, cAMP, and the bacterial "alarmone" (p)ppGpp are well-characterized examples of intracellular signaling molecules that serve important roles in modulating gene expression in response to environmental and physiological fluxes in bacteria (2, 119, 257). (p)ppGpp is responsible for the global down-regulation of transcription, translation, DNA replication, and growth rate that occurs during the stringent response to amino acid limitation (159, 199, 257). In more recent years, (p)ppGpp has been implicated in a number of non-stringent processes, including virulence (280-282), persister cell formation (283-285), biofilm production (286), maintaining balanced growth rate (287), and regulating GTP pools in response to nutrient downshift (210).

A role for (p)ppGpp in modulating cell motility has also been previously reported for several Gram-negative bacteria including *Vibrio cholera* (288), *Legionella pneumophila* (289), *and E. coli* (290-292). For example, (p)ppGpp and the regulatory protein DksA have been shown to act directly on flagella biosynthesis promoters to negatively regulate flagella production during *E. coli* stationary phase growth (292). In this study, we observe that a *B. subtilis relA* mutant deficient for (p)ppGpp hydrolysis

(185) grows as a homogeneous population of unchained, motile cells during exponential growth in rich media, a time when our wild-type laboratory strain is predominantly chained and non-motile. These results suggest that increased (p)ppGpp levels or decreased GTP levels promote differentiation of *B. subtilis* (Fig. 2.7).

Since the levels of (p)ppGpp present in the strain backgrounds and growth conditions presented in this study fall outside the current quantitative detection range, we tested our model genetically using (p)ppGpp synthetase mutants. We found that the increase in cell motility (Fig. 2.4B) and loss of cell chaining (Fig. 2.2B) directly correlates with the (p)ppGpp levels predicted to be produced in Δ*relA (highest)*, Δ*relA/*Δ*ywaC* (intermediate), and Δ*relA/*Δ*yjbM* (lowest) mutants during exponential growth (Fig. 2.2 and Fig. 2.7). In contrast, the increase in cell motility and loss of chaining inversely correlates with the GTP levels measured in the Δ*relA (lowest)*, Δ*relA/*Δ*ywaC* (intermediate), and Δ*relA/*Δ*yjbM* (highest) backgrounds {Nanamiya, 2008 #32). Our data also demonstrate that a Δ*relA* mutant has elevated levels of SigD activity compared to wild-type (Fig. 2.6B), consistent with the homogeneous population of unchained and flagellated cells we observed microscopically. These results support a model in which (p)ppGpp levels act as a modulator of SigD activity and, subsequently, cellular differentiation (Fig. 2.7). More specifically, our data suggest that even slight increases in (p)ppGpp may promote a SigD ON activation state during the exponential growth phase (Fig. 2.7). The absence of RelA activity clearly has a profound effect on bacterial decision making, dramatically shifting the bias of exponentially growing *B.*

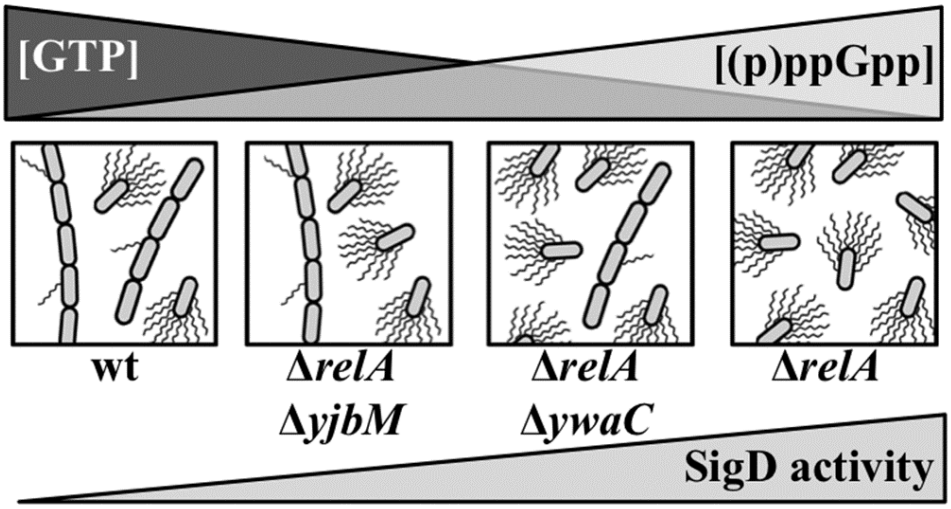

FIGURE 2.7 Model depicting the observed relationships between cell motility and chaining, SigD activity, GTP concentration, and putative (p)ppGpp levels in various (p)ppGpp synthetase/hydrolase backgrounds.

subtilis cells from a non-motile, chained wild-type population (85%) to a homogeneous population of unchained, motile cells in the Δ*relA* mutant (Fig. 2.2A and 2.2B).

How might changes in (p)ppGpp levels and/or a decrease in GTP levels promote the activation of the SigD and thus promote the increased frequency of unchained, swimming cells we observed in *relA* mutant backgrounds? SigD activity is regulated at the level of protein synthesis (102) and by being held in an inactive state through the action of the anti-sigma factor FlgM (110, 111). We showed that compared to wild-type, SigD is both more abundant and more active in the *relA* mutant (Fig. 2.6A and 2.6B). Since the global regulator DegU has been shown to repress SigD production (99) and promote FlgM synthesis (114) determining the role of DegU in the single cell, swimming phenotype we observed is a potential avenue for future investigations.

Interestingly, we observed that a Δ*relA/*Δ*sigD* mutant does not grow as long chains like the *ΔsigD* parent (Fig. 2.2C). This result suggests that the absence of *relA* is promoting activation of some SigD-independent autolysins (77). One attractive idea that could explain both the Δ*relA* and the Δ*relA/*Δ*sigD* phenotype is that elevated (p)ppGpp levels in *B. subtilis* may promote sigma factor switching, such has been reported in *E. coli* (293-295). In *E. coli*, (p)ppGpp has been shown to bind to RNA polymerase, and, in concert with DksA, directly regulate gene transcription (158). *B. subtilis* lacks a known DksA homolog, and direct regulation of RNA polymerase by (p)ppGpp has not been observed (74, 193).

The *B. subtilis* Δ*relA* mutant harbors reduced levels of GTP (185, 209), which may also contribute to the motile, unchained phenotype we observed. (p)ppGpp synthesis affects GTP levels through at least two independent mechanisms. First, GDP, GTP and ATP are the substrates for (p)ppGpp synthetic enzymes and (p)ppGpp synthesis is correlated with a subsequent drop in GTP levels (70, 74, 158, 207). Second, a recent study in *B. subtilis* showed that (p)ppGpp can also negatively regulate cellular GTP levels by binding directly to two key enzymes in the GTP synthesis pathway, HptR and Gmk, thereby negatively regulating their ability to synthesize GMP and GDP precursors, respectively (210).

It is possible that lower GTP levels present in the *relA* mutant may relieve transcriptional repression of some promoters in the *SigD* regulon through CodY derepression. CodY is a GTP-sensing protein that binds DNA and positively or negatively regulates the expression of over 100 *B. subtilis* gene products (228).

Although CodY has been shown to repress expression from *hag* (235), a recent global analysis found no evidence for binding of CodY to the *hag* promoter in vivo (228).

Previous studies also show that transcription can be affected by shifts in the GTP and ATP pools of cells. In *B. subtilis* undergoing stringent response through amino acid starvation, (p)ppGpp and ATP levels rise, while GTP levels fall (208, 210). Promoters beginning with +1G are apparently particularly sensitive to GTP pools, as GTP is rate-limiting for initiation (23, 208). Therefore, is is possible that the lower GTP levels of the *relA* mutant lead to decreased expression from +1G promoters. Both of the *fla*/*che* promoters P_{D-3} and P_A, which regulate the bulk of *sigD* expression, begin with a +1A (109), while the *flgM* promoter begins with a +1G (208).

In summary, our results show that during exponential growth, RelA activity leads to a modulation of gene expression in *B. subtilis* and support the idea that even minor fluxes in (p)ppGpp levels may greatly influence cellular decision making. More specifically we show that the *B. subtilis* Δ*relA* mutant is trapped in a SigD ON state, biasing cells toward a motile, unchained phenotype during exponential growth; future experiments will be aimed at elucidating the molecular mechanisms underlying this developmental outcome.

CHAPTER III

CodY REGULATES SigD LEVELS AND ACTIVITY BY BINDING TO THREE SITES IN THE *fla/che* OPERON

Introduction

Genetically identical populations of bacteria often exhibit phenotypic heterogeneity, possessing cells that switch between distinct physiological and/or developmental states. Phenotypic switching is most widely understood in the context of highly regulated responses to changes in environmental cues, such as nutrient status and cell density. However, phenotypic switching can also occur spontaneously, and stochastic switching between two stable phenotypes at the subpopulation level is termed phenotypic bistability (253, 296). Bistability likely confers a selective advantage to a species during unpredictable environmental conditions by increasing the chance that at least one alternative cell state will survive any given adverse condition (296-298). For example, in a given population of antibiotic-sensitive bacteria, small subpopulations of genetically identical, yet non-growing and antibiotic-tolerant bacteria known as "persisters" are detectable (285, 299). Since the persister subpopulation is non-growing, it is able to survive a sudden onslaught of antibiotic selection.

Exponentially growing populations of *Bacillus subtilis* are comprised of both chained, non-motile cells and unchained, motile cells presumably poised for dispersal (76). The two cell types differ from each other at the level of gene expression. More

specifically, motile cells have higher levels of active SigD, an alternative sigma factor that promotes expression of the genes responsible for flagellar assembly and cell separation (75, 76). During exponential growth, the switch between SigD "ON" and SigD "OFF" states is stochastic and exhibits bistability (102, 300). SigD levels also increase as cells exit exponential growth, reaching a maximum during the transition phase, suggesting that SigD expression is tightly linked to nutrient status and/or cell density cues (256).

In a previous study, we found that the proportion of chained, non-motile versus unchained, motile cells in exponentially growing *B. subtilis* cultures can be manipulated by introducing mutations that alter GTP levels (301). More specifically, we found that a Δ*relA* mutant harboring reduced levels of intracellular GTP (185, 209) is trapped in a SigD "ON" state, with 100% of the population exhibiting the unchained, motile phenotype. Mutants with GTP levels intermediate to wildtype and the Δ*relA* mutant exhibited intermediate chaining and motility phenotypes (301). These results suggested that GTP might be an important intracellular signal controlling SigD regulation. In this study, we investigated the idea that the GTP-sensing protein, CodY (70), previously shown to bind to promoters that regulate flagellin expression (P_{hag}) as well as promoters upstream of the *fla/che* operon (P_{D3} and $P_{fla/che}$) (235), might be responsible for mediating the shift between non-motile and motile cell states we observed in the Δ*relA* mutant background.

In the present work, we found that deletion of *codY* increases the proportion of unchained, motile cells in an exponentially growing population from 15% to 75%. We

also found that SigD levels in the Δ*codY* mutant are comparable to those produced by the Δ*relA* mutant, suggesting that CodY represses *sigD* expression. Using electrophoretic mobility shift assays, we found that CodY binds to three sites located in the *sigD*-containing *fla*/*che* operon and that point mutations in any one of these three binding sites results in production of SigD protein at levels comparable to the Δ*relA* and Δ*codY* mutants. These results suggest that the *fla*/*che* operon may be finely tuned to detect even small changes in GTP status. Lastly, we found that mutations in all three CodY binding sites were required to phenocopy the 75% unchained phenotype of the Δ*codY* mutant, suggesting that CodY binding in the *fla/che* operon may also be important for the post-translational regulation of SigD activity.

Materials and methods

General methods

The *B. subtilis* strains, plasmids are listed in Table 3.1 and oligos are listed in Table 3.2. All strains were grown in 250 ml baffled flasks in a shaking water bath (280 rpm) at 37°C in CH medium (Sterlini and Mandelstam 1969) or Luria-Bertani (LB) broth (10 g/L tryptone, 5 g/L yeast extract, 5 g/L NaCl), as indicated. To make solid media plates, CH and LB were supplemented with 1.5% (w/v) Bacto agar. All *Escherichia coli* strains were grown in LB medium. *E.coli* DH5α was used for isolation of plasmid DNA and cloning. Plasmids used to generate point mutations were isolated

from *E.coli* TG-1. *E.coli* BL21(λDE3) was used for protein overexpression. For *B. subtilis* natural transformation, cells were grown in MC medium (10.7 g K_2HPO_4, 5.2 g KH_2PO_4, 20 g dextrose, 0.88 g sodium citrate dehydrate, 2.2 g L-glutamic acid monopotassium salt, 1 ml of (2.2%) ferric ammonium citrate, and 1 g casein hydrolysate per 1000 ml). When appropriate, antibiotics were added to the growth media at the following concentrations: 100 µg/ml spectinomycin, 7.5 µg/ml chloramphenicol, 10 µg/ml tetracycline, and 1 µg/ml erythromycin plus 25 µg/ml lincomycin (mls), for *B. subtilis* strains; and 100 µg/ml ampicillin, for *E. coli* strains.

Strains and plasmid construction

PY79 genomic was used to amplify PCR products for cloning. All marked deletion strains were confirmed by PCR. To mutate the CodY binding sites, the region upstream of each binding site was PCR-amplified using the following primer pairs: P_{D3} site, oQA150/151; *fliE*, oQA154/155; *fliK*, oQA158/159. Similarly, the region downstream of each binding site was PCR-amplified using the following primer pairs: P_{D3} site, oQA152/153; *fliE*, oQA156/157; *fliK*, oQA160/161. The two PCR products for each binding site were used as template for overlap extension PCR using the following primer pairs: P_{D3} site, oQA150/153; *fliE*, oQA154/157; *fliK*, oQA158/161. The amplified fragments were gel-purified, digested with EcoRI and KpnI and cloned into pMiniMAD cut with the same enzymes. The resulting plasmids pQA23 (D_{mu}), pQA23 (E_{mu}) and pQA23 (K_{mu}) were introduced into the PY79 background by single cross-over

TABLE 3.1 Strains and plasmids

Strain	Genotype	Reference
BJH001	PY79 (wild-type)	[265]
BQA003	*ΔyjbM::erm*	(301)
BQA006	*ΔywaC::erm*	(301)
BQA009	*ΔrelA::spec*	(301)
BQA010	*ΔrelA::erm*	[294]
BQA022	*ΔsigD::tetR*	[294]
BQA046	*amyE::Phag-lacZ (cat)*	[294]
BQA047	*amyE::PlytA-lacZ (cat)*	[294]
BQA050	*amyE::Phag-lacZ (cat), ΔrelA::spec*	[294]
BQA051	*amyE::PlytA-lacZ (cat), ΔrelA::spec*	[294]
BQA067	*amyE::PrelA-relA (spec)*	[294]
BQA068	*amyE::PrelA-relA (spec), ΔrelA::erm*	[294]
BQA076	*Δhag::erm*	Bacillus Genetic Stock Center
BQA081	*ΔrelA::spec, ΔyjbM::erm*	[294]
BQA082	*ΔrelA::spec, ΔywaC::erm*	[294]
BQA090	*ΔcodY::erm*	Bacillus Genetic Stock Center
BQA091	*ΔcodY::erm, ΔrelA::spec*	[294]
BQA092	*ΔyjbM::cat*	[294]
BQA093	*ΔywaC::cat*	[294]
BQA094	*ΔyjbM::cat, ΔrelA::spec*	[294]
BQA095	*ΔywaC::cat, ΔrelA::spec*	[294]
BQA096	*ΔyjbM::cat , ΔrelA::spec, ΔcodY::erm*	This work
BQA097	*ΔywaC::cat, ΔrelA::spec, ΔcodY::erm*	This work
BQA102	*amyE::Phag-lacZ (cat), ΔcodY::erm*	This work
BQA103	*amyE::PlytA-lacZ (cat), ΔcodY::erm*	This work
BQA106	Dmu	This work
BQA107	Emu	This work
BQA108	Kmu	This work
BQA109	Emu Kmu	This work
BQA110	Dmu Emu	This work
BQA111	Dmu Kmu	This work
BQA112	Dmu Emu Kmu	This work

TABLE 3.1 continued

Plasmid	Description	Reference
pDR111	*amyE::Phyperspank (spec) (amp)*	David Z. Rudner
pMiniMAD2	*oriBsTs (amp) (erm)*	[266]
pDG1661	*amyE::lacZ (cat)*	Bacillus Genetic Stock Center
pET-24b(+)	expression vector (kan)	Novagen
pJW053	*ΔyjbM::spec*	[294]
pJW054	*ΔrelA::spec*	[294]
pJW055	*ΔyjbM::erm*	[294]
pJW058	*ΔrelA::erm*	[294]
pJW063	*ΔywaC::spec*	[294]
pJW064	*ΔywaC::erm*	[294]
pKM079	B. subtilis chromosomal integration vector (spec)	David Z. Rudner
pKM082	B. subtilis chromosomal integration vector (erm)	David Z. Rudner
pQA014	*amyE::PlytA-lacZ (cat)*	[294]
pQA015	*amyE::Phag-lacZ (cm)*	[294]
pQA020	*amyE::PrelA-relA* (spec)	[294]
pQA21	*amyE::PD3- fla/che-lacZ (cm)*	This work
pQA22	*amyE::PA-fla/che-lacZ (cm)*	This work
pQA23	pminiMAD –PD3 mu (amp) (erm)	This work
pQA24	pminiMAD –fliE mu (amp) (erm)	This work
pQA25	pminiMAD –fliK mu (amp) (erm)	This work
pQA26	codY-His6 (kan)	This work

TABLE 3.2 Oligonucleotides

Primer	Sequence (5' to 3')
oQA100	AGGAG GAA TTC CTGACCGTGTCGGCATTACCCGTT
oQA103	GATAAGGATCC ATCCGCTCTGCTCAAGGCATTTTCAAG
oQA106	GATAAGGATCCTCTCCTTTCTTTTCGGCATTTTTG
oQA107	AGGAG GAA TTC GAAAAAACAGAAATTCTGCTATTTTC
oQA130	TATGCATATGATGGCTTTATTACAAAAAACA
oQA131	GGTGCTCGAGATGAGATTTTAGATTTTCTAA
oQA136	TTTTTGAGGGTTCTTTTTTTA
oQA137	TTTTCGGCATTTTTGAAACTTTTTGAAGAA
oQA140	TTCTTCAAAAAGTTTCAAAAATGCCGAAAAAAGGCGTTAGAAATCGGA AAG
oQA143	CGAAAAGCTTGTTTGATTTGA
oQA146	TTCTTCAAAAAGTTTCAAAAATGCCGAAAACTTCCTCAAAAAGGGACCA AA
oQA149	TCCGATGCATTTTTGCTGGAT
oQA150	AGGAGGAATTCAATGACGATGACTTAATTCTA
oQA151	TTGAAGAAAAATGCAACATCTTTTACAACTATTACATAGAAAGAC
oQA152	GTCTTTCTATGTAATAGTTGTAAAAGATGTTGCATTTTTCTTCAA
oQA153	CTCCTGGTACCAAAATCAACATGACGATAGTC
oQA154	AGGAGGAATTCTTCAGCATCGGCTTTAACAGC
oQA155	ATTTGTTGCATTTTGCGTGTTTTGGGTGTTTTGAACCTGAAAAGG
oQA156	CCTTTTCAGGTTCAAAACACCCAAAACACGCAAAATGCAACAAAT
oQA157	CTCCTGGTACCGCCATTTTAGAATTTGAAGCA
oQA158	AGGAGGAATTCGCTCACAGAAACGGAGAAAAT
oQA159	TCCCAAAGTCTTGTGAGGACTCGGAGGACTTCGATAACAAGAAGG
oQA160	CCTTCTTGTTATCGAAGTCCTCCGAGTCCTCACAAGACTTTGGGA
oQA161	CTCCTGGTACCTTGGACCGGAAGAGTAAAACG

integration, propagated in the absence selection, and plated on LB agar. Colonies were patched to identify MLS sensitive colonies and the corresponding region was PCR amplified and sequenced to identify strains harboring the appropriate mutations.

Plasmids pJW053, pJW054, pJW055, pJW058, pJW063, pJW064, pQA014, pQA015 and pQA20 were constructed as described previously (301). Plasmid pQA21 was constructed by two-way ligation with a PCR product containing the DNA sequence upstream of the P_{D3} promoter in the *fla/che* operon (primer pair oQA100/106). The PCR product was digested with EcoRI and BamHI, and cloned into pDG1661 digested with the same enzymes. pDG1661 [*amyE::lacZ (cat)*] is an ectopic integration vector. Plasmid pQA22 was constructed by two-way ligation with a PCR product containing a DNA sequence upstream of the P_A promoter of the *fla/che* operon (primer pair oQA103/107). The PCR product was digested with EcoRI and BamHI, and cloned into pDG1661 cut with the same enzymes. Plasmid pQA26 was generated by amplifying the *codY* gene with primer pair oQA130/131. The PCR product was digested with NheI and XhoI and cloned into pET-24b(+) digested with the same enzymes.

Swim plate assay

Twenty five ml cultures of *B. subtilis* strains were grown at 37°C in CH medium until the optical density (OD_{600}) reached approximately 0.5. Cultures were centrifuged and cells were concentrated to an OD_{600} of 10 in PBS (137 mM NaCl, 2.7 mM KCl, 10 mM Na2HPO4, 2 mM KH2PO4, [pH 7.4]) containing 0.5% (w/v) India ink (Higgins).

Ten µl of the cell suspensions were spotted on top of 150 x 15 mm petri plates filled with ~100 ml of LB fortified with 0.25% Bacto-agar, dried for 30 min at room temperature to allow time for absorption, and incubated at 37°C inside a covered glass dish containing water-soaked paper towels to generate humid conditions. Plates were scanned after 5 hrs of incubation.

SDS-PAGE and western blotting

B. subtilis strains were grown to mid-logarithmic phases, the optical density was measured (for equivalent loading) at 600 nm, and 1 ml samples were harvested at an OD_{600} near 0.5. Cells were pelleted by centrifugation and resuspended in 50 µl lysis buffer (20 mM Tris [pH 7.0], 10 mM EDTA, 10 mg/ml lysozyme, 10 µg/ml DNase I, and 100 µg/ml RNase A, with 1 mM phenylmethylsulfonyl fluoride [PMSF]) and incubated for 15 min at 37°C. Fifty µl of sample buffer (0.25 M Tris [pH 6.8], 4% SDS, 20% glycerol, 10 mM EDTA) containing 10% 2-mercaptoethanol was added to an equal volume of lysate and the sample and the sample was boiled for 5 min prior to loading. Sample loads were normalized by OD_{600} values. Proteins were separated by SDS-PAGE on 4-20% mini-protean TGX polyacrylamide gels (Bio-Rad), transferred onto nitrocellulose membrane (Pall) and blocked in 5% (w/v) nonfat milk in PBS–0.5% (v/v) Tween-20. Membranes were probed with an anti-SigD antibody at a 1:5,000 dilution or anti-SigA antibody at a 1:20 000 dilution (Fujita Masaya, University of Houston, TX), followed by a 1:10 000 dilution of horseradish peroxidase-conjugated goat anti-rabbit

immunoglobulin G secondary antibody (Bio-Rad). Washed membranes were incubated with SuperSignal West Femto Chemiluminescent Substrate (Thermo) according to the manufacturer's instructions.

Purification of 6His-CodY

E.coli BL21(λDE3) was transformed with pQA26. To overexpress 6XHis-CodY protein, cultures were grown in 25 ml of Cinnabar high-yield protein expression media (Teknova) supplemented with 25 μg/ml kanamycin and 0.1% (w/v) glucose in a shaking waterbath at 300 rpm at 37°C. When the cell density of the cultures reached an OD_{600} of 2.5, protein expression was induced by the addition of 1 mM final IPTG. Cultures were grown to an OD_{600} of 7 and harvested by centrifugation at 15,000 x g. The cell pellets were stored at −80°C until needed. For lysis, pellets were resuspended in 25 ml of lysis buffer (50 mM Tris-HCl [pH 8.5], 300 mM NaCl, 50 ul of 1 mg/ml DNase I, and 50 ul of Protease Inhibitor Cocktail (Sigma)) and passed three times through a French pressure cell at 10,000 PSI. The cells lysate was centrifuged at 15,000 x g for 30 min at 4°C to remove cell debris. The supernatant was collected and loaded to a 1 ml bed volume of pre-equilibrated Ni-NTA (Qiagen) and washed with 5 ml wash buffer (50 mM Tris-HCl [pH 8.5], 300 mM NaCl, 20mM imidazole, and 10% glycerol). Protein was eluted with 2 ml elution buffer (50 mM Tris-HCl [pH 8.5], 300 mM NaCl, 250 mM imidazole, and 10% glycerol) and collected in 250 μl fractions. All fractions were subjected to SDS-

PAGE and peak fractions were pooled and dialyzed against binding buffer (see below). Aliquots were frozen at −80°C prior to use.

Electrophoretic mobility shift assays

The PCR products containing the CodY-binding sites upstream of promoter P_{D3} and in the coding sequence of *fliE* and *fliK* were amplified using the primer pair's oQA136/137, oQA140/143 and oQA146/149, respectively. PCR products were cleaned using the DNA concentrator kit (Zymogen).

The DNA-binding reaction mixtures contained 5 nM DNA, 25 mM 2-(*N*-morpholino) ethanesulfonic acid [pH 6.0], 200 mM sodium acetate, 1 mM dithiothreitol (DTT), 1 mM Tris (2-carboxyethyl) phosphine, 1 mM EDTA, 0.05% n-octylglucoside, 5% glycerol, 100 µg/ml bovine serum albumin, 2 mM GTP and 10 mM of each of valine, leucine and isoleucine, as described previously (246). The reactions contained various amounts of CodY and were incubated for 15 to 20 min at room temperature and separated on 5% non-denaturing polyacrylamide gels containing 50 mM bis(2-hydroxyethyl)amino-tris(hydroxymethyl)methane [pH 6.0] and 10 mM isoleucine. The running buffer was composed of 25 mM 2-(*N*-morpholino) ethanesulfonic acid plus 25 mM bis(2-hydroxyethyl)amino-tris(hydroxymethyl) methane running buffer [pH 6.0]. The gels were run at 175 V for 3 hr and then stained with SYBR Green EMSA gel stain (Life Technologies) for 10 min. The gels were washed with distilled H_20 and DNA was

visualized with a Typhoon Trio fluorescence imager (GE Healthcare) following excitation at 488 nm with a 520 nm band pass emission filter.

Microscopy

One ml samples were collected at an OD_{600} of 0.5 and cells were pelleted by centrifugation. To stain membranes, cells pellets were resuspended in PBS containing 0.02 TMA-DPH [1-(4-trimethylammoniumphenyl)-6-phenyl-1,3,5-hexatriene *p*-toluenesulfonate] and mounted on glass slides with polylysine-treated coverslips. Fluorescence microscopic analysis was performed with a Nikon Ti-E microscope equipped with a CFI Plan Apo lambda DM 100X objective, and Prior Scientific Lumen 200 Illumination system, C-FL UV-2E/C DAPI, C-FL GFP HC HISN Zero Shift, C-FL YFP HC HISN Zero Shift, and C-FL Cyan GFP, filter cubes, and a CoolSNAP HQ2 monochrome camera. All images were captured with NIS Elements Advanced Research (version 4.10), and processed with ImageJ64 (302).

Results

A ΔcodY *mutant grows primarily as unchained cells*

In a previous study, we found that a Δ*relA* mutant, which possesses decreased GTP levels, grows as a homogenous population of unchained, swimming cells during

exponential growth (301). We hypothesized that the GTP-sensing global regulator CodY, previously implicated in repression of flagellar gene expression (235), might become derepressed in the Δ*relA* mutant due to the lower levels of GTP. In this model, CodY derepression could be responsible for mediating the shift toward the unchained, motile cell state we observed in the Δ*relA* mutant. To test this idea, we first examined the cell chaining phenotype in a Δ*codY* mutant during exponential growth where the wildtype (PY79) strain grows as a mixed population of 85% chained and 15% unchained cells (76). We found that during exponential growth the Δ*codY* mutant is less chained than the wildtype, but unlike the Δ*relA* mutant, is comprised of both chained and unchained cells (Fig. 3.1). Quantitation revealed that the proportion of unchained cells increased from 15% in wildtype to 75% in the Δ*codY* mutant. We conclude that CodY has a significant role in preventing the switch from chained cells to unchained cells during exponential growth. This result suggests that derepression of CodY-regulated genes could account for most of the unchained cells observed in the Δ*relA* mutant. The result also indicates that CodY derepression alone cannot account for the 100% unchained phenotype observed in the Δ*relA* mutant, since 25% of Δ*codY* mutant cells remain chained.

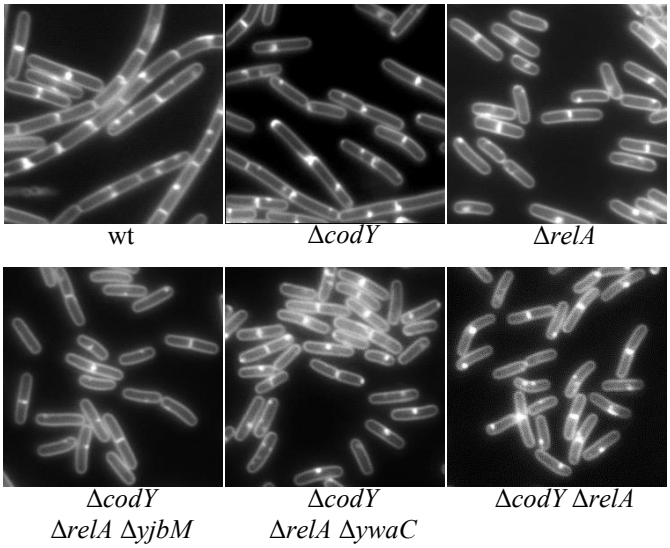

FIGURE 3.1 The Δ*codY* mutant is less chained than the wild type. Representative images of wildtype (BJH001), Δ*relA* (BQA009); Δ*codY* (BQA090), Δ*codY*/Δ*relA*/Δ*yjbM* (BQA096), Δ*codY*/Δ*relA*/Δ*ywaC* (BQA097) and Δ*relA*/Δ*codY* (BQA091) cells grown to mid-log in CH medium. Membranes were stained with TMA.

We hypothesized that reduced GTP levels in the Δ*relA* mutant could contribute to the CodY-independent unchained phenotype observed. In this case, strains harboring higher levels of GTP than Δ*relA*, but lower than wildtype, should shift the Δ*codY* mutant toward a more unchained phenotype. To test this hypothesis, we introduced the *codY* deletion into Δ*relA*/Δ*ywaC* and Δ*relA*/Δ*yjbM* mutant backgrounds, previously shown to have intermediate GTP levels (185) and be 66% and 22% unchained during exponential growth (301), respectively. In comparison to the *codY* deletion alone (75% unchained), the Δ*codY*/Δ*relA*/Δ*ywaC* and Δ*codY*/Δ*relA*/Δ*yjbM* triple mutants grew as 100% unchained populations (Fig. 3.1). These results suggest that the switch of the remaining chained cells to unchained cells could be accounted for by a GTP-dependent, but CodY-independent mechanism. The Δ*relA*/Δ*ywaC* and Δ*relA*/Δ*yjbM* mutant backgrounds likely harbor increased (p)ppGpp levels (185, 209, 301), so we do not rule out the possibility that (p)ppGpp levels may contribute to the phenotypic switch to unchained cells we observe.

The ΔcodY *mutant strain exhibits increased mobility on swim plates*

Cell chaining and cell motility are inversely correlated; unchained cells possess flagella and are motile, while chained cells are mainly aflagellate and non-motile (76). Since the Δ*codY* mutant population is less chained than wildtype, we expected that it

would also produce a more motile population compared to wildtype. To assess the motility behavior of a Δ*codY* mutant population, we performed a swim plate assay (301). Cultures were grown to mid-exponential phase and equal cell densities were spotted on semi-solid media. In the swim plate assay, motile cells migrate away from the original spot and produce a halo, the outer edge of which is referred to as the swim front. As expected, the Δ*codY* mutant swimming front migrated further than the wildtype, but not as far as the Δ*relA* mutant (Fig. 3.2). This result is consistent with the proportion of unchained cells observed in the Δ*codY* and Δ*relA* mutants (Fig. 3.1A). The Δ*sigD* mutant population, which is composed exclusively of chained, non-motile cells (76), did not migrate appreciably on the swim plate. We conclude that the Δ*codY* mutant population is not only more unchained, but also composed of more swimming cells than wild-type.

SigD levels and activity are elevated in the codY ***mutant***

The phenotypic switch to the unchained, motile cell phenotype is regulated by both SigD levels and activity, and we previously found that SigD levels and activity are elevated in the Δ*relA* mutant (301). Since the Δ*codY* mutant is less chained than wildtype, we hypothesized that the Δ*codY* mutant would also produce higher levels of SigD than wildtype. Western blot analysis on cell lysates collected from exponentially growing cultures showed that the Δ*codY* mutant exhibited higher levels of SigD levels relative to wildtype (Fig. 3.3A and 3.3B). Surprisingly, levels of SigD protein in the

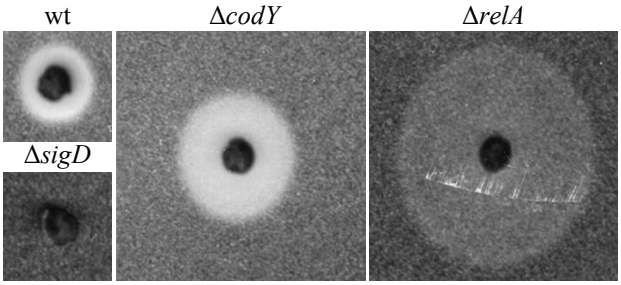

FIGURE 3.2 The Δ*codY* mutant strain exhibits increased mobility on swim plates**.** Wildtype (BJH001), Δ*relA* (BQA009); Δ*codY* (BQA090) and Δ*sigD* (BQA022) strains were inoculated on LB fortified with 0.25% agar. After 5 hr incubation at 37ºC, the plates were scanned against a black background. The images shown are cropped from the same petri plate and are representative of the swimming behavior of each strain for at least three biologically independent replicates. The density of cells around the Δ*relA* mutant is less than wildtype and Δ*codY* due to the slower growth rate and increased mobility of the strain.

Δ*codY* mutant were not statistically different from the Δ*relA* mutant (Fig. 3.3B), which exhibits a completely SigD "ON" state phenotypically (301). The Δ*codY*/Δ*relA*/Δ*ywaC* and Δ*codY*/Δ*relA*/Δ*yjbM* triple mutants phenocopied the Δ*relA* mutant with respect to SigD protein produced (Fig. 3.3A and 3.3B).

The Δ*relA* and Δ*codY* mutants accumulate similar levels of SigD during exponential growth (Fig. 3.3A and 3.3B). Although the average SigD levels were consistently lower in the Δ*codY* mutant, densitometric analysis of five independent biological replicates indicated that the observed difference is not significant within a 95% confidence interval. The Δ*codY* mutant is more chained and less motile than the Δ*relA* mutant, suggesting that SigD protein levels alone may not account for the differences in phenotypes. To examine SigD activity, we analyzed expression from two SigD-dependent promoters (P_{hag} and P_{lytA}) using transcriptional fusions to a *lacZ* reporter gene. CodY was previously shown to bind the *hag* promoter and to repress *hag* transcription (235, 256). Consistent with the prior data performed in another *B. subtilis* strain (JH642) under different growth conditions (235), we observe that P_{hag} becomes derepressed in the absence of *codY* in wildtype PY79 grown in CH medium (Fig. 3.3C). We also observed that expression from P_{lytA} is increased 2.2-fold compared to wildtype, suggesting that CodY also regulates expression from P_{lytA} (Fig. 3.3C), possibly indirectly through SigD. As expected based on the phenotypic differences we observed, expression from P_{hag} and P_{lytA} in the Δ*codY* mutant is lower than in a Δ*relA* mutant (Fig. 3.3C). Since SigD protein levels do not differ significantly between Δ*relA* and Δ*codY*

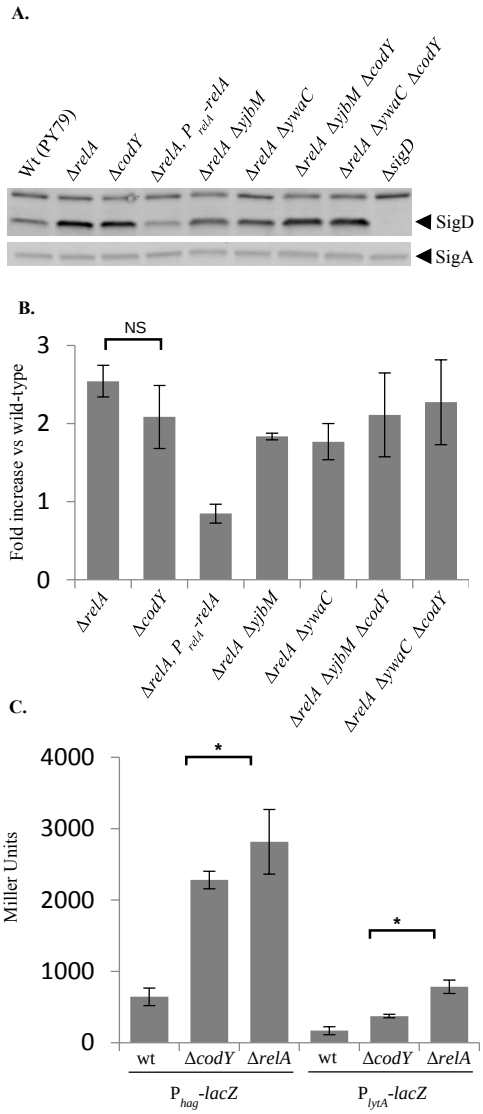

FIGURE 3.3 SigD levels and activity are elevated in the Δ*codY* mutant. A. Comparison of SigD protein levels in wildtype (BJH001), Δ*relA* (BQA009), Δ*relA*, P_{relA}-*relA* (BQA068), Δ*codY* (BQA090), Δ*relA*/Δ*yjbM* (BQA081), Δ*relA*/Δ*ywaC* (BQA082) Δ*codY*/Δ*relA*/Δ*yjbM* (BQA096), Δ*codY*/Δ*relA*/Δ*ywaC* (BQA097) and Δ*sigD* (BQA022). Samples were collected from mid-log cultures grown in CH media. Proteins from cell lysates were separated by SDS-PAGE and analyzed by western blot analysis by probing with anti-SigD antibodies. SigA is a loading control. B. Quantification of SigD protein from strains in (A). Five independent biological and experimental replicates were analyzed. C. β-galactosidase assays of P_{hag}-*lacZ* and P_{lytA}-*lacZ* transcriptional activities conducted on wildtype (BJH046 and BJH047), Δ*relA* (BQA050 and BQA051) and Δ*codY* (BQA102 and BQA103). Samples were collected from mid-log cultures grown in CH media. Data shown is the mean of three independent biological replicates with standard deviations. Significant ($P<0.05$) differences between Δ*codY* and Δ*relA* are indicated by asterisks.

(this study), these results suggest that the Δ*codY* mutant harbors a higher level of inactive SigD compared to the Δ*relA* mutant. Alternatively, it is also possible that there are small differences in SigD levels between the two strains that fall outside the limit of detection for western blot analysis.

CodY has three putative binding sites in the fla/che ***operon region***

CodY is a DNA-binding protein that globally regulates the expression of over one hundred gene products in response to changes in nutrient status (228). The DNA binding domain of CodY recognizes a 15-bp, AT-rich DNA motif, AATTTTCWGAAAATT (239, 243, 303). To determine if CodY could be directly regulating the accumulation of SigD by directly regulating *sigD* expression from the *fla/che* operon (82, 83), we searched the literature for previously reported CodY-binding sites in the region. Three putative CodY binding sites were identified. One site, found upstream of the SigD-dependent promoter, P_{D3} (referred to as Site D in this study) was previously shown to be bound by CodY directly (235). We also identified two untested, intragenic sites in the *fla/che* operon in *fliE* (Site E) and *fliK* (Site K) within a dataset from a CodY ChIP-seq study (228). The location and sequence of the three sites is shown in Figure 3.4. The Site D motif sequence has three mismatches with respect to the CodY-binding consensus motif, while Sites E and K have six and five mismatches, respectively (Fig. 3.4).

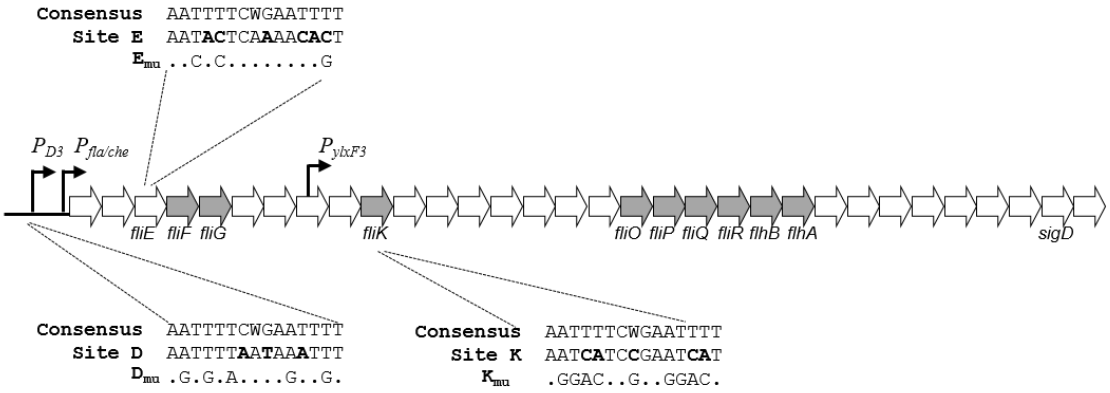

FIGURE 3.4 CodY has three putative binding sites in the *fla*/*che* operon**.** Genetic organization of the *fla/che* operon genes. Transcription of $P_{fla/che}$ is driven by SigA, while SigD directs transcription from P_{D-3} and P_{ylxF3}. Open reading frames are represented by arrows (not to scale). Components essential for FlgM secretion are shaded gray. The CodY consensus sequence, CodY binding sites, and point mutations made to the mutated versions of the sites are shown. Nucleotides that differ between the consensus and the sites are indicated by bold type.

To determine if CodY interacts directly with Sites E and K, we PCR amplified DNA fragments from the chromosome centered around each site and performed electrophoretic mobility gel shift assays with 6His-CodY in the presence of GTP and branched chain amino acids. As a positive control, we included the previously identified site, Site D (235). In vitro, CodY bound to all three sites, showing an apparent preference for Sites E and D compared to Site K (Fig. 3.5). DNA lacking the predicted binding motifs did not show altered mobility at any of the protein concentrations tested (data not shown), suggesting that the binding of CodY to each of these sites is specific.

Mutating the three CodY-binding sites in the fla/che ***operon phenocopies*** ΔcodY

CodY negatively regulates transcription by binding to promoter regions and preventing transcription initiation (243). CodY has also been shown to prevent synthesis of full-length transcripts by acting as a roadblock to RNA polymerase transit (249). Since CodY-binding Site D is located upstream of SigD-dependent and SigA-dependent promoters, P_{D3} and $P_{fla/che}$, respectively (Fig. 3.4), it could function to prevent initiation of transcription from P_{D3} and/or $P_{fla/che}$. On the other hand, Sites E and K lie within open reading frames (Fig. 3.4). If CodY is disrupting transcription from Sites E and K, then CodY is most likely be acting through a roadblock mechanism, preventing transcription of RNA downstream of each binding site (249).

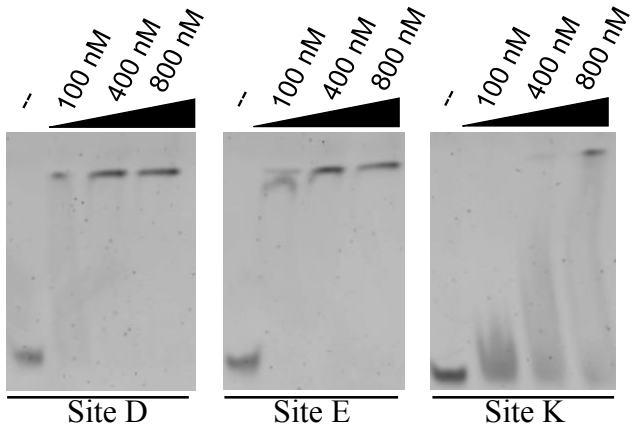

FIGURE 3.5 CodY binds directly to three sites in the *fla/che* operon. Electrophoretic mobility gel shift analysis of DNA fragments (5 nM) centered on the putative CodY binding motif incubated with the indicated concentrations of 6His-CodY. Gel shifts were performed in the presence of the CodY cofactors GTP, isoleucine, leucine, and valine.

To determine the contribution of each of the CodY binding sites to the unchained phenotype and increased SigD levels and activity we observed in the Δ*codY* mutant, we created point mutations within each of the sites on the chromosome (Fig. 3.4). Since sites E and K lie within genes, we introduced point mutations that did not disrupt the open reading frame of *fliE* and *fliK*, respectively. To determine the contribution of each binding site to the chaining phenotype, we determined the proportion of unchained versus chained cells in strains harboring all six possible combinations of mutant CodY-binding sites. The proportion of unchained cells was higher than wildtype by at least double for each of the mutants tested (Fig. 3.6A). The relative contribution of each single site to cell chaining showed the following pattern: Site D >Site E >Site K. Moreover, the double mutants that included D_{mu} were most similar to the Δ*codY* mutant. These results suggest that Site D has the strongest control over SigD activity, but that Sites E and K are also independently important.

We then examined SigD levels in backgrounds harboring all possible combinations of the mutant CodY binding sites. Surprisingly, mutating any one of the CodY-binding sites caused a significant increase in SigD levels compared to wildtype, each strain reaching SigD levels statistically indistinguishable from the Δ*codY* mutant (Fig. 3.6B and 3.6C). Strains in which either two or all three of the binding sites were mutated also showed SigD levels comparable to the Δ*codY* mutant (Fig. 3.6B and 3.6C). We conclude that Sites D, E, and K each contribute to preventing the accumulation of SigD during exponential growth.

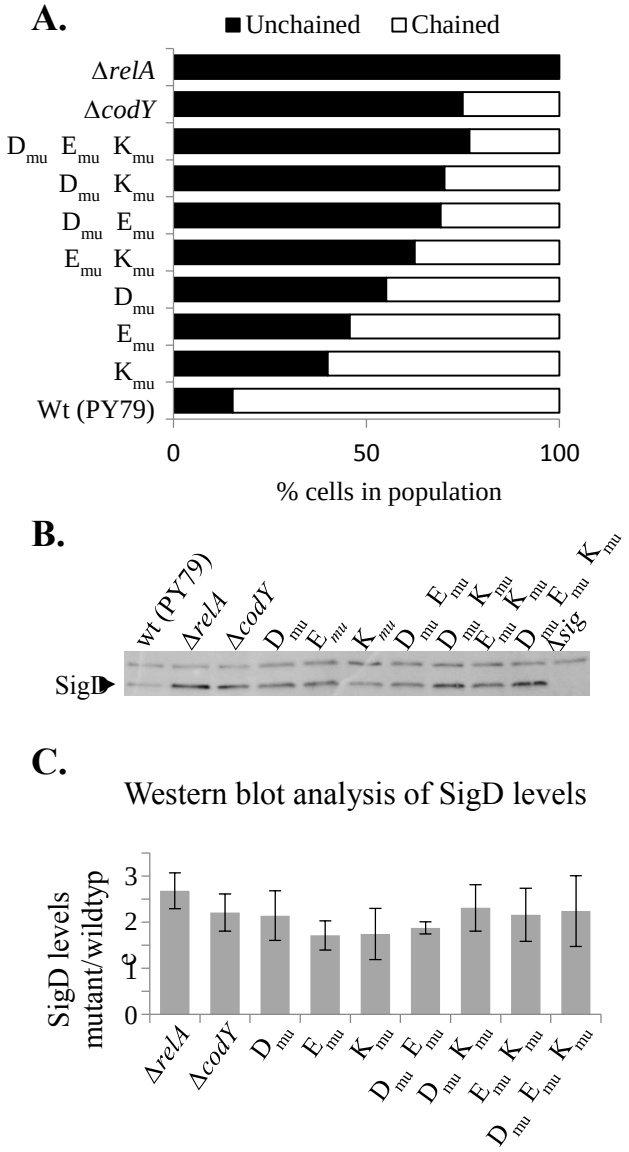

FIGURE 3.6 Mutating three CodY-binding sites in the *fla/che* phenocopies Δ*codY***.** A. Frequency of chained (three or more cells linked) and unchained (single and doublet) cells across a population. Images from at least three independent cultures were counted and no less than 3,000 cells were quantitated for each strain represented in the graph. B. Comparison of SigD protein levels from samples collected from mid-log cultures grown in CH media. C. Quantification of SigD protein from the strains indicated above. The average standard deviations for five independent biological replicates are shown normalized to wildtype (PY79). None of the codY binding site mutants or mutant combinations differ significantly at the 95% confidence level from the Δ*codY* mutant. Strains shown are: Wildtype (BJH001), Δ*relA* (BQA009), Δ*codY* (BQA090), D_{mu} (BQA106), E_{mu} (BQA107), K_{mu} (BQA108), D_{mu} E_{mu} (BQA110), D_{mu} K_{mu} (BQA111), E_{mu} K_{mu} (BQA109), D_{mu} E_{mu} K_{mu} (BQA112) and Δ*sigD* (BQA022).

Discussion

RelA is a dual-function (p)ppGpp synthetase and hydrolase enzyme, which along with two additional (p)ppGpp synthetases YjbM (RelQ, SasB) and YwaC (RelP, SasA), modulates (p)ppGpp levels in *B. subtilis* (185). (p)ppGpp synthesis by YjbM and YwaC in the absence of RelA (p)ppGpp hydrolysis activity is sufficient to bias cells toward the 100% motile, unchained phenotype (301).

Accumulation of (p)ppGpp induces a wide range of physiological alterations that affect many important cellular processes such as DNA replication, transcription, translation, and metabolism (206). In *E.coli*, (p)ppGpp and a co-regulator, DksA, bind directly to RNA polymerase to inhibit or activate transcription (191, 304). (p)ppGpp has also been shown be important for the association of alternative sigma factors with the RNA polymerase core (198). In the Gram-positive bacterium *B. subtilis* (p)ppGpp's effects on transcriptional regulation occur primarily through modulation of GTP levels (206). GTP is one of the substrates for (p)ppGpp synthesis, so as (p)ppGpp levels rise, GTP becomes depleted. In addition, (p)ppGpp inhibits hypoxanthine-guanine phosphribosyltransferase (HprT) and guanylate kinase (GMK), enzymes involved in the biosynthesis of GTP biosynthesis (210). GTP levels affect transcription in *B. subtilis* through at least two mechanisms. First, GTP is an important co-factor for the global transcriptional regulator CodY (212), so reductions in cellular GTP levels lead to derepression of CodY-repressed target genes (70, 213). Second, decreased GTP levels

reduce transcription from promoters that use GTP as the initiating nucleotide for transcription (23, 74, 208, 305, 306).

In this study, we investigated the role of CodY in regulating the switch between SigD "ON" and "OFF" states. We find that CodY represses expression of SigD by binding directly to three sites within the *fla/che* operon. To our surprise, cells harboring mutations in any one of the CodY binding sites produced SigD levels that were indistinguishable from the Δ*codY* mutant, suggesting that SigD expression in PY79 is largely a function of whether or not CodY is bound within the *fla*/*che* operon. We found that the SigD protein levels were not necessarily predictive of the phenotypic consequence of mutating each of the CodY-binding sites. For example, a Site D mutant (D_{mu}) and a Δ*codY* mutant produced similar SigD levels on average (Fig. 3.6C), however, D_{mu} possessed ~20% more chained cells than a Δ*codY* mutant (Fig. 6A). It is possible that subtle differences in SigD levels may explain the observed differences in cell chaining. Alternatively, the phenotypic differences could be explained by post-translational regulation of SigD activity (see below).

One model suggests that CodY's binding to various sites within the chromosome is hierarchical (248). In other words, when GTP is abundant, CodY-GTP would bind to all sites, but as GTP levels drop, CodY would be gradually released from lower affinity sites. Based on our electrophoretic gel mobility shift data, CodY has a higher affinity for Sites D and Site E compared to Site K (Fig. 3.5). If the same relative affinity is present in vivo, then it would suggest that CodY is released from Site K first, allowing transcription to occur from the P_{ylxF} promoter to the end of the operon (Fig. 3.4) (102).

A further drop in GTP levels would allow transcription through Site K from the $P_{fla/che}$ and P_{D3} promoters, respectively.

Our analysis of the CodY binding sites within the *fla*/*che* operon revealed that the newly characterized CodY binding sites (Sites E and K, Fig. 3.4) are positioned just upstream of flagellar apparatus genes important for FlgM secretion (Fig. 3.4)(112). FlgM is an anti-sigma factor that inhibits SigD activity by preventing its association with RNA polymerase (102, 110, 111). Upon completion of the hook–basal body complex, FlgM is secreted outside of the cell, where it is no longer competent to antagonize SigD (112). The minimal set of flagellar genes in the *fla/che* operon required for FlgM secretion are *fliF*, *fliG*, *fliK*, *fliO*, *fliP*, *fliQ*, *fliR*, *flhB*, and *flhA* (112)(Fig 3.4, shaded arrows). Therefore, in addition to regulating SigD levels, CodY may exert some control on SigD activity by specifically regulating expression of genes important for FlgM secretion.

We found that a Δ*codY* mutant is 75% unchained, suggesting that CodY derepression could contribute to the unchained, motile phenotype observed in the Δ*relA* mutant. We were unable to determine if CodY is required for 100% unchained phenotype of the Δ*relA* mutant because the double mutant is itself 100% unchained (Fig. 3.1). However, we were able to ascertain that varying the GTP levels in Δ*codY* mutant background through the inactivation of Δ*relA*/Δ*ywaC* or Δ*relA*/Δ*yjbM* was sufficient to phenocopy the 100% unchained phenotype of the Δ*relA* mutant (Fig. 3.1). Our results are consistent with the idea that both CodY-dependent and CodY-independent mechanisms contribute to the SigD "ON" state in the Δ*relA* mutant background and also

suggest each of these mechanisms is responsive to the cellular levels of GTP and/or (p)ppGpp. Finally, our results also support the idea that global transcriptional regulators like CodY are capable of finely tuning gene expression in response to even small changes in the concentration of important intracellular signaling molecules.

CHAPTER IV

A SECRETED FACTOR COORDINATES ENVIRONMENTAL QUALITY WITH *BACILLUS* DEVELOPMENT

Introduction

A major challenge in developmental biology is to uncover the signals that stimulate differentiation. Bacteria use cell-cell signaling to receive a variety of spatial, temporal and environmental cues that help them regulate and coordinate the requisite morphological and physiological changes needed for differentiation (307). Quorum sensing is one form of cell-cell signaling that enables bacteria to share information about the population density and to respond by reprogramming gene expression. In quorum sensing, bacteria use diffusible molecules, such as acyl-homoserine lactones, that increase in concentration with cell density. When a critical threshold of signal accumulates, a population-based community behavior, such as the production of bioluminescence, is induced (308, 309). The growing list of bacterial processes regulated by quorum sensing includes extracellular enzyme secretion (310), antibiotic production (311, 312), virulence (308), competence for DNA uptake (313, 314), biofilm formation (315, 316), sporulation (317, 318).

Bacillus subtilis is a Gram positive organism capable of differentiating into multiple cell types, including a heat and dessication resistant spores (254). Spore formation can be induced through nutrient exhaustion (319) or through conditions that

cause a rapid fall in cellular GTP levels (69, 320) However, Grossman and Losick observed that sudden drops in GTP levels are insufficient to trigger efficient sporulation when cell densities are very low (317). This observation lead to the discovery of oligopeptide-mediated quorum-sensing (317).

The oligopeptide signals of *B. subtilis* are synthesized ribosomally as pro-peptides, secreted outside the cell, processed into the mature oligopeptide forms, and then transported back into the cell by the oligopeptide uptake systems Opp and App (49, 321-323). Once internalized, the processed peptides promote the phosphorylation of the global response regulator Spo0A (28). Spo0A is always synthesized in *B. subtilis* (27, 29), but during transition and stationary phase the Spo0A levels rise and the active form, Spo0A-P, accumulates (27, 324). At lower levels, Spo0A-P activates and represses genes involved in growth phase adaptation nutrient scavenging and competence (27, 325). At higher levels of Spo0A-P, the developmental pathway of sporulation is initiated (27). The signaling network regulating Spo0A's phosphorylation state is complicated. Several sensor kinases, including KinA, promote Spo0A phosphorylation (20), (16). Conversely, several phosphatases antagonize Spo0A phosphorylation both directly and indirectly (16). The characterized quorum sensing oligopeptides of *B. subtilis* inhibit the activity of the phosphatases, promoting development by shifting Spo0A toward its phosphorylated form (45). Since, the known quorum-sensing peptides of *B. subtilis* act as modulators of Spo0A-P levels, these results suggest that the sporulation pathway is primarily a function of Spo0A-P levels, and that the contribution of cell density and/or growth phase is indirect.

In order to directly probe this question directly, Ireton and colleagues isolated a constitutively active allele of Spo0A called SAD67 and placed it under the control of an inducible promoter [326]. Although induction of SAD67 resulted in expression of early sporulation genes (27, 29, 326, 327) it was not sufficient to induce efficient sporulation under nutrient replete conditions unless the cells were also treated with decoyinine to cause a rapid drop in GTP levels (69, 326, 327). These results suggested that there are at least two requirements for efficient sporulation: sufficient levels of Spo0A-P and a signal indicating deteriorating environmental conditions.

In a subsequent study, Fujita and Losick found that *B. subtilis* could be triggered to sporulate efficiently in rich media if the Spo0A-P levels were elevated gradually; this gradual accumulation was achieved by artificially expressing KinA, one of several kinases that donate phosphoryl groups to the Spo0A phosphorelay. The authors concluded that Spo0A-P was both necessary and sufficient to promote sporulation during exponential growth in rich media (64). Moreover, the authors suggested that nutrient-dependent signals, such as GTP levels, likely act to promote sporulation indirectly, by feeding into the Spo0A phosphorelay.

In the present study, we find that *B. subtilis* cells continuously cultured at exponential phase cell densities ($<OD_{600}$ of 0.8 in CH medium) are unable to sporulate through KinA-dependent induction. Instead, we find that sporulation requires both KinA induction and the accumulation of at least one extracellular signal, which we call Factor X (FacX). FacX is retained by dialysis with a cutoff smaller than 8 kDa, heat stable, and sensitive to proteinase K, consistent with previously characterized quorum-sensing

peptide-based signals. However, unlike the characterized peptides, FacX activity is not dependent on Spo0A or SigH (46), and does not require the known oligopeptide transporters Opp and App (49, 321, 323). Finally, spiking cultures with concentrated Factor X is sufficient to induce sporulation at low cell densities via KinA or Spo0A (SAD67), suggesting that there is no formal requirement for gradual Spo0A-P accumulation in sporulation induction. In sum, our results suggest that Spo0A-P is necessary, but not sufficient to trigger sporulation. Instead, efficient sporulation requires both Spo0A-P and at least one other signal.

Materials and methods

General methods

The *B. subtilis* strains and plasmids used in this study are listed in Table 4.1 Primers are listed in table 4.2. All strains were streaked on Luria-Bertani (LB) plates (10 g/L tryptone, 5 g/L yeast extract, 5 g/L NaCl, 1.5% Bacto agar). Cultures were grown aerobically at 37°C in liquid CH medium (Sterlini and Mandelstam 1969). *Escherichia coli* DH5α and TG-1 were used for isolation of plasmid DNA and were grown in LB medium. *B. subtilis* was transformed with DNA following growth in MC medium (10.7 g K_2HPO_4, 5.2 g KH_2PO_4, 20 g dextrose, 0.88 g sodium citrate dehydrate, 2.2 g L-glutamic acid monopotassium salt, 1 ml of 2.2% ferric ammonium citrate, and 1 g casein hydrolysate per 1000 ml). When needed, antibiotics were added to the growth media at

the following concentrations: 100 µg/ml spectinomycin, 7.5 µg/ml chloramphenicol, and 1 µg/ml erythromycin plus 25 µg/ml lincomycin (mls), for *B. subtilis* strains; and 100 µg/ml ampicillin, for *E. coli* strains.

Strains and plasmids construction

To generate a spectinomycin marked *oppC* deletion strain (*ΔoppC::spec*), the PY79 genomic was used to amplify a PCR product with the primer pair oJW113 and oJW114. The resulting fragment was digested with EcoRI and BamHI and cloned into pKM079 cut with the same enzymes to generate plasmid pJW080. Another PCR product from oJW121 and oJW122 was cut with EagI and SalI and introduced into pJW080 cut with the same enzymes to generate plasmid pJW081. Plasmid pJW080 was linearized with ScaI and introduced to the PY79 through selected for on plates supplemented with spectinomycin. The spectinomycin marked *opp operon* deletion strain was constructed as described for the *ΔoppC::spec.* PCR product from oJH219 and oJH220 (EcoRI-BamHI) was cloned into pKM079 to generate pJH041. Another PCR product from oJH217 and oJH218 (EagI-SalI) was introduced into pHJ040 to generate pJH041. The resulting pJH041 was introduced in *B. subtilis* as described above.

TABLE 4.1 Bacterial strains and plasmids

Strain	**Genotype**	**Reference**
BJH001	PY79 (wild-type)	[265]
BJH004	168 (*trpC2*)	Bacillus Genetic Stock Center
BDR2333	*spo0AΩ$P_{hyper\text{-}spank}$-spo0A(sad67) (spec)*	(64)
BDR2345	*amyE::P_{spac}-spo0A(sad67)(D56N) (cat),* Δ*spo0A::erm, trpC2, pheA1*	(326)
BJH012	*kinAΩ$P_{hyper\text{-}spank}$-kinA(cat)in B. subtilis PY79*	(64)
BJH160	Δ*spo0A*::*kan*	Errett Hobbs in the Losick Lab
BJH052	Δ*oppC::spec*	[294]
BQA022	Δ*sigH*::*cat*	Paul Straight
BQA052	*kinAΩPhyper-spank-kinA(cat) in B. subtilis 168*	This work
BQA055	Δ*oppC::spec; kinAΩ$P_{hyper\text{-}spank}$-kinA(cat) in B. subtilis 168*	This work
BQA061	Δ*oppABCDF::spec*	This work
BQA066	Δ*oppABCDF::spec; kinAΩPhyper-spank-kinA(cat) in B. subtilis 168*	This work

Plasmid	**Description**	**Reference**
pJW081	Δ*oppC::spec*	David Z. Rudner
pJH042`	Δ*oppABCDF::spec*	This work
pKM079	*B. subtilis chromosomal integration vector (spec)*	David Z. Rudner

TABLE 4.2 Primers

Primer	**1. Sequence (5’ to 3’)**
oJW113	GACGGATCCGATCCTAAGTTACGTAAATAAGGG
oJW114	CTGGAATTCCATGCGGAAATTGGTTCACC
oJW121	ATGCGGCCGGTTCTGCAATATGTGTTCTCC
oJW055	AATGTCGACCATGGCCTAGGCTCCTTT
oJH217	TTACTCGAGCTCTTAACTGATCTGCTGCTT
oJH218	AAGCAGCAGATCAGTTAAGAGCTCGAGTAA
oJH219	CCGAGCCGAATTCTTTCTCTA
oJH220	GGATCGGCCGGCTGGATTCAA

Microscopy

Culture samples (1 ml) were collected and pelleted by centrifugation. Membranes with either TMA-DPH (0.02 mM) or FM4-64 (3 µg ml^{-1}) (Life Technologies) and imaged with exposure times of 200-800 msec. Stained samples were mounted on glass slides with polylysine-treated coverslips. Fluorescence microscopic analysis was performed with a Nikon Ti-E microscope equipped with a CFI Plan Apo lambda DM 100X objective, and Prior Scientific Lumen 200 Illumination system, C-FL GFP HC HISN Zero Shift, and C-FL Texas Red HC HISN Zero Shift filter cubes, and a CoolSNAP HQ2 monochrome camera. All obtained images were captured with NIS Elements Advanced Research (version 4.10), and processed with ImageJ64 (302).

Conditioned CH media preparation

Single colonies were used to inoculate a 3 ml glass tube containing CH media and incubated for 4 hrs. The starter cultures was then used to inoculate at one to 1000 ratio a 500 ml CH media flask. The culture was grown in a shaking waterbath at 300 rpm, 37°C to an OD_{600} nm between 1.3 and 1.5. Cell were removed by centrifugation at 10,000 xg for 10 min and the conditioned media was filter sterilized by passing it through a 0.45 µm filter. All conditioned media prepared was tested by the sporulation assay (described below) and stored at 4ºC until needed. The activity was found to be stable for at least one month at 4ºC.

Proteinase K treatment and dialysis of the conditioned media

Conditioned CH media was treated with proteinase K at a final concentration of 75 µg/ml and incubated at 37°C for 30 min. Proteinase K was inactivated by incubation at 95°C for 10 min. Conditioned CH media was dialyzed against fresh CH media at least 3 times at 4°C. The first and the third dialysis steps were carried out overnight, while the second for 8-10 hrs. Heat treatment of conditioned CH media was carried out by transferring the conditioned media to a glass tube and submerging the glass tube in a bath of boiling water for X min. The heat-treated media was cooled before testing in the sporulation assay.

Sporulation assay

A 25 ml culture in a 250 ml baffled flask was grown in a shaking waterbath at 300 rpm, 37°C to an OD_{600} of approximately 0.6. Two hundred microliter of this culture are added to 2.3 ml of conditioned CH in 14-mm glass tubes containing 4-5 glass beads. To induce KinA expression, 20 µM final concentration of IPTG was added to the 2.5 ml sporulation assay tube. Culture tubes were incubated in a shaking waterbath at 300 rpm, 37°C for 2 hrs. The OD_{600} of the sporulation assay cultures at the end of the incubation period generally fell between 0.2 and 0.4, and were always below an OD_{600} of 0.6. One milliliter of samples were collected to check for sporulation by microscopic analysis as described above.

Results

Sporulation through KinA requires exit from exponential growth

While investigating the effects of KinA induction on DNA replication during vegetative growth in CH medium, we observed KinA-induced cells continuously cultured at OD_{600} values of less than 0.8 did not show morphological signs of sporulation (polar septa, axial filament formation, and engulfment) even after two hours of growth (Fig. 4.1). Instead, the cells appeared similar to the uninduced control (Fig. 4.1). In contrast, if KinA-induced cells were allowed to exit exponential growth, morphological changes characteristic of robust sporulation were readily observed (Fig. 4.1). These sporulating cells appeared similar to those induced to sporulate by resuspension in DSM (319). We conclude that sporulation in rich media via KinA requires exit from exponential growth.

FacX is present in conditioned media

B. subtilis is known to produce extracellular oligopeptides that stimulate sporulation in a cell density dependent manner (45), so we hypothesized that KinA-dependent sporulation might require the accumulation of an extracellular factor. To test this idea, we grew wildtype *B. subtilis* in liquid media until the culture reached early stationary phase (OD_{600} = 1.3-1.5) and removed the cells by centrifugation and filtration

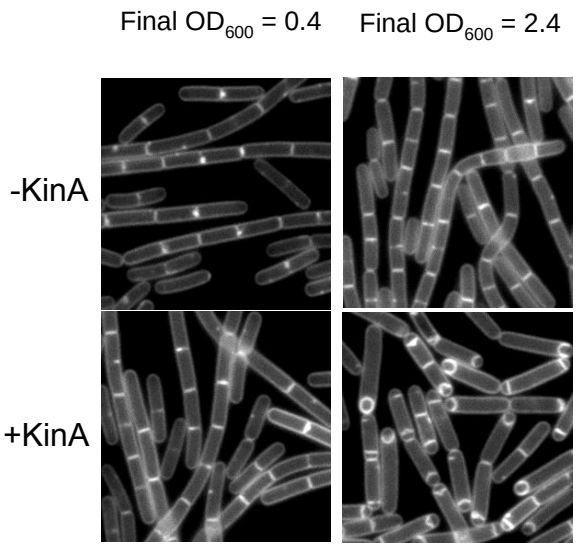

FIGURE 4.1 Triggering sporulation by KinA induction. Forespore formation in strain BJH012 ($P_{hy\text{-}spank}$-*kinA*). Cells were grown in CH medium and treated with IPTG (20 μM) at the mid-exponential phase of growth. Membranes were stained with TMA.

to generate the "conditioned media" (Fig 4.2A). We then inoculated the conditioned media with a small volume of exponentially growing cells harboring P*hy-kinA.* If no inducer (IPTG) was added, the cells continued to grow (final OD_{600} ~0.4 at 2 hrs) and exhibited no sporulation phenotypes (Fig. 4.2). These results indicate that the conditioned media itself is not sufficient to induce sporulation in the timecourse of this experiment. In contrast, when KinA was induced in cells growing in the conditioned media, robust sporulation occurred (Fig. 4.2). We next determined if the sporulation-inducing activity could be concentrated or diluted, which would suggest the presence rather than the absence of a factor. Cells were able to trigger sporulation successfully when the cultures growing in fresh CH medium were spiked with concentrated conditioned media at a 1X concentration (Fig. 4.3, upper panel). However, diluting the conditioned media by 25% prevented efficient sporulation (Fig. 4.3, lower panel). These results suggest that FacX's activity is concentration-dependent, and that a critical threshold of FacX is required to stimulate KinA-dependent sporulation. We conclude that in addition to the accumulation of Spo0A-P (in this case via KinA) (64), cells require the presence of at least one other factor for efficient sporulation at low cell densities. We refer to this factor (or factors) as FacX.

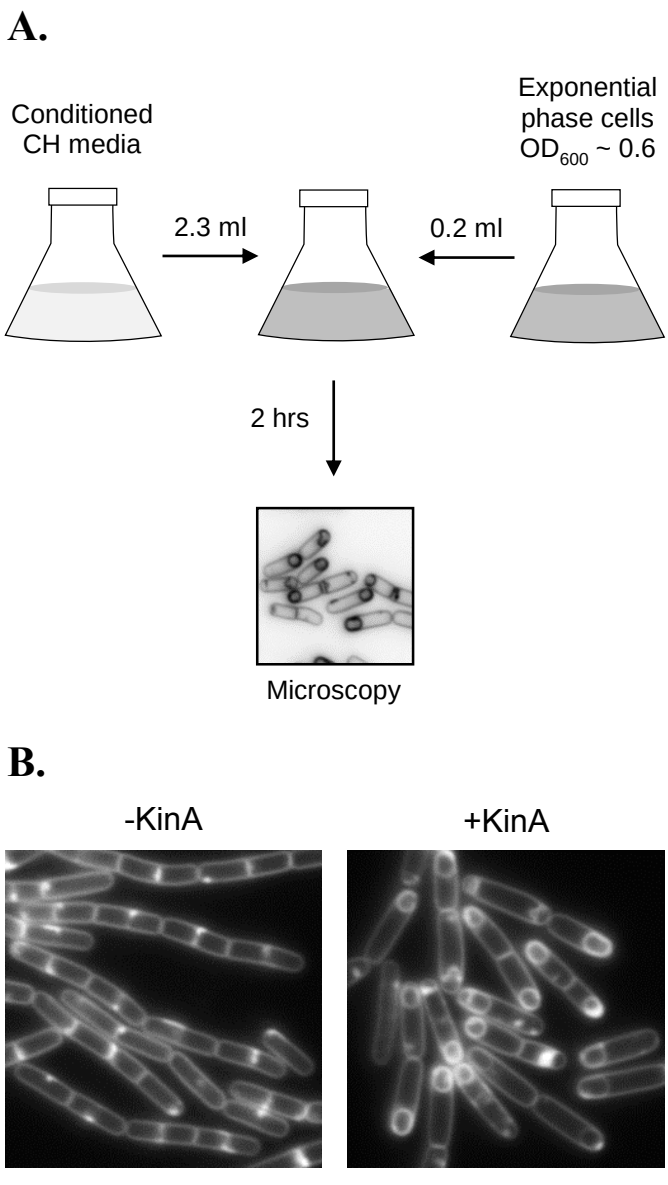

FIGURE 4.2 Conditioned media and KinA-dependent sporulation assay. (A) Schematic representation of the KinA-dependent sporulation assay used in this study. (B) Forespore formation in strain BJH012 ($P_{hy\text{-}spank}$-*kinA*). Cells were grown in conditioned CH medium and treated with IPTG (20 μM). Membranes were stained with TMA.

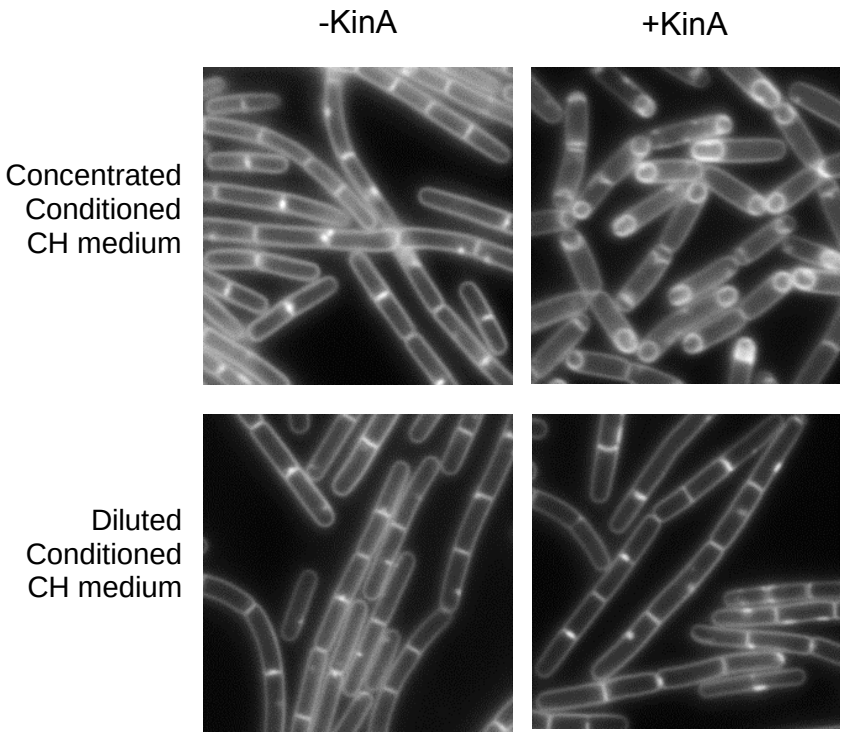

FIGURE 4.3 KinA-dependent sporulation assay following conditioned media concentration and dilution. Forespore formation in strains BJH012 ($P_{hy\text{-}spank}$-*kinA*). (Upper panel) Conditioned CH medium was diluted with fresh CH (1 part conditioned:3 parts fresh). (Lower panel) Fresh CH medium spiked with concentrated conditioned media at a 1X concentration. Membranes were stained with TMA.

FacX is sensitive to protease and retained by dialysis membranes smaller than 8 kDa

Since the characterized quorum-sensing signals of *B. subtilis* are peptides, we tested the susceptibility of FacX to heat and Proteinase K. FacX's sporulation stimulating activity was only mildly affected by boiling (Fig. 4.4A), but the activity was completely lost following proteinase K digestion (Fig. 4.4A). These results indicate that FacX is heat stable and composed, at least in part, of protein.

To determine the approximate size of FacX, we assayed for KinA-dependent sporulation at low cell densities using dialyzed conditioned media. We found that FacX activity was retained by both 0.1-5 kDa and 1-3.5 kDa molecular weight cutoff tubing, although the sporulation from the 0.1-5 kDa dialysate was more robust (Fig. 4.4B). In contrast, FacX activity was lost in the dialysate retained in the 6.0-8.0 kDa cutoff tubing (Fig 4.4B). We conclude that FacX is most likely between 500 and 8000 Daltons. We do not rule out the possibility that more than one molecule in the 500 to 8000 Dalton size range is responsible for FacX activity.

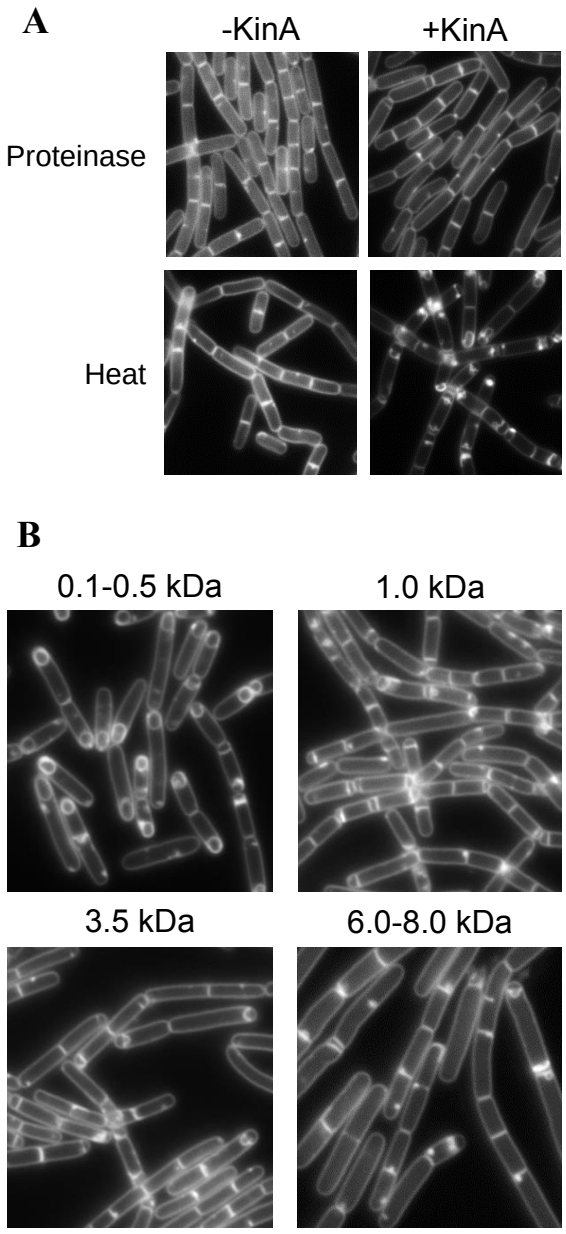

FIGURE 4.4 Assay for KinA-dependent sporulation following conditioned media dialysis, and treatment with heat and proteinase K. (A) Forespore formation in strain BJH012 ($P_{hy\text{-}spank}$-*kinA*). Conditioned CH medium was boiled and treated with proteinase K as described in the methods before used for the KinA- dependent sporulation assay with and without IPTG (20 μM). (B) Forespore formation in strain BJH012 ($P_{hy\text{-}spank}$-*kinA*). Conditioned CH medium was dialyzed as described in the method section before used for the KinA- dependent sporulation assay with and without IPTG (20 μM). Membranes were stained with TMA.

FacX activity is not dependent on SigH, Spo0A, or known oligopeptide transporters

Several secreted peptides, including CSF, PhrC, PhrE, and PhrF (44, 45, 314, 328) fall within the SigH regulon (46). To determine if FacX was a previously described sporulation modulating peptide or factor, we prepared conditioned media from cells lacking SigH or Spo0A. SigH is known to control the expression of a number of peptides that participate in the regulation of Spo0A activation (45) and Spo0A also regulates a number of post-exponential phase factors (27, 29). Conditioned media collected from either Δ*sigH* or Δ*spo0A* mutant cultures were still capable of stimulating sporulation at low cell densities when combined with KinA induction (Fig.4.4 and Table 4.3). These results indicate that FacX does not depend on SigH or Spo0A for its accumulation to sporulation-inducing levels.

The known oligopeptide signals are transported back into *B. subtilis* through the Opp (321, 323) and App (49) ABC transporter systems. To test if FacX requires transport through Opp or App, we assayed for KinA-dependent sporulation at low cell densities in a Δ*oppABCDF*Δ*appA* mutant. The cells sporulated efficiently similar to the wildtype control (Fig. 4.5 and Table 4.3). We conclude that FacX activity does not require transport back into the cell via Opp or App. Since FacX does not require SigH for synthesis and does not require Opp or App for transport, which strongly suggests that FacX is not one of the previously characterized quorum-sensing peptides.

TABLE 4.3 Summary of KinA-dependent sporulation assay

Genotype [a]	Sporulation initiation	
	-KinA	+KinA
Conditioned CH prepared from [b]		
WT (*Bs.* PY79)	x	o
ΔsigH	x	x
Δspo0A	x	x
Cells responding to conditioned CH [c]		
WT (*Bs.* PY79)	x	o
ΔoppABCDF	x	x
appA168 (*Bs* 168)	x	x
ΔoppABCDF, appA168	x	x

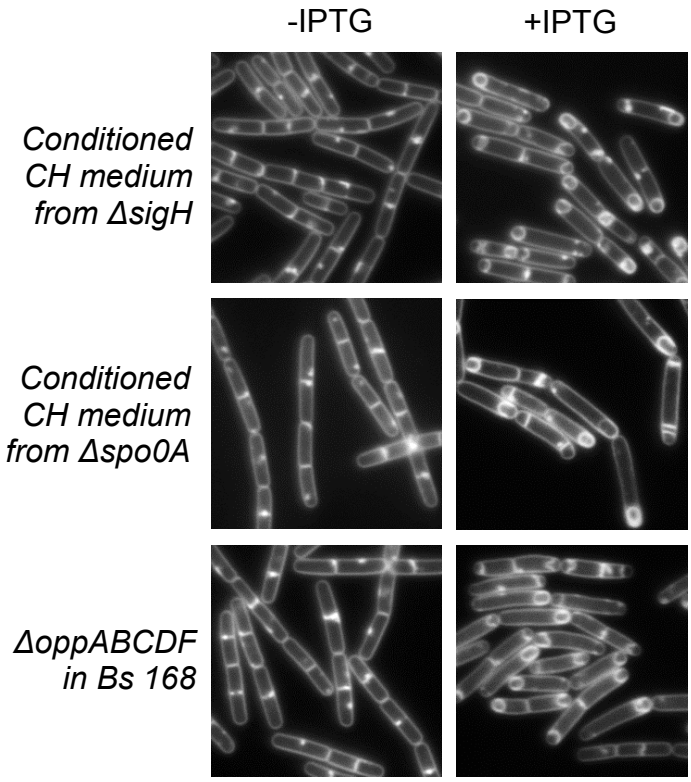

FIGURE 4.5 Conditioned media and KinA-dependent sporulation assay. Forespore formation in strains BJH012($P_{hy\text{-}spank}$-*kinA*) (Upper and middle panel) and BQA066 ($P_{hy\text{-}spank}$-*kinA*; Δ*oppABCDF* in *B.subtilis* 168) (Lower panel). (Upper panel) Conditioned CH medium was prepared from BQA012 (Δ*sigH*::*cat*) culture. (Upper panel) Conditioned CH medium was prepared from BJH160 (Δ*spo0A*::*kan*). (Lower panel) Conditioned CH medium was prepared from BJH001 (Wildtype). Membranes were stained with TMA.

FacX creates a permissive condition for sporulation

The observation that KinA-dependent sporulation at low cell densities required FacX lead us to revisit the model that sporulation requires a gradual accumulation of Spo0A-P (64). We hypothesized that the reason that exponentially growing cells cannot be induced to sporulate via SAD67 (the constitutively active allele) was not due to the acute induction of all Spo0A-P regulated genes, but could instead be attributed to the absence of FacX. To test this idea, we inoculated exponentially growing cells harboring P_{hy}-*SAD67* in conditioned media and induced expression using IPTG. Cells expressing *SAD67* in fresh CH media showed pleotropic phenotypes consistent with the up-regulation of high-threshold Spo0A-P genes (27), including occasional asymmetric septa (329), movement of chromosomes towards poles (330), and inhibition of DNA replication (331), however the cells also appeared unhealthy, lysed, and did not sporulate. In contrast, cells expressing *SAD67* in conditioned CH appeared to sporulate efficiently. We conclude that Spo0A-P is only sufficient to induce sporulation if a second signal, such as FacX (this study) or a sudden drop in GTP levels is also present (69).

Discussion

We report here that cultures of *B. subtilis* secrete a novel extracellular factor, FacX that accumulates with cell density. FacX is highly stable and exhibits many of the characteristics of previously characterized oligopeptide signaling molecules of *B.*

subtilis, including susceptibility to protease and a relatively small size (less than 8 kDa). However, FacX accumulation is not affected in the absence of SigH and does not require the Opp or App ABC transporters for activity, consistent with it comprising a novel signaling pathway for entry into sporulation.

Conditions required for the extracellular factor activity argue against the possibility that this factor is a previously described Phr peptide. First, production of FacX is not dependent on either SigH or Spo0A (Fig. 4.5 and Table 4.3), whereas the *phr* genes have both SigA and SigH-dependent promoters (45, 46). Expression of *phrC* is undetectable in a *sigH* mutant (332) and 50% lower in a *phrE* mutant (42). Second, the activities of the peptide products of PhrA, PhrC, PhrE and PhrH are absolutely dependent upon reimportation by the Opp/App oligopeptide transporters (42, 43, 313, 314, 318, 321, 323). In contrast, FacX doesn't require these transport systems for its activity (Fig. 4.5 and Table 4.3). Third, FacX allowed exponentially growing cells to initiate sporulation following acute induction of SAD67, suggesting that FacX either creates (or signals) a permissive condition for sporulation. Given the difference in phenotypes observed following SAD67 induction in fresh and conditioned CH media, we speculate that FacX somehow triggers cells to slow down growth processes associated with mid-exponential growth. How this might occur remains an area of open investigation, however the fact that rapidly falling GTP levels can substitute for FacX's activity may suggest that the levels of important signaling molecules such as (p)ppGpp and GTP play a critical role in the ultimate decision of whether or not to sporulate in addition to absolute Spo0A-P levels.

Our attempts to determine the identity of FacX from conditioned media were unsuccessful. However partial purification and characterization revealed many properties of FacX that may be useful. For example, FacX could not be bound to either anionic or cationic exchange resins, suggesting it may have a non-polar character. Consistent with this observation, FacX binds efficiently to C18 resin, but conditions to elute the activity from the column in a peak fraction were not successful. This could suggest that FacX activity comprised of more than one molecule or requires processing to a mature form before it is active, similar to the Phr peptides (333). Future experiments will be aimed at determining the identity of FacX and investigating how FacX changes the physiology of the cells. These investigations will shed new light on how bacteria make developmental decisions.

CHAPTER V

CONCLUSIONS AND FUTURE DIRECTIONS

In the ever changing and dynamic environment, bacteria continuously modulate their metabolism to thrive in local environments. To further increase their fitness and chances of survival, bacteria integrate the expression of a variety of developmental pathways into complex global signaling networks controlling carbon and nitrogen metabolism. The stringent response has emerged as an important central modulator of complex regulatory networks in bacteria. Previous work in our laboratory revealed that deletion of a gene responsible for (p)ppGpp metabolism in *B. subtilis* led to a dramatic shift of exponentially growing *B. subtilis* cells from a non-motile, chained wild-type population (85%) to a homogeneous population of unchained, motile cells. Thus, indicating that non-stringent (p)ppGpp levels may greatly influence the developmental decision-making outcomes. The goal of this work was to understand the role of (p)ppGpp in coordinating the transition from nonmotile, chained cells into motile, single cells in *B. subtilis*.

We found that a *relA* mutant deficient in the major (p)ppGpp hydrolase grows exclusively as unchained, motile cells and shows a significant increase in the synthesis and activity of SigD; likely due to elevated (p)ppGpp levels in this mutant. Although we did not quantitatively measure (p)ppGpp levels in strain backgrounds and growth conditions presented in this study, we were able to infer from the (p)ppGpp synthetase mutant phenotypes that the increase in cell motility and loss of cell chaining directly

correlates with the (p)ppGpp levels. In addition, based on the results obtained in Chapter II and other published data (185), we also found that the increase in cell motility and loss of cell chaining inversely correlates with the GTP levels. These results support a model in which (p)ppGpp levels act as a modulator of SigD activity, and subsequently, cellular differentiation. More specifically, our data suggest that even slight increases in (p)ppGpp may promote a SigD ON activation state during the exponential growth phase. Thus, cell chaining and motility in *B. subtilis* is regulated by RelA through its activity as a (p)ppGpp hydrolase.

In the course of elucidating the molecular mechanisms underlying the (p)ppGpp mediated cell motility and chaining developmental outcome, we found that deletion of *codY* gene resulted in a significant increase in SigD accumulation and activity and shifted the proportion of unchained cells up from 15% to 75%, suggesting that CodY is an important regulator of SigD. CodY was previously shown to bind to the promoter region upstream of the first gene in the *sigD*-containing *fla/che* operon. Using electrophoretic mobility shift assays, we found that CodY also binds to two other previously uncharacterized sites within the *fla*/*che* operon. Mutations in any one of the three binding sites resulted in SigD levels similar to the Δ*codY* mutant, suggesting that each site is sufficient to tip cells toward a maximal level of CodY-dependent SigD accumulation. However, mutations in all three sites were required to phenocopy the Δ*codY* mutant's reduced level of cell chaining, consistent with the idea that CodY binding in the *fla/che* is also important for post-translational control of SigD activity. Finally, our results support the idea that global transcriptional regulators like CodY are

capable of finely tuning gene expression in response to even small changes in the concentration of important intracellular signaling molecules.

Basal (p)ppGpp levels and differential regulation of cell chaining and motility by ppGpp versus pppGpp

Since its discovery, most research has focus on the protective and regulatory roles of (p)ppGpp during the stringent response, which is characterized by a rapid and dramatic accumulation of (p)ppGpp. However, more recent studies suggest that (p)ppGpp is also an important effector in many non-stringent processes at concentrations below those needed to activate the SR. During phenotypic characterization of Δ*relA,* Δ*relA/*Δ*ywaC*, and Δ*relA/*Δ*yjbM* mutants, we observed two important differences between these three strains that could be clearly attributed to differences in the amount and wether pppGpp or ppGpp accumulated in each one of these strains.

First, the increase in cell motility, loss of cell chaining, increase in SigD levels and activity, is directly correlated with the (p)ppGpp levels predicted to be produced in Δ*relA (highest)*, Δ*relA/*Δ*ywaC* (intermediate), and Δ*relA/*Δ*yjbM* (lowest) mutants. What is common about these three mutants is the absence of (p)ppGpp hydrolyzing enzyme. Thus, the differences in (p)ppGpp levels accumulating in each of the Δ*relA,* Δ*relA/*Δ*ywaC*, and Δ*relA/*Δ*yjbM* mutants are attributed to differences in activity of (p)ppGpp synthases YjbM and/or YwaC. Future work should focus on detecting the absolute quantitative (p)ppGpp levels in the three above mentioned mutants. This can be accomplished by developing a

sensitive HPLC-based technique for quantitative basal (p)ppGpp levels detection. When the basal (p)ppGpp concentrations from the three mutants are compared to concentrations from the wild type cultures, we will be able to determine the (p)ppGpp concentration threshold required to promote the differentiation into motile cells. To further explore the relationship between (p)ppGpp levels and developmental decision-making outcomes, we can examine the developmental consequences of artificially and gradually raising the (p)ppGpp concentrations in *B subtilis*, which can be carried out in a (p)ppGpp^0 strain (Δ*relA/*Δ*ywaC/*Δ*yjbM*) expressing an inducible (p)ppGpp synthase.

Second, as described earlier, the Δ*relA/*Δ*ywaC* mutant (YjbM is active) exhibited less chaining, more motility and higher SigD levels and activity than the Δ*relA/*Δ*yjbM* mutant (YwaC is active), indicating that YjbM is a more significant contributor to (p)ppGpp synthesis during exponential growth than YwaC. However, to our surprise the Δ*relA/*Δ*yjbM* mutant grows slower than the Δ*relA/*Δ*ywaC* mutant (data not shown), which disagree with the expected (p)ppGpp levels predicted to be produced in each mutant. In addition, YjbM appeared to preferentially synthesize pppGpp more than ppGpp (185). These results indicate that the slow growth and the cell chaining/motility observed in the *relA* mutant might be differentially regulated by ppGpp and pppGpp, respectively. Consistent with this idea, Cashel and colleague have demonstrated recently that pppGpp is less potent than ppGpp with respect to regulation of growth rate in *E. coli* (151). Furthermore, assays of *B. subtilis* DNA primase suggest that pppGpp is a more potent inhibitor of this enzyme than ppGpp (261). Expression profiles suggest that the level of *yjbM* transcription peaks during rapid growth and transition state in rich media

(185, 270). In addition, YjbM contributes, albeit less substantially than RelA, to the basal levels of (p)ppGpp present during exponential growth (185), while YwaC has been suggested to be responsible for the increase in (p)ppGpp observed during alkaline shock (185). Future experiments should be designed to estimate the relative regulatory activities of ppGpp versus pppGpp in influencing the developmental decision-making outcomes in *B subtilis*. These experiments can be carried out by manipulating the expression of two ectopic (p)ppGpp synthetases in (p)ppGpp^0, to obtain a preferential accumulation of ppGpp or pppGpp. Lastly, the findings of the above proposed experiments could have important implications with respect to (p)ppGpp synthesis inhibitors drug design. Researchers are now developing drugs that can act as (p)ppGpp analogues to inhibit (p)ppGpp synthesis (334-336). Relacin is one drug candidate that was demonstrated to inhibit (p)ppGpp synthesis in vitro and in vivo by blocking the dissociation of RelA from stalled ribosomes (336). Consequently, Relacin was shown to affect entry into stationary phase and causes cell death. Furthermore, Relacin inhibits spore and biofilm formation (336). Relacin mode of action was not examined against the small monofunctional (p)ppGpp synthases such as YjbM or YwaC. Unlike RelA, these enzymes have not been reported to interact with ribosomes, but are responsible for the accumulation of basal (p)ppGpp levels. Thus, small monofunctional (p)ppGpp synthases enzymes could provide cell with a resistance mechanism against the (p)ppGpp inhibitors, like Relacin.

The contribution of changes in (p)ppGpp and GTP pools to cell chaining and motility

In Gram positive bacteria, transcriptional regulation exerted by (p)ppGpp relies heavily on modulating GTP levels (206, 210). The accumulation of (p)ppGpp reduces intracellular GTP levels. When the GTP-sensing repressor CodY is inactivated in *B. subtilis*, 75% of the population grows as unchained cells. In contrast, 100% of the *relA* mutant population grow exclusively as unchained cells. Thus, the Δ*relA* cell unchaining phenotype cannot be fully explained by derepression of expression by CodY. Future experiment should be design to uncover the other mechanism(s) responsible for Δ*relA* cell unchaining phenotype. These mechanisms might be mediated by the accumulation of (p)ppGpp and/or by GTP pool reduction, independent of CodY. To separate the possible roles that (p)ppGpp or GTP play in the Δ*relA* cell unchaining phenotype, the GMP synthase inhibitor decoyinine could be used to deplete GTP independent of (p)ppGpp accumulation. The loss of chaining, increase in motility, SigD level and activity in Δ*codY* cultures treated with decoyinine would allow us to determine if the Δ*relA* cell unchaining phenotype could be also explained by GTP pool reduction, independent of CodY. Also, to distinguish the effect of (p)ppGpp accumulation from GTP pool reduction on Δ*relA* cell unchaining phenotype, Δ*codY* cultures treated with decoyinine are compared to Δ*codY* cultures similarly treated with mupirocin. Mupirocin causes (p)ppGpp accumulation and subsequent GTP pool reduction. Another strategy to

deplete GTP independent of (p)ppGpp accumulation is through mutation of enzymes in the *de novo* GTP biosynthesis pathway, such as GmK or HprT (210).

Identification of components required for FacX mediated activity

Our result indicates that FacX is an extracellular quorum-sensing signal, accumulating to assayable levels at higher cell densities. Conditioned media prepared from late exponential phase cultures were able to induce sporulation when combined with KinA in exponentially growing cells. In addition, diluting stationary phase conditioned media with fresh media resulted in severe reduction in the number of spore-forming cells when KinA was also induced. These results suggest that the levels of FacX are critical to its role in coordinating sporulation with growth phase. Moreover, cells expressing the constitutively active Spo0A-SAD67 were also able to sporulate when grown in the conditioned media. This particular result indicates that FacX triggers sporulation without affecting the canonical phosphorelay and phosphorelay modulating proteins. One possible mechanism by which FacX promote sporulation is through lowering GTP levels. Spo0A-SAD67 was shown to be sufficient to trigger sporulation if cells are also given compound (decoyinine) to a drop in cellular GTP levels (iteron 1993). Furure experiments should be designed to test if FacX can cause a drop in GTP levels.

Attempts to purify and identify FacX were unsuccessful. Currently, we are still working on identifying FacX using LC-MS. Future work should focus on

complementary approaches to identify genetic components required for FacX activity. Genetic screens can be designed to identify genes required for FacX synthesis, secretion, processing, uptake and/or activity.

REFERENCES

1. Lopez D & Kolter R (2010) Extracellular signals that define distinct and coexisting cell fates in *Bacillus subtilis*. *FEMS Microbiol Rev* 34(2):134-149.

2. Camilli A & Bassler BL (2006) Bacterial small-molecule signaling pathways. *Science* 311(5764):1113-1116.

3. Burkholder PR & Giles NH, Jr. (1947) Induced biochemical mutations in *Bacillus subtilis*. *Am J Bot* 34(6):345-348.

4. Aguilar C, Vlamakis H, Losick R, & Kolter R (2007) Thinking about *Bacillus subtilis* as a multicellular organism. *Curr Opin Microbiol* 10(6):638-643.

5. Britton RA, Eichenberger P, Gonzalez-Pastor JE, Fawcett P, *et al.* (2002) Genome-wide analysis of the stationary-phase sigma factor (sigma-H) regulon of *Bacillus subtilis*. *J Bacteriol* 184(17):4881-4890.

6. Lee JM, Zhang S, Saha S, Santa Anna S, *et al.* (2001) RNA expression analysis using an antisense *Bacillus subtilis* genome array. *J Bacteriol* 183(24):7371-7380.

7. Molle V, Nakaura Y, Shivers RP, Yamaguchi H, *et al.* (2003) Additional targets of the *Bacillus subtilis* global regulator CodY identified by chromatin immunoprecipitation and genome-wide transcript analysis. *J Bacteriol* 185(6):1911-1922.

8. Silvaggi JM, Perkins JB, & Losick R (2006) Genes for small, noncoding RNAs under sporulation control in *Bacillus subtilis*. *J Bacteriol* 188(2):532-541.

9. Youngman P, Perkins JB, & Losick R (1984) Construction of a cloning site near one end of Tn917 into which foreign DNA may be inserted without affecting transposition in *Bacillus subtilis* or expression of the transposon-borne erm gene. *Plasmid* 12(1):1-9.

10. Auchtung JM, Lee CA, Monson RE, Lehman AP, *et al.* (2005) Regulation of a *Bacillus subtilis* mobile genetic element by intercellular signaling and the global DNA damage response. *Proc Natl Acad Sci U S A* 102(35):12554-12559.

11. Zeigler DR, Pragai Z, Rodriguez S, Chevreux B, *et al.* (2008) The origins of 168, W23, and other *Bacillus subtilis* legacy strains. *J Bacteriol* 190(21):6983-6995.

12. Errington J (2003) Regulation of endospore formation in *Bacillus subtilis*. *Nat Rev Microbiol* 1(2):117-126.

13. Errington J (1996) Determination of cell fate in *Bacillus subtilis*. *Trends Genet* 12(1):31-34.

14. Errington J (1993) *Bacillus subtilis* sporulation: regulation of gene expression and control of morphogenesis. *Microbiol Rev* 57(1):1-33.

15. Hilbert DW & Piggot PJ (2004) Compartmentalization of gene expression during *Bacillus subtilis* spore formation. *Microbiol Mol Biol Rev* 68(2):234-262.

16. Higgins D & Dworkin J (2012) Recent progress in *Bacillus subtilis* sporulation. *FEMS Microbiol Rev* 36(1):131-148.

17. Parker GF, Daniel RA, & Errington J (1996) Timing and genetic regulation of commitment to sporulation in *Bacillus subtilis*. *Microbiology* 142 (Pt 12):3445-3452.

18. Sonenshein AL (2000) Control of sporulation initiation in *Bacillus subtilis*. *Curr Opin Microbiol* 3(6):561-566.

19. Stragier P & Losick R (1996) Molecular genetics of sporulation in *Bacillus subtilis*. *Annu Rev Genet* 30:297-241.

20. Jiang M, Shao W, Perego M, & Hoch JA (2000) Multiple histidine kinases regulate entry into stationary phase and sporulation in *Bacillus subtilis*. *Mol Microbiol* 38(3):535-542.

21. LeDeaux JR, Yu N, & Grossman AD (1995) Different roles for KinA, KinB, and KinC in the initiation of sporulation in *Bacillus subtilis*. *J Bacteriol* 177(3):861-863.

22. Eswaramoorthy P & Fujita M (2010) Systematic domain deletion analysis of the major sporulation kinase in *Bacillus subtilis*. *J Bacteriol* 192(6):1744-1748.

23. Tojo S, Hirooka K, & Fujita Y (2013) Expression of *kinA* and *kinB* of *Bacillus subtilis*, necessary for sporulation initiation, is under positive stringent transcription control. *J Bacteriol* 195(8):1656-1665.

24. Devi SN, Vishnoi M, Kiehler B, Haggett L, *et al.* (2015) In vivo functional characterization of the transmembrane histidine kinase KinC in *Bacillus subtilis*. *Microbiology* 161(5): 1092-1104.

25. Vishnoi M, Narula J, Devi SN, Dao HA, *et al.* (2013) Triggering sporulation in *Bacillus subtilis* with artificial two-component systems reveals the importance of proper Spo0A activation dynamics. *Mol Microbiol* 90(1):181-194.

26. Lopez D, Vlamakis H, Losick R, & Kolter R (2009) Cannibalism enhances biofilm development in *Bacillus subtilis*. *Mol Microbiol* 74(3):609-618.

27. Fujita M, Gonzalez-Pastor JE, & Losick R (2005) High- and low-threshold genes in the Spo0A regulon of *Bacillus subtilis*. *J Bacteriol* 187(4):1357-1368.

28. Burbulys D, Trach KA, & Hoch JA (1991) Initiation of sporulation in *B. subtilis* is controlled by a multicomponent phosphorelay. *Cell* 64(3):545-552.

29. Molle V, Fujita M, Jensen ST, Eichenberger P, *et al.* (2003) The Spo0A regulon of *Bacillus subtilis*. *Mol Microbiol* 50(5):1683-1701.

30. Wang L, Grau R, Perego M, & Hoch JA (1997) A novel histidine kinase inhibitor regulating development in *Bacillus subtilis*. *Genes Dev* 11(19):2569-2579.

31. Jacques DA, Langley DB, Hynson RM, Whitten AE, *et al.* (2011) A novel structure of an antikinase and its inhibitor. *J Mol Biol* 405(1):214-226.

32. Cunningham KA & Burkholder WF (2009) The histidine kinase inhibitor Sda binds near the site of autophosphorylation and may sterically hinder autophosphorylation and phosphotransfer to Spo0F. *Mol Microbiol* 71(3):659-677.

33. Antoniewski C, Savelli B, & Stragier P (1990) The *spoIIJ* gene, which regulates early developmental steps in *Bacillus subtilis*, belongs to a class of environmentally responsive genes. *J Bacteriol* 172(1):86-93.

34. Perego M, Hanstein C, Welsh KM, Djavakhishvili T, *et al.* (1994) Multiple protein-aspartate phosphatases provide a mechanism for the integration of diverse signals in the control of development in *B. subtilis*. *Cell* 79(6):1047-1055.

35. Tzeng YL, Zhou XZ, & Hoch JA (1998) Phosphorylation of the Spo0B response regulator phosphotransferase of the phosphorelay initiating development in *Bacillus subtilis*. *J Biol Chem* 273(37):23849-23855.

36. Veening JW, Hamoen LW, & Kuipers OP (2005) Phosphatases modulate the bistable sporulation gene expression pattern in *Bacillus subtilis*. *Mol Microbiol* 56(6):1481-1494.

37. Smits WK, Bongiorni C, Veening JW, Hamoen LW, *et al.* (2007) Temporal separation of distinct differentiation pathways by a dual specificity Rap-Phr system in *Bacillus subtilis*. *Mol Microbiol* 65(1):103-120.

38. Parashar V, Mirouze N, Dubnau DA, & Neiditch MB (2011) Structural basis of response regulator dephosphorylation by Rap phosphatases. *PLoS Biol* 9(2):e1000589.

39. Perego M (2001) A new family of aspartyl phosphate phosphatases targeting the sporulation transcription factor Spo0A of *Bacillus subtilis*. *Mol Microbiol* 42(1):133-143.

40. Solomon JM, Lazazzera BA, & Grossman AD (1996) Purification and characterization of an extracellular peptide factor that affects two different developmental pathways in *Bacillus subtilis*. *Genes Dev* 10(16):2014-2024.

41. Mueller JP, Bukusoglu G, & Sonenshein AL (1992) Transcriptional regulation of *Bacillus subtilis* glucose starvation-inducible genes: control of *gsiA* by the ComP-ComA signal transduction system. *J Bacteriol* 174(13):4361-4373.

42. Jiang M, Grau R, & Perego M (2000) Differential processing of propeptide inhibitors of Rap phosphatases in *Bacillus subtilis*. *J Bacteriol* 182(2):303-310.

43. Mirouze N, Parashar V, Baker MD, Dubnau DA, *et al.* (2011) An atypical Phr peptide regulates the developmental switch protein RapH. *J Bacteriol* 193(22):6197-6206.

44. Baker MD & Neiditch MB (2011) Structural basis of response regulator inhibition by a bacterial anti-activator protein. *PLoS Biol* 9(12):e1001226.

45. Lazazzera BA & Grossman AD (1998) The ins and outs of peptide signaling. *Trends Microbiol* 6(7):288-294.

46. McQuade RS, Comella N, & Grossman AD (2001) Control of a family of phosphatase regulatory genes (phr) by the alternate sigma factor sigma-H of *Bacillus subtilis*. *J Bacteriol* 183(16):4905-4909.

47. Healy J, Weir J, Smith I, & Losick R (1991) Post-transcriptional control of a sporulation regulatory gene encoding transcription factor sigma H in *Bacillus subtilis*. *Mol Microbiol* 5(2):477-487.

48. Pottathil M & Lazazzera BA (2003) The extracellular Phr peptide-Rap phosphatase signaling circuit of *Bacillus subtilis*. *Front Biosci* 8:d32-45.

49. Koide A & Hoch JA (1994) Identification of a second oligopeptide transport system in *Bacillus subtilis* and determination of its role in sporulation. *Mol Microbiol* 13(3):417-426.

50. Gallego del Sol F & Marina A (2013) Structural basis of Rap phosphatase inhibition by Phr peptides. *PLoS Biol* 11(3):e1001511.

51. Parashar V, Jeffrey PD, & Neiditch MB (2013) Conformational change-induced repeat domain expansion regulates Rap phosphatase quorum-sensing signal receptors. *PLoS Biol* 11(3):e1001512.

52. Predich M, Nair G, & Smith I (1992) *Bacillus subtilis* early sporulation genes *kinA*, *spo0F*, and *spo0A* are transcribed by the RNA polymerase containing sigma H. *J Bacteriol* 174(9):2771-2778.

53. Fujita M & Sadaie Y (1998) Feedback loops involving Spo0A and AbrB in in vitro transcription of the genes involved in the initiation of sporulation in *Bacillus subtilis*. *J Biochem* 124(1):98-104.

54. Strauch MA, Trach KA, Day J, & Hoch JA (1992) Spo0A activates and represses its own synthesis by binding at its dual promoters. *Biochimie* 74(7-8):619-626.

55. Chastanet A & Losick R (2011) Just-in-time control of Spo0A synthesis in *Bacillus subtilis* by multiple regulatory mechanisms. *J Bacteriol* 193(22):6366-6374.

56. Chibazakura T, Kawamura F, & Takahashi H (1991) Differential regulation of spo0A transcription in *Bacillus subtilis*: glucose represses promoter switching at the initiation of sporulation. *J Bacteriol* 173(8):2625-2632.

57. Banse AV, Chastanet A, Rahn-Lee L, Hobbs EC, *et al.* (2008) Parallel pathways of repression and antirepression governing the transition to stationary phase in *Bacillus subtilis*. *Proc Natl Acad Sci U S A* 105(40):15547-15552.

58. Bai U, Mandic-Mulec I, & Smith I (1993) SinI modulates the activity of SinR, a developmental switch protein of *Bacillus subtilis*, by protein-protein interaction. *Genes Dev* 7(1):139-148.

59. Chai Y, Norman T, Kolter R, & Losick R (2011) Evidence that metabolism and chromosome copy number control mutually exclusive cell fates in *Bacillus subtilis*. *EMBO J* 30(7):1402-1413.

60. Hahn J, Kong L, & Dubnau D (1994) The regulation of competence transcription factor synthesis constitutes a critical control point in the regulation of competence in *Bacillus subtilis*. *J Bacteriol* 176(18):5753-5761.

61. Kearns DB, Chu F, Branda SS, Kolter R, *et al.* (2005) A master regulator for biofilm formation by *Bacillus subtilis*. *Mol Microbiol* 55(3):739-749.

62. Hoa TT, Tortosa P, Albano M, & Dubnau D (2002) Rok (YkuW) regulates genetic competence in *Bacillus subtilis* by directly repressing *comK*. *Mol Microbiol* 43(1):15-26.

63. Albano M, Smits WK, Ho LT, Kraigher B, *et al.* (2005) The Rok protein of *Bacillus subtilis* represses genes for cell surface and extracellular functions. *J Bacteriol* 187(6):2010-2019.

64. Fujita M & Losick R (2005) Evidence that entry into sporulation in *Bacillus subtilis* is governed by a gradual increase in the level and activity of the master regulator Spo0A. *Genes Dev* 19(18):2236-2244.

65. Eswaramoorthy P, Dinh J, Duan D, Igoshin OA, *et al.* (2010) Single-cell measurement of the levels and distributions of the phosphorelay components in a population of sporulating *Bacillus subtilis* cells. *Microbiology* 156(Pt 8):2294-2304.

66. Levine JH, Fontes ME, Dworkin J, & Elowitz MB (2012) Pulsed feedback defers cellular differentiation. *PLoS Biol* 10(1):e1001252.

67. Narula J, Devi SN, Fujita M, & Igoshin OA (2012) Ultrasensitivity of the *Bacillus subtilis* sporulation decision. *Proc Natl Acad Sci U S A* 109(50):E3513-3522.

68. Freese E, Heinze JE, & Galliers EM (1979) Partial purine deprivation causes sporulation of *Bacillus subtilis* in the presence of excess ammonia, glucose and phosphate. *J Gen Microbiol* 115(1):193-205.

69. Lopez JM, Dromerick A, & Freese E (1981) Response of guanosine 5'-triphosphate concentration to nutritional changes and its significance for *Bacillus subtilis* sporulation. *J Bacteriol* 146(2):605-613.

70. Ratnayake-Lecamwasam M, Serror P, Wong KW, & Sonenshein AL (2001) *Bacillus subtilis* CodY represses early-stationary-phase genes by sensing GTP levels. *Genes Dev* 15(9):1093-1103.

71. Slack FJ, Serror P, Joyce E, & Sonenshein AL (1995) A gene required for nutritional repression of the *Bacillus subtilis* dipeptide permease operon. *Mol Microbiol* 15(4):689-702.

72. Guedon E, Serror P, Ehrlich SD, Renault P, *et al.* (2001) Pleiotropic transcriptional repressor CodY senses the intracellular pool of branched-chain amino acids in *Lactococcus lactis*. *Mol Microbiol* 40(5):1227-1239.

73. Shivers RP & Sonenshein AL (2004) Activation of the *Bacillus subtilis* global regulator CodY by direct interaction with branched-chain amino acids. *Mol Microbiol* 53(2):599-611.

74. Krasny L & Gourse RL (2004) An alternative strategy for bacterial ribosome synthesis: *Bacillus subtilis* rRNA transcription regulation. *EMBO J* 23(22):4473-4483.

75. Chen R, Guttenplan SB, Blair KM, & Kearns DB (2009) Role of the sigmaD-dependent autolysins in *Bacillus subtilis* population heterogeneity. *J Bacteriol* 191(18):5775-5784.

76. Kearns DB & Losick R (2005) Cell population heterogeneity during growth of *Bacillus subtilis*. *Genes Dev* 19(24):3083-3094.

77. Smith TJ, Blackman SA, & Foster SJ (2000) Autolysins of *Bacillus subtilis*: multiple enzymes with multiple functions. *Microbiology* 146 (Pt 2):249-262.

78. Kuroda A & Sekiguchi J (1991) Molecular cloning and sequencing of a major *Bacillus subtilis* autolysin gene. *J Bacteriol* 173(22):7304-7312.

79. Lazarevic V, Margot P, Soldo B, & Karamata D (1992) Sequencing and analysis of the *Bacillus subtilis lytRABC* divergon: a regulatory unit encompassing the structural genes of the N-acetylmuramoyl-L-alanine amidase and its modifier. *J Gen Microbiol* 138(9):1949-1961.

80. Margot P, Mauel C, & Karamata D (1994) The gene of the N-acetylglucosaminidase, a *Bacillus subtilis* 168 cell wall hydrolase not involved in vegetative cell autolysis. *Mol Microbiol* 12(4):535-545.

81. Margot P, Pagni M, & Karamata D (1999) *Bacillus subtilis* 168 gene *lytF* encodes a gamma-D-glutamate-meso-diaminopimelate muropeptidase expressed by the alternative vegetative sigma factor, sigmaD. *Microbiology* 145 (Pt 1):57-65.

82. Helmann JD, Marquez LM, & Chamberlin MJ (1988) Cloning, sequencing, and disruption of the *Bacillus subtilis* sigma 28 gene. *J Bacteriol* 170(4):1568-1574.

83. Marquez LM, Helmann JD, Ferrari E, Parker HM, *et al.* (1990) Studies of sigma D-dependent functions in *Bacillus subtilis*. *J Bacteriol* 172(6):3435-3443.

84. Pooley HM & Karamata D (1984) Genetic analysis of autolysin-deficient and flagellaless mutants of *Bacillus subtilis*. *J Bacteriol* 160(3):1123-1129.

85. Blackman SA, Smith TJ, & Foster SJ (1998) The role of autolysins during vegetative growth of *Bacillus subtilis* 168. *Microbiology* 144 (Pt 1):73-82.

86. Kearns DB (2010) A field guide to bacterial swarming motility. *Nat Rev Microbiol* 8(9):634-644.

87. Kearns DB & Losick R (2003) Swarming motility in undomesticated *Bacillus subtilis*. *Mol Microbiol* 49(3):581-590.

88. Henrichsen J (1972) Bacterial surface translocation: a survey and a classification. *Bacteriol Rev* 36(4):478-503.

89. Kearns DB (2013) You get what you select for: better swarming through more flagella. *Trends Microbiol* 21(10):508-509.

90. Macnab RM (2003) How bacteria assemble flagella. *Annu Rev Microbiol* 57:77-100.

91. Chevance FF & Hughes KT (2008) Coordinating assembly of a bacterial macromolecular machine. *Nat Rev Microbiol* 6(6):455-465.

92. Mukherjee S & Kearns DB (2014) The structure and regulation of flagella in *Bacillus subtilis*. *Annu Rev Genet* 48:319-340.

93. Macnab RM (1992) Genetics and biogenesis of bacterial flagella. *Annu Rev Genet* 26:131-158.

94. Calvio C, Celandroni F, Ghelardi E, Amati G, *et al.* (2005) Swarming differentiation and swimming motility in *Bacillus subtilis* are controlled by *swrA*, a newly identified dicistronic operon. *J Bacteriol* 187(15):5356-5366.

95. Kearns DB, Chu F, Rudner R, & Losick R (2004) Genes governing swarming in *Bacillus subtilis* and evidence for a phase variation mechanism controlling surface motility. *Mol Microbiol* 52(2):357-369.

96. Calvio C, Osera C, Amati G, & Galizzi A (2008) Autoregulation of *swrAA* and motility in *Bacillus subtilis*. *J Bacteriol* 190(16):5720-5728.

97. Tsukahara K & Ogura M (2008) Promoter selectivity of the *Bacillus subtilis* response regulator DegU, a positive regulator of the *fla/che* operon and *sacB*. *BMC Microbiol* 8:8.

98. Murray EJ, Kiley TB, & Stanley-Wall NR (2009) A pivotal role for the response regulator DegU in controlling multicellular behaviour. *Microbiology* 155(Pt 1):1-8.

99. Amati G, Bisicchia P, & Galizzi A (2004) DegU-P represses expression of the motility *fla-che* operon in *Bacillus subtilis*. *J Bacteriol* 186(18):6003-6014.

100. Kobayashi K (2007) Gradual activation of the response regulator DegU controls serial expression of genes for flagellum formation and biofilm formation in *Bacillus subtilis*. *Mol Microbiol* 66(2):395-409.

101. Chen L & Helmann JD (1994) The *Bacillus subtilis* sigma D-dependent operon encoding the flagellar proteins FliD, FliS, and FliT. *J Bacteriol* 176(11):3093-3101.

102. Cozy LM & Kearns DB (2010) Gene position in a long operon governs motility development in *Bacillus subtilis*. *Mol Microbiol* 76(2):273-285.

103. Kobayashi K (2008) SlrR/SlrA controls the initiation of biofilm formation in *Bacillus subtilis*. *Mol Microbiol* 69(6):1399-1410.

104. Cozy LM, Phillips AM, Calvo RA, Bate AR, *et al.* (2012) SlrA/SinR/SlrR inhibits motility gene expression upstream of a hypersensitive and hysteretic switch at the level of sigma(D) in *Bacillus subtilis*. *Mol Microbiol* 83(6):1210-1228.

105. Chai Y, Kolter R, & Losick R (2009) Paralogous antirepressors acting on the master regulator for biofilm formation in *Bacillus subtilis*. *Mol Microbiol* 74(4):876-887.

106. Chai Y, Kolter R, & Losick R (2010) Reversal of an epigenetic switch governing cell chaining in *Bacillus subtilis* by protein instability. *Mol Microbiol* 78(1):218-229.

107. Chai Y, Norman T, Kolter R, & Losick R (2010) An epigenetic switch governing daughter cell separation in *Bacillus subtilis*. *Genes Dev* 24(8):754-765.

108. Estacio W, Anna-Arriola SS, Adedipe M, & Marquez-Magana LM (1998) Dual promoters are responsible for transcription initiation of the *fla/che* operon in *Bacillus subtilis*. *J Bacteriol* 180(14):3548-3555.

109. West JT, Estacio W, & Marquez-Magana L (2000) Relative roles of the *fla/che* P(*A*), P(*D-3*), and P(*sigD*) promoters in regulating motility and *sigD* expression in *Bacillus subtilis*. *J Bacteriol* 182(17):4841-4848.

110. Caramori T, Barilla D, Nessi C, Sacchi L, *et al.* (1996) Role of FlgM in sigma D-dependent gene expression in *Bacillus subtilis*. *J Bacteriol* 178(11):3113-3118.

111. Bertero MG, Gonzales B, Tarricone C, Ceciliani F, *et al.* (1999) Overproduction and characterization of the *Bacillus subtilis* anti-sigma factor FlgM. *J Biol Chem* 274(17):12103-12107.

112. Calvo RA & Kearns DB (2015) FlgM is secreted by the flagellar export apparatus in *Bacillus subtilis*. *J Bacteriol* 197(1):81-91.

113. Mirel DB, Lauer P, & Chamberlin MJ (1994) Identification of flagellar synthesis regulatory and structural genes in a sigma D-dependent operon of *Bacillus subtilis*. *J Bacteriol* 176(15):4492-4500.

114. Hsueh YH, Cozy LM, Sham LT, Calvo RA, *et al.* (2011) DegU-phosphate activates expression of the anti-sigma factor FlgM in *Bacillus subtilis*. *Mol Microbiol* 81(4):1092-1108.

115. Hamoen LW, Eshuis H, Jongbloed J, Venema G, *et al.* (1995) A small gene, designated comS, located within the coding region of the fourth amino acid-activation domain of *srfA*, is required for competence development in *Bacillus subtilis*. *Mol Microbiol* 15(1):55-63.

116. Berthet J, Rall TW, & Sutherland EW (1957) The relationship of epinephrine and glucagon to liver phosphorylase. IV. Effect of epinephrine and glucagon on the reactivation of phosphorylase in liver homogenates. *J Biol Chem* 224(1):463-475.

117. Ashman DF, Lipton R, Melicow MM, & Price TD (1963) Isolation of adenosine 3', 5'-monophosphate and guanosine 3', 5'-monophosphate from rat urine. *Biochem Biophys Res Commun* 11:330-334.

118. Bernlohr RW, Haddox MK, & Goldberg ND (1974) Cyclic guanosine 3':5'-monophosphate in *Escherichia coli* and *Bacillus lichenformis*. *J Biol Chem* 249(13):4329-4331.

119. Kalia D, Merey G, Nakayama S, Zheng Y, *et al.* (2013) Nucleotide, c-di-GMP, c-di-AMP, cGMP, cAMP, (p)ppGpp signaling in bacteria and implications in pathogenesis. *Chem Soc Rev* 42(1):305-341.

120. Busby S & Ebright RH (1999) Transcription activation by catabolite activator protein (CAP). *J Mol Biol* 293(2):199-213.

121. Jackson DW, Simecka JW, & Romeo T (2002) Catabolite repression of *Escherichia coli* biofilm formation. *J Bacteriol* 184(12):3406-3410.

122. Gorke B & Stulke J (2008) Carbon catabolite repression in bacteria: many ways to make the most out of nutrients. *Nat Rev Microbiol* 6(8):613-624.

123. Soutourina O, Kolb A, Krin E, Laurent-Winter C, *et al.* (1999) Multiple control of flagellum biosynthesis in Escherichia coli: role of H-NS protein and the cyclic AMP-catabolite activator protein complex in transcription of the *flhDC* master operon. *J Bacteriol* 181(24):7500-7508.

124. Liang W, Pascual-Montano A, Silva AJ, & Benitez JA (2007) The cyclic AMP receptor protein modulates quorum sensing, motility and multiple genes that affect intestinal colonization in *Vibrio cholerae*. *Microbiology* 153(Pt 9):2964-2975.

125. Setlow B & Setlow P (1978) Levels of cyclic GMP in dormant, germinated, and outgrowing spores and growing and sporulating cells of *Bacillus megaterium*. *J Bacteriol* 136(1):433-436.

126. Bhatnagar NB, Bhatnagar R, & Venkitasubramanian TA (1984) Characterization and metabolism of cyclic guanosine 3'5'-monophosphate in Mycobacterium smegmatis. *Biochem Biophys Res Commun* 121(2):634-640.

127. Marden JN, Dong Q, Roychowdhury S, Berleman JE, *et al.* (2011) Cyclic GMP controls *Rhodospirillum centenum* cyst development. *Mol Microbiol* 79(3):600-615.

128. Ross P, Weinhouse H, Aloni Y, Michaeli D, *et al.* (1987) Regulation of cellulose synthesis in *Acetobacter xylinum* by cyclic diguanylic acid. *Nature* 325(6101):279-281.

129. Paul R, Weiser S, Amiot NC, Chan C, *et al.* (2004) Cell cycle-dependent dynamic localization of a bacterial response regulator with a novel di-guanylate cyclase output domain. *Genes Dev* 18(6):715-727.

130. Ryjenkov DA, Tarutina M, Moskvin OV, & Gomelsky M (2005) Cyclic diguanylate is a ubiquitous signaling molecule in bacteria: insights into biochemistry of the GGDEF protein domain. *J Bacteriol* 187(5):1792-1798.

131. Tal R, Wong HC, Calhoon R, Gelfand D, *et al.* (1998) Three cdg operons control cellular turnover of cyclic di-GMP in *Acetobacter xylinum*: genetic organization and occurrence of conserved domains in isoenzymes. *J Bacteriol* 180(17):4416-4425.

132. Schmidt AJ, Ryjenkov DA, & Gomelsky M (2005) The ubiquitous protein domain EAL is a cyclic diguanylate-specific phosphodiesterase: enzymatically active and inactive EAL domains. *J Bacteriol* 187(14):4774-4781.

133. Ryan RP, Fouhy Y, Lucey JF, Crossman LC, *et al.* (2006) Cell-cell signaling in Xanthomonas campestris involves an HD-GYP domain protein that functions in cyclic di-GMP turnover. *Proc Natl Acad Sci U S A* 103(17):6712-6717.

134. D'Argenio DA & Miller SI (2004) Cyclic di-GMP as a bacterial second messenger. *Microbiology* 150(Pt 8):2497-2502.

135. Romling U, Gomelsky M, & Galperin MY (2005) C-di-GMP: the dawning of a novel bacterial signalling system. *Mol Microbiol* 57(3):629-639.

136. Jenal U & Malone J (2006) Mechanisms of cyclic-di-GMP signaling in bacteria. *Annu Rev Genet* 40:385-407.

137. Ryjenkov DA, Simm R, Romling U, & Gomelsky M (2006) The PilZ domain is a receptor for the second messenger c-di-GMP: the PilZ domain protein YcgR controls motility in enterobacteria. *J Biol Chem* 281(41):30310-30314.

138. Pratt JT, Tamayo R, Tischler AD, & Camilli A (2007) PilZ domain proteins bind cyclic diguanylate and regulate diverse processes in *Vibrio cholerae*. *J Biol Chem* 282(17):12860-12870.

139. Tuckerman JR, Gonzalez G, & Gilles-Gonzalez MA (2011) Cyclic di-GMP activation of polynucleotide phosphorylase signal-dependent RNA processing. *J Mol Biol* 407(5):633-639.

140. Hickman JW & Harwood CS (2008) Identification of FleQ from Pseudomonas aeruginosa as a c-di-GMP-responsive transcription factor. *Mol Microbiol* 69(2):376-389.

141. Krasteva PV, Fong JC, Shikuma NJ, Beyhan S, *et al.* (2010) *Vibrio cholerae* VpsT regulates matrix production and motility by directly sensing cyclic di-GMP. *Science* 327(5967):866-868.

142. Leduc JL & Roberts GP (2009) Cyclic di-GMP allosterically inhibits the CRP-like protein (Clp) of *Xanthomonas axonopodis* pv. citri. *J Bacteriol* 191(22):7121-7122.

143. Fazli M, O'Connell A, Nilsson M, Niehaus K, *et al.* (2011) The CRP/FNR family protein Bcam1349 is a c-di-GMP effector that regulates biofilm formation in the respiratory pathogen *Burkholderia cenocepacia*. *Mol Microbiol* 82(2):327-341.

144. Lee ER, Baker JL, Weinberg Z, Sudarsan N, *et al.* (2010) An allosteric self-splicing ribozyme triggered by a bacterial second messenger. *Science* 329(5993):845-848.

145. Sudarsan N, Lee ER, Weinberg Z, Moy RH, *et al.* (2008) Riboswitches in eubacteria sense the second messenger cyclic di-GMP. *Science* 321(5887):411-413.

146. Lee VT, Matewish JM, Kessler JL, Hyodo M, *et al.* (2007) A cyclic-di-GMP receptor required for bacterial exopolysaccharide production. *Mol Microbiol* 65(6):1474-1484.

147. Abel S, Chien P, Wassmann P, Schirmer T, *et al.* (2011) Regulatory cohesion of cell cycle and cell differentiation through interlinked phosphorylation and second messenger networks. *Mol Cell* 43(4):550-560.

148. Qi Y, Chuah ML, Dong X, Xie K, *et al.* (2011) Binding of cyclic diguanylate in the non-catalytic EAL domain of FimX induces a long-range conformational change. *J Biol Chem* 286(4):2910-2917.

149. Navarro MV, Newell PD, Krasteva PV, Chatterjee D, *et al.* (2011) Structural basis for c-di-GMP-mediated inside-out signaling controlling periplasmic proteolysis. *PLoS Biol* 9(2):e1000588.

150. Witte G, Hartung S, Buttner K, & Hopfner KP (2008) Structural biochemistry of a bacterial checkpoint protein reveals diadenylate cyclase activity regulated by DNA recombination intermediates. *Mol Cell* 30(2):167-178.

151. Mehne FM, Gunka K, Eilers H, Herzberg C, *et al.* (2013) Cyclic di-AMP homeostasis in *Bacillus subtilis*: both lack and high level accumulation of the nucleotide are detrimental for cell growth. *J Biol Chem* 288(3):2004-2017.

152. Bejerano-Sagie M, Oppenheimer-Shaanan Y, Berlatzky I, Rouvinski A, *et al.* (2006) A checkpoint protein that scans the chromosome for damage at the start of sporulation in *Bacillus subtilis*. *Cell* 125(4):679-690.

153. Corrigan RM & Grundling A (2013) Cyclic di-AMP: another second messenger enters the fray. *Nat Rev Microbiol* 11(8):513-524.

154. Zhang L, Li W, & He ZG (2013) DarR, a TetR-like transcriptional factor, is a cyclic di-AMP-responsive repressor in *Mycobacterium smegmatis*. *J Biol Chem* 288(5):3085-3096.

155. Corrigan RM, Campeotto I, Jeganathan T, Roelofs KG, *et al.* (2013) Systematic identification of conserved bacterial c-di-AMP receptor proteins. *Proc Natl Acad Sci U S A* 110(22):9084-9089.

156. Corrigan RM, Abbott JC, Burhenne H, Kaever V, *et al.* (2011) c-di-AMP is a new second messenger in *Staphylococcus aureus* with a role in controlling cell size and envelope stress. *PLoS Pathog* 7(9):e1002217.

157. Luo Y & Helmann JD (2012) Analysis of the role of *Bacillus subtilis* sigma(M) in beta-lactam resistance reveals an essential role for c-di-AMP in peptidoglycan homeostasis. *Mol Microbiol* 83(3):623-639.

158. Cashel M, Gentry, D.M., Hernandez, V.J., and Vinella, D. (1996) The stringent response. *Escherichia coli and Salmonella typhimurium Cellular and Molecular Biology*, ed Neidhardt FC (ASM Press, Washington D.C.), Vol 1, pp 1458-1496.

159. Potrykus K & Cashel M (2008) (p)ppGpp: still magical? *Annu Rev Microbiol* 62:35-51.

160. Cashel M & Gallant J (1969) Two compounds implicated in the function of the RC gene of Escherichia coli. *Nature* 221(5183):838-841.

161. Spira B, Silberstein N, & Yagil E (1995) Guanosine 3',5'-bispyrophosphate (ppGpp) synthesis in cells of *Escherichia coli* starved for Pi. *J Bacteriol* 177(14):4053-4058.

162. Battesti A & Bouveret E (2006) Acyl carrier protein/SpoT interaction, the switch linking SpoT-dependent stress response to fatty acid metabolism. *Mol Microbiol* 62(4):1048-1063.

163. Lapouge K, Schubert M, Allain FH, & Haas D (2008) Gac/Rsm signal transduction pathway of gamma-proteobacteria: from RNA recognition to regulation of social behaviour. *Mol Microbiol* 67(2):241-253.

164. Irr JD (1972) Control of nucleotide metabolism and ribosomal ribonucleic acid synthesis during nitrogen starvation of *Escherichia coli*. *J Bacteriol* 110(2):554-561.

165. Vinella D, Albrecht C, Cashel M, & D'Ari R (2005) Iron limitation induces SpoT-dependent accumulation of ppGpp in *Escherichia coli*. *Mol Microbiol* 56(4):958-970.

166. Xiao H, Kalman M, Ikehara K, Zemel S, *et al.* (1991) Residual guanosine 3',5'-bispyrophosphate synthetic activity of *relA* null mutants can be eliminated by *spoT* null mutations. *J Biol Chem* 266(9):5980-5990.

167. Atkinson GC, Tenson T, & Hauryliuk V (2011) The RelA/SpoT homolog (RSH) superfamily: distribution and functional evolution of ppGpp synthetases and hydrolases across the tree of life. *PLoS One* 6(8):e23479.

168. Sun D, Lee G, Lee JH, Kim HY, *et al.* (2010) A metazoan ortholog of SpoT hydrolyzes ppGpp and functions in starvation responses. *Nat Struct Mol Biol* 17(10):1188-1194.

169. Goldman E & Jakubowski H (1990) Uncharged tRNA, protein synthesis, and the bacterial stringent response. *Mol Microbiol* 4(12):2035-2040.

170. Wendrich TM, Blaha G, Wilson DN, Marahiel MA, *et al.* (2002) Dissection of the mechanism for the stringent factor RelA. *Mol Cell* 10(4):779-788.

171. English BP, Hauryliuk V, Sanamrad A, Tankov S, *et al.* (2011) Single-molecule investigations of the stringent response machinery in living bacterial cells. *Proc Natl Acad Sci U S A* 108(31):E365-373.

172. Gropp M, Strausz Y, Gross M, & Glaser G (2001) Regulation of *Escherichia coli* RelA requires oligomerization of the C-terminal domain. *J Bacteriol* 183(2):570-579.

173. An G, Justesen J, Watson RJ, & Friesen JD (1979) Cloning the *spoT* gene of *Escherichia coli*: identification of the spoT gene product. *J Bacteriol* 137(3):1100-1110.

174. Bougdour A & Gottesman S (2007) ppGpp regulation of RpoS degradation via anti-adaptor protein IraP. *Proc Natl Acad Sci U S A* 104(31):12896-12901.

175. Wout P, Pu K, Sullivan SM, Reese V, *et al.* (2004) The *Escherichia coli* GTPase CgtAE cofractionates with the 50S ribosomal subunit and interacts with SpoT, a ppGpp synthetase/hydrolase. *J Bacteriol* 186(16):5249-5257.

176. Jiang M, Sullivan SM, Wout PK, & Maddock JR (2007) G-protein control of the ribosome-associated stress response protein SpoT. *J Bacteriol* 189(17):6140-6147.

177. Raskin DM, Judson N, & Mekalanos JJ (2007) Regulation of the stringent response is the essential function of the conserved bacterial G protein CgtA in *Vibrio cholerae*. *Proc Natl Acad Sci U S A* 104(11):4636-4641.

178. Mechold U, Cashel M, Steiner K, Gentry D, *et al.* (1996) Functional analysis of a relA/spoT gene homolog from *Streptococcus equisimilis*. *J Bacteriol* 178(5):1401-1411.

179. Avarbock D, Avarbock A, & Rubin H (2000) Differential regulation of opposing RelMtb activities by the aminoacylation state of a tRNA.ribosome.mRNA.RelMtb complex. *Biochemistry* 39(38):11640-11648.

180. Mechold U, Murphy H, Brown L, & Cashel M (2002) Intramolecular regulation of the opposing (p)ppGpp catalytic activities of Rel(Seq), the Rel/Spo enzyme from *Streptococcus equisimilis*. *J Bacteriol* 184(11):2878-2888.

181. Hogg T, Mechold U, Malke H, Cashel M, *et al.* (2004) Conformational antagonism between opposing active sites in a bifunctional RelA/SpoT homolog modulates (p)ppGpp metabolism during the stringent response [corrected]. *Cell* 117(1):57-68.

182. Lemos JA, Lin VK, Nascimento MM, Abranches J, *et al.* (2007) Three gene products govern (p)ppGpp production by *Streptococcus mutans*. *Mol Microbiol* 65(6):1568-1581.

183. Abranches J, Martinez AR, Kajfasz JK, Chavez V, *et al.* (2009) The molecular alarmone (p)ppGpp mediates stress responses, vancomycin tolerance, and virulence in *Enterococcus faecalis*. *J Bacteriol* 191(7):2248-2256.

184. Das B, Pal RR, Bag S, & Bhadra RK (2009) Stringent response in *Vibrio cholerae*: genetic analysis of *spoT* gene function and identification of a novel (p)ppGpp synthetase gene. *Mol Microbiol* 72(2):380-398.

185. Nanamiya H, Kasai K, Nozawa A, Yun CS, *et al.* (2008) Identification and functional analysis of novel (p)ppGpp synthetase genes in *Bacillus subtilis*. *Mol Microbiol* 67(2):291-304.

186. Yan X, Zhao C, Budin-Verneuil A, Hartke A, *et al.* (2009) The (p)ppGpp synthetase RelA contributes to stress adaptation and virulence in *Enterococcus faecalis* V583. *Microbiology* 155(Pt 10):3226-3237.

187. Srivatsan A, Han Y, Peng J, Tehranchi AK, *et al.* (2008) High-precision, whole-genome sequencing of laboratory strains facilitates genetic studies. *PLoS Genet* 4(8):e1000139.

188. Geiger T, Kastle B, Gratani FL, Goerke C, *et al.* (2014) Two small (p)ppGpp synthases in *Staphylococcus aureus* mediate tolerance against cell envelope stress conditions. *J Bacteriol* 196(4):894-902.

189. Kim JN, Ahn SJ, Seaton K, Garrett S, *et al.* (2012) Transcriptional organization and physiological contributions of the *relQ* operon of *Streptococcus mutans. J Bacteriol* 194(8):1968-1978.

190. Paul BJ, Barker MM, Ross W, Schneider DA, *et al.* (2004) DksA: a critical component of the transcription initiation machinery that potentiates the regulation of rRNA promoters by ppGpp and the initiating NTP. *Cell* 118(3):311-322.

191. Paul BJ, Berkmen MB, & Gourse RL (2005) DksA potentiates direct activation of amino acid promoters by ppGpp. *Proc Natl Acad Sci U S A* 102(22):7823-7828.

192. Mechold U, Potrykus K, Murphy H, Murakami KS, *et al.* (2013) Differential regulation by ppGpp versus pppGpp in *Escherichia coli*. *Nucleic Acids Res* 41(12):6175-6189.

193. Ross W, Vrentas CE, Sanchez-Vazquez P, Gaal T, *et al.* (2013) The magic spot: a ppGpp binding site on *E. coli* RNA polymerase responsible for regulation of transcription initiation. *Mol Cell* 50(3):420-429.

194. Zuo Y, Wang Y, & Steitz TA (2013) The mechanism of *E. coli* RNA polymerase regulation by ppGpp is suggested by the structure of their complex. *Mol Cell* 50(3):430-436.

195. Lennon CW, Ross W, Martin-Tumasz S, Toulokhonov I, *et al.* (2012) Direct interactions between the coiled-coil tip of DksA and the trigger loop of RNA polymerase mediate transcriptional regulation. *Genes Dev* 26(23):2634-2646.

196. Srivatsan A & Wang JD (2008) Control of bacterial transcription, translation and replication by (p)ppGpp. *Curr Opin Microbiol* 11(2):100-105.

197. Wagner R (2002) Regulation of ribosomal RNA synthesis in *E. coli*: effects of the global regulator guanosine tetraphosphate (ppGpp). *J Mol Microbiol Biotechnol* 4(3):331-340.

198. Jishage M, Kvint K, Shingler V, & Nystrom T (2002) Regulation of sigma factor competition by the alarmone ppGpp. *Genes Dev* 16(10):1260-1270.

199. Magnusson LU, Farewell A, & Nystrom T (2005) ppGpp: a global regulator in *Escherichia coli*. *Trends Microbiol* 13(5):236-242.

200. Schneider DA, Gaal T, & Gourse RL (2002) NTP-sensing by rRNA promoters in *Escherichia coli* is direct. *Proc Natl Acad Sci U S A* 99(13):8602-8607.

201. Gaal T, Bartlett MS, Ross W, Turnbough CL, Jr., *et al.* (1997) Transcription regulation by initiating NTP concentration: rRNA synthesis in bacteria. *Science* 278(5346):2092-2097.

202. Irr J & Gallant J (1969) The control of ribonucleic acid synthesis in *Escherichia coli*. II. Stringent control of energy metabolism. *J Biol Chem* 244(8):2233-2239.

203. Stayton MM & Fromm HJ (1979) Guanosine 5'-diphosphate-3'-diphosphate inhibition of adenylosuccinate synthetase. *J Biol Chem* 254(8):2579-2581.

204. Jores L & Wagner R (2003) Essential steps in the ppGpp-dependent regulation of bacterial ribosomal RNA promoters can be explained by substrate competition. *J Biol Chem* 278(19):16834-16843.

205. Artsimovitch I, Patlan V, Sekine S, Vassylyeva MN, *et al.* (2004) Structural basis for transcription regulation by alarmone ppGpp. *Cell* 117(3):299-310.

206. Liu K, Bittner AN, & Wang JD (2015) Diversity in (p)ppGpp metabolism and effectors. *Curr Opin Microbiol* 24:72-79.

207. Inaoka T & Ochi K (2002) RelA protein is involved in induction of genetic competence in certain *Bacillus subtilis* strains by moderating the level of intracellular GTP. *J Bacteriol* 184(14):3923-3930.

208. Krasny L, Tiserova H, Jonak J, Rejman D, *et al.* (2008) The identity of the transcription +1 position is crucial for changes in gene expression in response to amino acid starvation in *Bacillus subtilis*. *Mol Microbiol* 69(1):42-54.

209. Natori Y, Tagami K, Murakami K, Yoshida S, *et al.* (2009) Transcription activity of individual rrn operons in *Bacillus subtilis* mutants deficient in (p)ppGpp synthetase genes, relA, yjbM, and ywaC. *J Bacteriol* 191(14):4555-4561.

210. Kriel A, Bittner AN, Kim SH, Liu K, *et al.* (2012) Direct regulation of GTP homeostasis by (p)ppGpp: a critical component of viability and stress resistance. *Mol Cell* 48(2):231-241.

211. Tojo S, Satomura T, Kumamoto K, Hirooka K, *et al.* (2008) Molecular mechanisms underlying the positive stringent response of the *Bacillus subtilis* ilv-leu operon, involved in the biosynthesis of branched-chain amino acids. *J Bacteriol* 190(18):6134-6147.

212. Handke LD, Shivers RP, & Sonenshein AL (2008) Interaction of *Bacillus subtilis* CodY with GTP. *J Bacteriol* 190(3):798-806.

213. Brinsmade SR & Sonenshein AL (2011) Dissecting complex metabolic integration provides direct genetic evidence for CodY activation by guanine nucleotides. *J Bacteriol* 193(20):5637-5648.

214. Hamel E & Cashel M (1973) Role of guanine nucleotides in protein synthesis. Elongation factor G and guanosine 5'-triphosphate,3'-diphosphate. *Proc Natl Acad Sci U S A* 70(11):3250-3254.

215. Pingoud A & Block W (1981) The elongation factor Tu . guanosine tetraphosphate complex. *Eur J Biochem* 116(3):631-634.

216. Mitkevich VA, Ermakov A, Kulikova AA, Tankov S, *et al.* (2010) Thermodynamic characterization of ppGpp binding to EF-G or IF2 and of initiator tRNA binding to free IF2 in the presence of GDP, GTP, or ppGpp. *J Mol Biol* 402(5):838-846.

217. Milon P, Tischenko E, Tomsic J, Caserta E, *et al.* (2006) The nucleotide-binding site of bacterial translation initiation factor 2 (IF2) as a metabolic sensor. *Proc Natl Acad Sci U S A* 103(38):13962-13967.

218. Nomura T, Fujita N, & Ishihama A (1986) Promoter selectivity of *Escherichia coli* RNA polymerase: alteration by fMet-tRNAfMet. *Nucleic Acids Res* 14(17):6857-6870.

219. Mandelstam J (1958) Turnover of protein in growing and non-growing populations of *Escherichia coli*. *Biochem J* 69(1):110-119.

220. Sussman AJ & Gilvarg C (1969) Protein turnover in amino acid-starved strains of *Escherichia coli* K-12 differing in their ribonucleic acid control. *J Biol Chem* 244(22):6304-6306.

221. Kuroda A (2006) A polyphosphate-lon protease complex in the adaptation of *Escherichia coli* to amino acid starvation. *Biosci Biotechnol Biochem* 70(2):325-331.

222. Levine A, Vannier F, Dehbi M, Henckes G, *et al.* (1991) The stringent response blocks DNA replication outside the ori region in *Bacillus subtilis* and at the origin in *Escherichia coli*. *J Mol Biol* 219(4):605-613.

223. Wegrzyn G (1999) Replication of plasmids during bacterial response to amino acid starvation. *Plasmid* 41(1):1-16.

224. Levine A, Autret S, & Seror SJ (1995) A checkpoint involving RTP, the replication terminator protein, arrests replication downstream of the origin during the stringent response in *Bacillus subtilis*. *Mol Microbiol* 15(2):287-295.

225. Ferullo DJ & Lovett ST (2008) The stringent response and cell cycle arrest in *Escherichia coli*. *PLoS Genet* 4(12):e1000300.

226. Slack FJ, Mueller JP, & Sonenshein AL (1993) Mutations that relieve nutritional repression of the *Bacillus subtilis* dipeptide permease operon. *J Bacteriol* 175(15):4605-4614.

227. Fisher SH, Rohrer K, & Ferson AE (1996) Role of CodY in regulation of the *Bacillus subtilis hut* operon. *J Bacteriol* 178(13):3779-3784.

228. Belitsky BR & Sonenshein AL (2013) Genome-wide identification of *Bacillus subtilis* CodY-binding sites at single-nucleotide resolution. *Proc Natl Acad Sci U S A* 110(17):7026-7031.

229. Debarbouille M, Gardan R, Arnaud M, & Rapoport G (1999) Role of *bkdR*, a transcriptional activator of the *sigL*-dependent isoleucine and valine degradation pathway in *Bacillus subtilis*. *J Bacteriol* 181(7):2059-2066.

230. Ferson AE, Wray LV, Jr., & Fisher SH (1996) Expression of the *Bacillus subtilis* gabP gene is regulated independently in response to nitrogen and amino acid availability. *Mol Microbiol* 22(4):693-701.

231. Mathiopoulos C, Mueller JP, Slack FJ, Murphy CG, *et al.* (1991) A *Bacillus subtilis* dipeptide transport system expressed early during sporulation. *Mol Microbiol* 5(8):1903-1913.

232. Fouet A & Sonenshein AL (1990) A target for carbon source-dependent negative regulation of the *citB* promoter of *Bacillus subtilis*. *J Bacteriol* 172(2):835-844.

233. Serror P & Sonenshein AL (1996) CodY is required for nutritional repression of *Bacillus subtilis* genetic competence. *J Bacteriol* 178(20):5910-5915.

234. Inaoka T, Takahashi K, Ohnishi-Kameyama M, Yoshida M, *et al.* (2003) Guanine nucleotides guanosine 5'-diphosphate 3'-diphosphate and GTP co-operatively regulate the production of an antibiotic bacilysin in *Bacillus subtilis*. *J Biol Chem* 278(4):2169-2176.

235. Bergara F, Ibarra C, Iwamasa J, Patarroyo JC, *et al.* (2003) CodY is a nutritional repressor of flagellar gene expression in *Bacillus subtilis*. *J Bacteriol* 185(10):3118-3126.

236. van Schaik W, Chateau A, Dillies MA, Coppee JY, *et al.* (2009) The global regulator CodY regulates toxin gene expression in *Bacillus anthracis* and is required for full virulence. *Infect Immun* 77(10):4437-4445.

237. Majerczyk CD, Dunman PM, Luong TT, Lee CY, *et al.* (2010) Direct targets of CodY in *Staphylococcus aureus*. *J Bacteriol* 192(11):2861-2877.

238. Dineen SS, McBride SM, & Sonenshein AL (2010) Integration of metabolism and virulence by *Clostridium difficile* CodY. *J Bacteriol* 192(20):5350-5362.

239. Guedon E, Sperandio B, Pons N, Ehrlich SD, *et al.* (2005) Overall control of nitrogen metabolism in *Lactococcus lactis* by CodY, and possible models for CodY regulation in Firmicutes. *Microbiology* 151(Pt 12):3895-3909.

240. Chateau A, van Schaik W, Joseph P, Handke LD, *et al.* (2013) Identification of CodY targets in *Bacillus anthracis* by genome-wide in vitro binding analysis. *J Bacteriol* 195(6):1204-1213.

241. Levdikov VM, Blagova E, Colledge VL, Lebedev AA, *et al.* (2009) Structural rearrangement accompanying ligand binding in the GAF domain of CodY from *Bacillus subtilis*. *J Mol Biol* 390(5):1007-1018.

242. Levdikov VM, Blagova E, Joseph P, Sonenshein AL, *et al.* (2006) The structure of CodY, a GTP- and isoleucine-responsive regulator of stationary phase and virulence in gram-positive bacteria. *J Biol Chem* 281(16):11366-11373.

243. Belitsky BR & Sonenshein AL (2008) Genetic and biochemical analysis of CodY-binding sites in *Bacillus subtilis*. *J Bacteriol* 190(4):1224-1236.

244. Petranovic D, Guedon E, Sperandio B, Delorme C, *et al.* (2004) Intracellular effectors regulating the activity of the *Lactococcus lactis* CodY pleiotropic transcription regulator. *Mol Microbiol* 53(2):613-621.

245. Lemos JA, Nascimento MM, Lin VK, Abranches J, *et al.* (2008) Global regulation by (p)ppGpp and CodY in *Streptococcus mutans*. *J Bacteriol* 190(15):5291-5299.

246. Wray LV, Jr. & Fisher SH (2011) *Bacillus subtilis* CodY operators contain overlapping CodY binding sites. *J Bacteriol* 193(18):4841-4848.

247. Majerczyk CD, Sadykov MR, Luong TT, Lee C, *et al.* (2008) *Staphylococcus aureus* CodY negatively regulates virulence gene expression. *J Bacteriol* 190(7):2257-2265.

248. Brinsmade SR, Alexander EL, Livny J, Stettner AI, *et al.* (2014) Hierarchical expression of genes controlled by the *Bacillus subtilis* global regulatory protein CodY. *Proc Natl Acad Sci U S A* 111(22):8227-8232.

249. Belitsky BR & Sonenshein AL (2011) Roadblock repression of transcription by *Bacillus subtilis* CodY. *J Mol Biol* 411(4):729-743.

250. Mitani T, Heinze JE, & Freese E (1977) Induction of sporulation in *Bacillus subtilis* by decoyinine or hadacidin. *Biochem Biophys Res Commun* 77(3):1118-1125.

251. Geiger T, Goerke C, Fritz M, Schafer T, *et al.* (2010) Role of the (p)ppGpp synthase RSH, a RelA/SpoT homolog, in stringent response and virulence of *Staphylococcus aureus*. *Infect Immun* 78(5):1873-1883.

252. Bennett HJ, Pearce DM, Glenn S, Taylor CM, *et al.* (2007) Characterization of *relA* and *codY* mutants of Listeria monocytogenes: identification of the CodY regulon and its role in virulence. *Mol Microbiol* 63(5):1453-1467.

253. Dubnau D & Losick R (2006) Bistability in bacteria. *Mol Microbiol* 61(3):564-572.

254. Shank EA & Kolter R (2011) Extracellular signaling and multicellularity in *Bacillus subtilis*. *Curr Opin Microbiol* 14(6):741-747.

255. Mirouze N, Desai Y, Raj A, & Dubnau D (2012) Spo0A~P imposes a temporal gate for the bimodal expression of competence in *Bacillus subtilis*. *PLoS Genet* 8(3):e1002586.

256. Mirel DB, Estacio WF, Mathieu M, Olmsted E, *et al.* (2000) Environmental regulation of *Bacillus subtilis* sigma(D)-dependent gene expression. *J Bacteriol* 182(11):3055-3062.

257. Dalebroux ZD & Swanson MS (2012) ppGpp: magic beyond RNA polymerase. *Nat Rev Microbiol* 10(3):203-212.

258. Sarubbi E, Rudd KE, & Cashel M (1988) Basal ppGpp level adjustment shown by new *spoT* mutants affect steady state growth rates and *rrnA* ribosomal promoter regulation in *Escherichia coli*. *Mol Gener Genet* 213(2-3):214-222.

259. Ryals J, Little R, & Bremer H (1982) Control of rRNA and tRNA syntheses in *Escherichia coli* by guanosine tetraphosphate. *J Bacteriol* 151(3):1261-1268.

260. Nishino T, Gallant J, Shalit P, Palmer L, *et al.* (1979) Regulatory nucleotides involved in the Rel function of *Bacillus subtilis*. *J Bacteriol* 140(2):671-679.

261. Wang JD, Sanders GM, & Grossman AD (2007) Nutritional control of elongation of DNA replication by (p)ppGpp. *Cell* 128(5):865-875.

262. Zhang S & Haldenwang WG (2003) RelA is a component of the nutritional stress activation pathway of the *Bacillus subtilis* transcription factor sigma B. *J Bacteriol* 185(19):5714-5721.

263. Primm TP, Andersen SJ, Mizrahi V, Avarbock D, *et al.* (2000) The stringent response of *Mycobacterium tuberculosis* is required for long-term survival. *J Bacteriol* 182(17):4889-4898.

264. Nomura M, Gourse R, & Baughman G (1984) Regulation of the synthesis of ribosomes and ribosomal components. *Annu Rev Biochem* 53:75-117.

265. Traxler MF, Summers SM, Nguyen HT, Zacharia VM, *et al.* (2008) The global, ppGpp-mediated stringent response to amino acid starvation in *Escherichia coli*. *Mol Microbiol* 68(5):1128-1148.

266. Smith I, Paress P, Cabane K, & Dubnau E (1980) Genetics and physiology of the rel system of *Bacillus subtilis*. *Mol Gener Genet* 178(2):271-279.

267. Czarny TL, Perri AL, French S, & Brown ED (2014) Discovery of novel cell wall-active compounds using PywaC, a sensitive reporter of cell wall stress in the model Gram-positive *Bacillus subtilis*. *Antimicrob Agents Chemother* 58(6):3261-269

268. Eiamphungporn W & Helmann JD (2008) The *Bacillus subtilis* sigma(M) regulon and its contribution to cell envelope stress responses. *Mol Microbiol* 67(4):830-848.

269. Guariglia-Oropeza V & Helmann JD (2011) *Bacillus subtilis* sigma(V) confers lysozyme resistance by activation of two cell wall modification pathways, peptidoglycan O-acetylation and D-alanylation of teichoic acids. *J Bacteriol* 193(22):6223-6232.

270. Nicolas P, Mader U, Dervyn E, Rochat T, *et al.* (2012) Condition-dependent transcriptome reveals high-level regulatory architecture in *Bacillus subtilis*. *Science* 335(6072):1103-1106.

271. Cutting CRHaSM (1990) Molecular biological methods for *Bacillus*. John Wiley & Sons, Ltd., West Sussex, UK, p. 391 - 450.

272. Youngman PJ, Perkins JB, & Losick R (1983) Genetic transposition and insertional mutagenesis in *Bacillus subtilis* with Streptococcus faecalis transposon Tn917. *Proc Natl Acad Sci U S A* 80(8):2305-2309.

273. Patrick JE & Kearns DB (2008) MinJ (YvjD) is a topological determinant of cell division in *Bacillus subtilis*. *Mol Microbiol* 70(5):1166-1179.

274. Soutourina O, Soutourina J, Blanquet S, & Plateau P (2004) Formation of D-tyrosyl-tRNATyr accounts for the toxicity of D-tyrosine toward *Escherichia coli*. *J Biol Chem* 279(41):42560-42565.

275. Yang H, Zheng G, Peng X, Qiang B, *et al.* (2003) D-Amino acids and D-Tyr-tRNA(Tyr) deacylase: stereospecificity of the translation machine revisited. *FEBS letters* 552(2-3):95-98.

276. Blair KM, Turner L, Winkelman JT, Berg HC, *et al.* (2008) A molecular clutch disables flagella in the *Bacillus subtilis* biofilm. *Science* 320(5883):1636-1638.

277. Mirel DB & Chamberlin MJ (1989) The *Bacillus subtilis* flagellin gene (hag) is transcribed by the sigma 28 form of RNA polymerase. *J Bacteriol* 171(6):3095-3101.

278. Patrick JE & Kearns DB (2009) Laboratory strains of *Bacillus subtilis* do not exhibit swarming motility. *J Bacteriol* 191(22):7129-7133.

279. Patrick JE & Kearns DB (2012) Swarming motility and the control of master regulators of flagellar biosynthesis. *Mol Microbiol* 83(1):14-23.

280. Vogt SL, Green C, Stevens KM, Day B, *et al.* (2011) The stringent response is essential for *Pseudomonas aeruginosa* virulence in the rat lung agar bead and Drosophila melanogaster feeding models of infection. *Infect Immun* 79(10):4094-4104.

281. Weiss LA & Stallings CL (2013) Essential roles for *Mycobacterium tuberculosis* Rel beyond the production of (p)ppGpp. *J Bacteriol* 195(24):5629-5638.

282. Dalebroux ZD, Svensson SL, Gaynor EC, & Swanson MS (2010) ppGpp conjures bacterial virulence. *Microbiol Mol Biol Rev* 74(2):171-199.

283. Lewis K (2010) Persister cells. *Annu Rev Microbiol* 64:357-372.

284. Amato SM, Orman MA, & Brynildsen MP (2013) Metabolic control of persister formation in *Escherichia coli*. *Mol Cell* 50(4):475-487.

285. Jayaraman R (2008) Bacterial persistence: some new insights into an old phenomenon. *J Biosci* 33(5):795-805.

286. He H, Cooper JN, Mishra A, & Raskin DM (2012) Stringent response regulation of biofilm formation in *Vibrio cholerae*. *J Bacteriol* 194(11):2962-2972.

287. Potrykus K, Murphy H, Philippe N, & Cashel M (2011) ppGpp is the major source of growth rate control in *E. coli*. *Enviro Microbiol* 13(3):563-575.

288. Pal RR, Bag S, Dasgupta S, Das B, *et al.* (2012) Functional characterization of the stringent response regulatory gene *dksA* of *Vibrio cholerae* and its role in modulation of virulence phenotypes. *J Bacteriol* 194(20):5638-5648.

289. Dalebroux ZD, Yagi BF, Sahr T, Buchrieser C, *et al.* (2010) Distinct roles of ppGpp and DksA in *Legionella pneumophila* differentiation. *Mol Microbiol* 76(1):200-219.

290. Aberg A, Fernandez-Vazquez J, Cabrer-Panes JD, Sanchez A, *et al.* (2009) Similar and divergent effects of ppGpp and DksA deficiencies on transcription in *Escherichia coli*. *J Bacteriol* 191(10):3226-3236.

291. Magnusson LU, Gummesson B, Joksimovic P, Farewell A, *et al.* (2007) Identical, independent, and opposing roles of ppGpp and DksA in *Escherichia coli*. *J Bacteriol* 189(14):5193-5202.

292. Lemke JJ, Durfee T, & Gourse RL (2009) DksA and ppGpp directly regulate transcription of the *Escherichia coli* flagellar cascade. *Mol Microbiol* 74(6):1368-1379.

293. Osterberg S, del Peso-Santos T, & Shingler V (2011) Regulation of alternative sigma factor use. *Annu Rev Microbiol* 65:37-55.

294. Costanzo A, Nicoloff H, Barchinger SE, Banta AB, *et al.* (2008) ppGpp and DksA likely regulate the activity of the extracytoplasmic stress factor sigmaE in *Escherichia coli* by both direct and indirect mechanisms. *Mol Microbiol* 67(3):619-632.

295. Sharma UK & Chatterji D (2010) Transcriptional switching in *Escherichia coli* during stress and starvation by modulation of sigma activity. *FEMS Microbiol Rev* 34(5):646-657.

296. Veening JW, Smits WK, & Kuipers OP (2008) Bistability, epigenetics, and bet-hedging in bacteria. *Annu Rev Microbiol* 62:193-210.

297. Maisonneuve E, Castro-Camargo M, & Gerdes K (2013) (p)ppGpp controls bacterial persistence by stochastic induction of toxin-antitoxin activity. *Cell* 154(5):1140-1150.

298. Losick R & Desplan C (2008) Stochasticity and cell fate. *Science* 320(5872):65-68.

299. Balaban NQ, Merrin J, Chait R, Kowalik L, *et al.* (2004) Bacterial persistence as a phenotypic switch. *Science* 305(5690):1622-1625.

300. Norman TM, Lord ND, Paulsson J, & Losick R (2013) Memory and modularity in cell-fate decision making. *Nature* 503(7477):481-486.

301. Ababneh QO & Herman JK (2015) RelA inhibits *Bacillus subtilis* motility and chaining. *J Bacteriol* 197(1):128-137.

302. Rasband WS (1997-2014) ImageJ (U.S. National Institutes of Health, Bethesda, Maryland).

303. den Hengst CD, van Hijum SA, Geurts JM, Nauta A, *et al.* (2005) The *Lactococcus lactis* CodY regulon: identification of a conserved cis-regulatory element. *J Biol Chem* 280(40):34332-34342.

304. Haugen SP, Ross W, & Gourse RL (2008) Advances in bacterial promoter recognition and its control by factors that do not bind DNA. *Nat Rev Microbiol* 6(7):507-519.

305. Sojka L, Kouba T, Barvik I, Sanderova H, *et al.* (2011) Rapid changes in gene expression: DNA determinants of promoter regulation by the concentration of the transcription initiating NTP in *Bacillus subtilis*. *Nucleic Acids Res* 39(11):4598-4611.

306. Tojo S, Kumamoto K, Hirooka K, & Fujita Y (2010) Heavy involvement of stringent transcription control depending on the adenine or guanine species of the transcription initiation site in glucose and pyruvate metabolism in *Bacillus subtilis*. *J Bacteriol* 192(6):1573-1585.

307. Magnuson R, Solomon J, & Grossman AD (1994) Biochemical and genetic characterization of a competence pheromone from *B. subtilis*. *Cell* 77(2):207-216.

308. Rutherford ST & Bassler BL (2012) Bacterial quorum sensing: its role in virulence and possibilities for its control. *Cold Spring Harb Perspect Med* 2(11).

309. Fuqua C, Parsek MR, & Greenberg EP (2001) Regulation of gene expression by cell-to-cell communication: acyl-homoserine lactone quorum sensing. *Annu Rev Genet* 35:439-468.

310. Whitehead NA, Barnard AM, Slater H, Simpson NJ, *et al.* (2001) Quorum-sensing in Gram-negative bacteria. *FEMS Microbiol Rev* 25(4):365-404.

311. Kleerebezem M & Quadri LE (2001) Peptide pheromone-dependent regulation of antimicrobial peptide production in Gram-positive bacteria: a case of multicellular behavior. *Peptides* 22(10):1579-1596.

312. Thomson NR, Crow MA, McGowan SJ, Cox A, *et al.* (2000) Biosynthesis of carbapenem antibiotic and prodigiosin pigment in Serratia is under quorum sensing control. *Mol Microbiol* 36(3):539-556.

313. Solomon JM, Magnuson R, Srivastava A, & Grossman AD (1995) Convergent sensing pathways mediate response to two extracellular competence factors in *Bacillus subtilis*. *Genes Dev* 9(5):547-558.

314. Solomon JM & Grossman AD (1996) Who's competent and when: regulation of natural genetic competence in bacteria. *Trends Genet* 12(4):150-155.

315. Parsek MR & Greenberg EP (1999) Quorum sensing signals in development of *Pseudomonas aeruginosa* biofilms. *Methods Enzymol* 310:43-55.

316. Hammer BK & Bassler BL (2003) Quorum sensing controls biofilm formation in *Vibrio cholerae*. *Mol Microbiol* 50(1):101-104.

317. Grossman AD & Losick R (1988) Extracellular control of spore formation in *Bacillus subtilis*. *Proc Natl Acad Sci U S A* 85(12):4369-4373.

318. Perego M & Hoch JA (1996) Cell-cell communication regulates the effects of protein aspartate phosphatases on the phosphorelay controlling development in *Bacillus subtilis*. *Proc Natl Acad Sci U S A* 93(4):1549-1553.

319. Schaeffer P, Millet J, & Aubert JP (1965) Catabolic repression of bacterial sporulation. *Proc Natl Acad Sci U S A* 54(3):704-711.

320. Lopez JM, Marks CL, & Freese E (1979) The decrease of guanine nucleotides initiates sporulation of *Bacillus subtilis*. *Biochim Biophys Acta* 587(2):238-252.

321. Rudner DZ, LeDeaux JR, Ireton K, & Grossman AD (1991) The spo0K locus of *Bacillus subtilis* is homologous to the oligopeptide permease locus and is required for sporulation and competence. *J Bacteriol* 173(4):1388-1398.

322. LeDeaux JR, Solomon JM, & Grossman AD (1997) Analysis of non-polar deletion mutations in the genes of the *spo0K* (opp) operon of *Bacillus subtilis*. *FEMS Microbiol Lett* 153(1):63-69.

323. Perego M, Higgins CF, Pearce SR, Gallagher MP, *et al.* (1991) The oligopeptide transport system of *Bacillus subtilis* plays a role in the initiation of sporulation. *Mol Microbiol* 5(1):173-185.

324. Phillips ZE & Strauch MA (2002) *Bacillus subtilis* sporulation and stationary phase gene expression. *Cell Mol Life Sci* 59(3):392-402.

325. Lopez D, Vlamakis H, & Kolter R (2009) Generation of multiple cell types in *Bacillus subtilis*. *FEMS Microbiol Rev* 33(1):152-163.

326. Ireton K, Rudner DZ, Siranosian KJ, & Grossman AD (1993) Integration of multiple developmental signals in *Bacillus subtilis* through the Spo0A transcription factor. *Genes Dev* 7(2):283-294.

327. Fujita M & Losick R (2003) The master regulator for entry into sporulation in *Bacillus subtilis* becomes a cell-specific transcription factor after asymmetric division. *Genes Dev* 17(9):1166-1174.

328. Mueller JP & Sonenshein AL (1992) Role of the *Bacillus subtilis* gsiA gene in regulation of early sporulation gene expression. *J Bacteriol* 174(13):4374-4383.

329. Ben-Yehuda S & Losick R (2002) Asymmetric cell division in *B. subtilis* involves a spiral-like intermediate of the cytokinetic protein FtsZ. *Cell* 109(2):257-266.

330. Ben-Yehuda S, Rudner DZ, & Losick R (2003) RacA, a bacterial protein that anchors chromosomes to the cell poles. *Science* 299(5606):532-536.

331. Wagner JK, Marquis KA, & Rudner DZ (2009) SirA enforces diploidy by inhibiting the replication initiator DnaA during spore formation in *Bacillus subtilis*. *Mol Microbiol* 73(5):963-974.

332. Lazazzera BA, Kurtser IG, McQuade RS, & Grossman AD (1999) An autoregulatory circuit affecting peptide signaling in *Bacillus subtilis*. *J Bacteriol* 181(17):5193-5200.

333. Lanigan-Gerdes S, Dooley AN, Faull KF, & Lazazzera BA (2007) Identification of subtilisin, Epr and Vpr as enzymes that produce CSF, an extracellular signalling peptide of *Bacillus subtilis*. *Mol Microbiol* 65(5):1321-1333.

334. Wexselblatt E, Katzhendler J, Saleem-Batcha R, Hansen G, *et al.* (2010) ppGpp analogues inhibit synthetase activity of Rel proteins from Gram-negative and Gram-positive bacteria. *Bioorg Med Chem* 18(12):4485-4497.

335. Wexselblatt E, Kaspy I, Glaser G, Katzhendler J, *et al.* (2013) Design, synthesis and structure-activity relationship of novel Relacin analogs as inhibitors of Rel proteins. *Eur J Med Chem* 70:497-504.

336. Wexselblatt E, Oppenheimer-Shaanan Y, Kaspy I, London N, *et al.* (2012) Relacin, a novel antibacterial agent targeting the Stringent Response. *PLoS Pathog* 8(9):e1002925.